Ph.D. DISSERTATION

GAME THEORETICAL APPROACHES FOR WIRELESS NETWORKS

무선 네트워크 운용을 위한 게임 이론적 접근

BY

LEE WOONG-HEE

FEBRUARY 2017

DEPARTMENT OF ELECTRICAL ENGINEERING AND
COMPUTER SCIENCE
COLLEGE OF ENGINEERING
SEOUL NATIONAL UNIVERSITY

Ph.D. DISSERTATION

GAME THEORETICAL APPROACHES FOR WIRELESS NETWORKS

무선 네트워크 운용을 위한 게임 이론적 접근

BY

LEE WOONG-HEE

FEBRUARY 2017

DEPARTMENT OF ELECTRICAL ENGINEERING AND
COMPUTER SCIENCE
COLLEGE OF ENGINEERING
SEOUL NATIONAL UNIVERSITY

GAME THEORETICAL APPROACHES FOR WIRELESS NETWORKS

무선 네트워크 운용을 위한 게임 이론적 접근

지도교수 김 성 철
이 논문을 공학박사 학위논문으로 제출함

2017년 2월

서울대학교 대학원

전기 컴퓨터 공학부

이 웅 희

이웅희의 공학박사 학위 논문을 인준함

2017년 2월

위 원 장: _____
부위원장: _____
위 원: _____
위 원: _____
위 원: _____

Abstract

In this dissertation, I introduce three algorithms, which are connectivity reconstruction game (CRG), adaptive sector coloring game (ASCG), and asymmetric transmission game (ATG), by mainly using supermodular game and exact potential game with considerations of various objectives (e.g., energy consumption and interference management) in wireless sensor and cellular networks. My main contributions are threefold: 1) connectivity relaxation (energy saving) in wireless localization; 2) inter-cell interference coordination in wireless cellular networks; 3) interference minimization in wireless ad-hoc relay networks. The corresponding explanations are as follows.

1) In geographically dense and energy limited wireless sensor networks, connectivity based localization with full power transmission can be inefficient in terms of energy consumption. In this work, I propose a distributed power control based connectivity reconstruction game, which takes into considerations of both energy efficiency and the quality of localization. The proposed scheme results in a better performance with an improved 61.9% reduction in energy consumption while maintaining the performance of localization at a level similar to the conventional algorithm with full power transmission.

2) Inter-cell interference coordination (ICIC) is a promising technique to improve the performance of frequency-domain packet scheduling (FDPS) in downlink LTE/LTE-A networks. However, it is difficult to maximize the performance of FDPS using static ICIC schemes because of insufficient consideration of signal-to-interference-and-noise ratio (SINR) distribution and user fairness. On the other hand, dynamic ICIC schemes based on channel state information (CSI) also have difficulty presented in the excessive signaling overhead and X2 interface latency. In order to overcome these drawbacks, I introduce a new concept of ICIC problem based on geometric network information (GNI) and propose an ASCG as a decentralized solution of the GNI based ICIC prob-

lem. Furthermore, I develop an ASCG with a dominant strategy space noted as ASCG-D to secure a stable solution through proving the existence of Nash equilibrium (NE). The proposed scheme provides better performance in terms of system throughput gain of up to about 44.1%, and especially of up to about 221% for the worst 10% users than static ICIC schemes. Moreover, the performance of the CSI based ICIC, which require too much computational load and signaling overhead, is only 13.0% and 5.6% higher than that of ASCG-D regarding the total user throughput and the worst 10% user throughput, respectively. The most interesting outcome is that the signaling overhead of ASCG-D is 1/144 of dynamic ICIC schemes' one.

3) In this work, I introduce the new concept of temporal diversity utilization based on asymmetric transmission to minimize network interference in wireless ad-hoc networks with a two-hop half-duplex relaying (HDR) protocol. Asymmetric transmission is an interference-aware backoff technique, in which each communication session (source-relay-destination link) adaptively chooses a certain subset of spectrally-orthogonal data streaming which should be delayed by the duration of one time-slot (i.e., half of one subframe). I design the problem in the HDR scenario by applying the concept of asymmetric transmission, and evaluate the game-theoretical algorithm, called ATG, to derive the suboptimal solution. I show that ATG is an exact potential game, and derive its convergence and optimality properties. Furthermore, I develop an approximated version of ATG (termed A-ATG) in order to reduce signaling and computational complexity. Numerical results verify that two algorithms proposed show significant synergistic effects when collaborating with the conventional methods in terms of interference coordination. Ultimately, the energy consumption to satisfy the rate requirement is reduced by up to 17.4% compared to the conventional schemes alone.

Keywords: Supermodular game, wireless localization, connectivity relaxation, energy consumption, exact potential game, LTE networks, inter-cell interference coordination, geometric network information, two-hop relaying protocol, interference coordination

Student number: 2009-23136

Contents

Abstract **i**

Contents **iii**

List of Tables **vii**

List of Figures **viii**

1 INTRODUCTION **1**

1.1 Application of Supermodular Game for Connectivity Relaxation in Wireless Localization 2

1.2 Application of Exact Potential Game for Effective Inter-Cell Interference Coordination in Wireless Cellular Networks 3

1.3 Application of Exact Potential Game for Interference Minimization in Wireless Ad-hoc Relay Networks 7

1.4 Dissertation Outline 11

2 APPLICATION OF SUPERMODULAR GAME: Distributed Power Control based Connectivity Reconstruction Game in Wireless Localization **13**

2.1 Brief Introduction 13

2.2 System Model 13

2.3 Proposed Power Control Algorithm 14

2.3.1 Reliability Function 14

2.3.2 Game Formulation 15
2.3.3 Convergence Properties of CRG 17
2.4 Simulation Results 20

3 APPLICATION OF EXACT POTENTIAL GAME: Adaptive Sector Coloring Game for Geometric Network Information based Inter-Cell Interference Coordination in Wireless Cellular Networks 24

3.1 Brief Introduction 24
3.2 Network Model 26
3.2.1 System Preliminaries 26
3.2.2 Determination of Time Policy 27
3.2.3 Two-Stage Framework of RB Allocation 27
3.3 PROBLEM FORMULATION: Geometric Network Information based ICIC 28
3.3.1 Outline 28
3.3.2 What Is the GNI? 28
3.3.3 Temporal Perspective: Why GNI? 29
3.3.4 Spatial Perspective: How do I Design a Suitable Utility Function? 29
3.3.5 GNI based ICIC Problem 33
3.4 ADAPTIVE SECTOR COLORING GAME 33
3.4.1 Design of ASCG 33
3.4.2 ASCG with a Dominant Strategy Space 35
3.4.3 Summary of System Operation 40
3.5 PERFORMANCE EVALUATION 41
3.5.1 Simulation Settings and Baselines for Comparison 41
3.5.2 SINR Distribution and Average User Throughput 43
3.5.3 Signaling Overhead for ICIC and FDPS 47
3.5.4 Reduction of Feasible ASCG Strategy Space 49

4 APPLICATION OF EXACT POTENTIAL GAME: Asymmetric Transmission Game for Interference Coordination in Wireless Ad-hoc Relay Networks **51**

4.1 Brief Introduction 51

4.2 Problem Formulation 52

4.2.1 System Preliminaries 52

4.2.2 The Concept of Asymmetric Transmission for Interference Coordination: A Simple Example 53

4.2.3 Optimization Problem 54

4.3 Asymmetric Transmission Game 55

4.3.1 Game Formulation 55

4.3.2 Convergence and Optimality Properties of Asymmetric Transmission Game 55

4.3.3 Approximated Version of Asymmetric Transmission Game . . 58

4.4 Simulation Results 61

4.4.1 Parameters Settings 61

4.4.2 Network Interference in One-shot Game 62

4.4.3 Individual Power Consumption in One-shot Game 66

4.4.4 Total Energy Consumption in 1000-shot Games 70

4.4.5 Complexity Analysis for Varying K and M 71

5 CONCLUSION **74**

Appendix A Derivation of number of partitions for extracting the dominant feasible strategy set **76**

Appendix B Derivation of the cardinal number of the dominant feasible strategy set **78**

Appendix C Existence of NE in ASCG-D **79**

Appendix D The Required Signaling overhead of ASCG-D **82**

Abstract (In Korean) **93**

List of Tables

1.1 List of main abbreviations 12

3.1 List of symbols 25
3.2 Minimization of number of cases of brute force search 35
3.3 System simulation parameters 42

4.1 Computational complexity and signaling overhead 59

List of Figures

2.1 NEs of CRG ($L = 20$, $M = 4$, and $R = 20$m). 17

2.2 Individual energy consumption for localization versus α. 20

2.3 RMSE versus L. 21

2.4 Comparison between $\mathbf{P}^*$ and $\tilde{\mathbf{P}}^*$ in terms of RMSE ($\alpha = 0.1$ and $L = 20$). 22

3.1 Concepts of potential gain and suffered/suffering interference. 31

3.2 Process of minimizing number of cases of brute-force search in ASCG. 36

3.3 Improvement path of ASCG-D in one-drop ($L = 7, M = 140, N = 25, K = 3, P = 43\mathrm{dBm}$, and detailed parameter settings are described in section 3.5). 38

3.4 Framework of ASCG-D and FDPS. 39

3.5 Average user SINR versus subframe for $\lambda = 0.6$. 44

3.6 Performance of FDPS with each ICIC schemes for a varying number of users per cell ($\lambda = 0.6$). 45

3.7 Average signaling overhead per TTI for a varying number of users per cell ($\lambda = 0.6$). 47

3.8 Computational load of ASCG according to irregularity of user distribution. 49

4.1 Link activation flow for data streaming and change of interference topology on a certain subchannel. 52
4.2 Improvement path of ATG in one drop ($M = 10$, $K = 6$, $W = 5$ MHz, $P = 23$ dBm (equal power allocation to all subchannels)); detailed parameter settings and graphical representation of the locations of the communication sessions are described in section 4.4. 56
4.3 Graphical representation of the locations of the communication sessions. 62
4.4 Trend of network interference with $M = 10$. 63
4.5 Individual power consumption for satisfying rate demand (= 6 Mbps) (a) without SA and (b) with SA. 64
4.6 Total energy consumption per minute with $M = 10$ (a) without SA and (b) with SA. 67
4.7 Computation load for varying (a) K (M is set to 10) and (b) M (K is set to 6). 69

Chapter 1

INTRODUCTION

As game theory can reflect to various phenomenons in real world, game theoretical approach is widely and deeply used in economics, political science, psychology, and even gambling. Fortunately, game theory can also provide stable and suboptimal solutions by distributed manner in wireless networks, because the construction of game can be suitably applied to those of various scenarios in wireless networks. As interest in decentralized wireless networks grew, game theoretic approaches to help us understand and predict the performance of complex wireless systems that cannot be completely modeled using traditional optimization tools. More concretely, the behavior of a given wireless device may affect the communication capabilities of a neighboring device, notably because the radio communication channel or the dedicated transmission time is usually shared in wireless networks. In addition, as energy consumption become capable of more sophisticated adaptations, the assumptions of game theoretic models become a still better match for future wireless networks. With these considerations, in this dissertation, I use two well-known games, which are supermodular game [1] and exact potential game [2], for achieving various objectives in wireless networks. The corresponding motivation, related work, and contribution of each of my works are introduced in the following three sections.

1.1 Application of Supermodular Game for Connectivity Relaxation in Wireless Localization

Localization in wireless sensor networks (WSNs) is crucial to establish self-configuration for surveillance, navigation, and communications. In WSN composed by small and cheap nodes, localization by measuring received-signal-strength (RSS) and determining connectivity has become popular because of the low complexity and low cost of sensor devices [3–6]. Among wireless localization techniques using RSS and connectivity, the distributed weighted multidimensional scaling (dw-MDS) algorithm is a well-known method that reduces computational complexity and localization error compared to the classical multidimensional scaling (MDS) algorithm [7] based on all pairwise distance measurements of sensors. The dw-MDS utilizes distance measurements in one-hop coverage and iteratively solves the scaling by majorizing a complicated function (SMACOF) algorithm based on the weighted cost function related that allows distance measurements that are believed to be more accurate to be weighted more heavily; consequently, dw-MDS outperforms the classical MDS in terms of localization error in spite of its distributed manner [8].

Because of the benefits of dw-MDS, it is used to develop several algorithms to optimize the quality of localization [8–10]. However, most of these studies on the wireless localization schemes have overlooked the amount of energy consumed in the excessively high density of network connection among wireless nodes. In dw-MDS, each node searches the neighboring nodes to exchange information for localization by full or heuristically regulated transmission power. Even if quality of localization could be guaranteed, these ambiguous power allocation are inefficient in a dense and energy-limited WSN. A suitable approach for localization that optimizes network connectivity in WSN is necessary.

To deal with the above considerations, I formulate the connectivity reconstruction game (CRG) based on distributed power control as a solution for energy-efficient op-

timization in WSN localization.[1] Furthermore, I show that the CRG satisfies the conditions of supermodular game; consequently, I am able to characterize convergence using the properties of supermodular game [1]. Simulation results show that dw-MDS combined with CRG significantly reduces energy consumption when compared to dw-MDS alone, while maintaining the performance of localization at a similar level.

1.2 Application of Exact Potential Game for Effective Inter-Cell Interference Coordination in Wireless Cellular Networks

Orthogonal frequency-division multiple access (OFDMA) is the envisioned air interface selected by the Third-Generation Partnership Project Long-Term Evolution (3GPP LTE) standard on account of its high spectrum efficiency. In OFDMA-based systems, the system bandwidth is divided into small radio resources known as resource blocks (RBs), and it is the smallest packet scheduling unit in LTE and LTE-Advanced (LTE-A) architectures [13, 14, 73]. The performance of downlink packet scheduling in OFDMA-based systems is considerably influenced by the spatial and temporal effectiveness of RB utilization. In RB utilization for downlink packet scheduling, frequency-domain packet scheduling (FDPS) is well known as the optimal solution to achieve the high system throughput and user fairness [16–19]. The FDPS is an extended version of proportional fairness scheduling (PFS) such as two-dimensional (2-D) packet scheduling in consideration of mapping between the RB domain and the user domain.

Further, the performance of FDPS depends on how the feasible FDPS space is coordinated well by a temporally and spatially suitable RB clusterings. The feasible

[1] In the previous works of [11] and [12], they also have the intuition related to energy saving for localization. However, they focus on localizing sensor nodes based on cooperation among sets of anchor nodes; thus, they are inappropriate to be applied to connectivity based localization.

FDPS space based RB clustering determines the current state of signal-to-interference-plus-noise ratio (SINR) distribution and multiuser diversity gain, which have a strong impact on the performance of FDPS. A kind of scheme developed to construct the feasible FDPS space to achieve the increased FDPS performance is called inter-cell interference coordination (ICIC)[2] [20–39].

The ICIC has been investigated as an approach to alleviate the impact of interference in the OFDMA-based systems. Conventional ICIC schemes are categorized, according to the update period for the current feasible FDPS space, into static ICIC schemes and dynamic ICIC schemes [20]. Static ICIC schemes are frequency reuse-based schemes and include the reuse-1, reuse-3, and partial frequency reuse (PFR) schemes [21–25]. These are predetermined frequency reuse patterns, because they do not require additional signaling overhead and system computational load. However, they are inappropriate for use with different cell layouts with the existence of dynamic network conditions such as the geometric user distribution and fast fading channel condition. In realistic systems, the network conditions may have significant variations over time. Symmetric and apriori frequency reuse patterns are highly inefficient in time-varying network conditions.

Various dynamic ICIC schemes to overcome these drawbacks have recently attracted research interest [26–39]. These dynamic ICIC schemes have emerged as efficient solutions to cope with changes in dynamic network conditions. Dynamic ICIC schemes are also called cell coordination-based schemes. Dynamic ICIC schemes can be categorized, based on the form of coordination and the level of optimizing ICIC, into centralized schemes, semi-distributed schemes, coordinated-distributed schemes, and autonomous-distributed schemes. In [20], the authors concretely introduce these four levels of classification of dynamic ICIC schemes. In centralized schemes, a radio

[2]Coordinated multi-point (CoMP) transmission is another attractive radio access technique in an LTE-A architecture. However, it incurs larger signaling overhead than ICIC schemes owing to the exchange of users' data as well as channel state information (CSI). In this study, I focus on ICIC rather than on CoMP.

network controller (RNC) collects all of the CSI of every user in the network and optimizes the feasible FDPS space of every cell. This process naturally yields extreme computational load because of a large number of potential solutions [26]. Even though semi-distributed schemes, in which each evolved Node-B (eNB) relieves the computational load of RNC, the corresponding computational load is still high to optimize ICIC properly in practical systems [30]. On the other hand, emerging cellular networks such as LTE-A systems rely on inter-eNB connections over the X2 interface without any central coordinator in a flat architecture [13]. LTE-A architectures solve the problem of constructing the feasible FDPS space by using a coordinated-distributed scheme by the exchange of CSI among eNBs, and not in a centralized or semi-distributed method as done by an RNC. In coordinated-distributed schemes, the decision of ICIC is made only at the eNB level. Thus, they are more attractive for practical implementation by virtue of reducing the network infrastructure complexity to eliminate the central entity.

However, most of these studies on the coordinated-distributed schemes for the CSI based ICIC have overlooked the temporal consideration of the signaling latency and signaling overhead. Latency on the X2 interface is a particularly critical factor for satisfying the performance requirements in LTE-A systems. Generally, the X2 interface latency in an LTE-A system is approximately on the order of several tens of milliseconds [41–43]; therefore, it is difficult to implement coordinated-distributed schemes in fast fading environments, such as those with a CSI coherence time of[3] 1-2 ms. Even after the message for CSI including information of inter-cell interference has been transmitted, it could be useless since the channel conditions have already changed. This contradiction has been overlooked in several studies on the CSI based ICIC [30–35]. Moreover, extremely large signaling overhead is necessary for exchanging global CSI. The exchange of global CSI for ICIC is not acceptable for large networks because the total feedback signaling overhead for ICIC increases exponentially due to the combi-

[3] After recognizing the need for resolving this temporal contradiction, LTE-A working groups have been actively conducting research toward minimizing the latencies across the X2 interface.

natorial nature of users. The signaling overhead must be reduced, which in turn may degrade the overall performance of the system.[4]

Considering the above background, I introduce a new concept of the ICIC problem based on geometric network information (GNI), which is the alternative to CSI. To develop the well-constructed coordinated-distributed ICIC scheme for realistic systems, a new ICIC problem with a long consistent period has to be established. The feasibility of GNI based ICIC problem comes from the fact that the GNI is changed much slower than the CSI. Based on this time-correlation property, the temporal limitations related to the X2 interface latency and signaling overhead can be solved. I define the new concepts of potential gain and suffered/suffering interference to formulate GNI based utility function effectively. These new concepts are formulated by the correlation between the GNI and the current state of RB clustering at network-level. The interesting outcome from this approach is that the signaling overhead of GNI based ICIC are much smaller than that of CSI based ICIC. However, it is a rather complex task to search a global optimal GNI based ICIC solution at the network level. Consequently, I propose a game-theoretic coordinated-distributed scheme denoted as an adaptive sector coloring game (ASCG) in order to resolve the GNI based ICIC problem with the reduced computational load. Game theory provides analytical tools for predicting the outcome of complicated interactions between rational entities. Game theoretic mechanism adapted to GNI based ICIC problems is designed as follows: each eNB determines a feasible FDPS space to maximize its own utility function of the GNI based ICIC problem, and the decision is made only at eNB level[5]. This game-theoretic approach can be effec-

[4]Even though autonomous-distributed schemes can significantly reduce the computational load and message exchange among eNBs, these schemes may bring other problems related to SINR distribution and system throughput due to the absence of sharing ICIC strategies among eNBs. Thus, similar to static ICIC schemes, autonomous-distributed schemes are also inappropriate for use with extremely irregular and dynamic networks.

[5]Because the mechanisms of non-cooperative games and coordinated-distributed schemes for ICIC are naturally similar, several studies on the use of game theoretic approaches, especially potential games, for the CSI based ICIC in LTE-A are presently underway [36–38]. However, they also have the temporal

tive implementation to obtain a suboptimal solution of the GNI based ICIC problem. The name "ASCG" is based on the concept of an adaptive mapping between RBs and beams (i.e., sectors), which appears similar to the action of the eNB coloring its sectors. In ASCG, a set of players is eNBs in the entire network. During their turn to update the strategy, all players myopically choose the best feasible FDPS space with the fixed strategies of other players. Moreover, convergence to equilibrium is assured by the conversion of ASCG to the form of an exact potential game [2], which is denoted as ASCG with dominant strategy space (ASCG-D). These new game theoretic approaches are expected to be capable of finding a meaningful solutions compared to conventional CSI based ICIC over the X2 interface.

My main contributions in this study can be summarized as follows: i) the formulation of GNI based ICIC problem with low signaling overhead and insensitivity to the X2 interface latency, ii) the construction of ASCG as the suboptimal solution of the GNI problem with low complexity, iii) the development of ASCG to ASCG-D with assurance of the stable solution.

1.3 Application of Exact Potential Game for Interference Minimization in Wireless Ad-hoc Relay Networks

The interest in energy efficiency in wireless networks has been increasing in recent years. Energy-constrained wireless systems, such as device-to-device (D2D) communication [45, 46] and WSNs [47, 48], are composed of mobile devices typically powered by lifetime-limited batteries, which inconvenience the serviced users in practice. In addition, the congestion by a large number of users sharing the same wireless resource would generate significant network interference among users, and therefore aggravate the energy efficiency issue at the system level. The fundamental challenge to utilize scarce energy efficiently in wireless systems is how to suppress network

limitation owing to the X2 interface latency.

interference by well coordinating temporally and spectrally suitable schemes. The amount of network interference is strongly tied to power consumption satisfying the rate requirements of end-users, therefore, well-coordinated network interference management methods are necessary for extending the network lifetime. Furthermore, especially in an ad-hoc network that creates multi-hop links with a relaying protocol, which is widely utilized in D2D communication and WSNs by virtue of its advantages in extending communication coverage [49], improving spectral efficiency [50], and reducing outage probability [51], it is not easy to optimize network interference reduction. The addition of a relaying protocol naturally makes interference coordination more difficult because the interference links are more complex compared to ad-hoc networks consisting of one-hop links.

To resolve the problems related to interference coordination and energy efficiency in wireless ad-hoc relay networks, various approaches for algorithmic solutions, which are categorized into relay selection, subchannel allocation (SA), and power allocation, have been developed [39, 40, 52–64]. First, considering that the network interference from relays to another destination is jointly affected by the relay selection of all source-and-destination pairs, many interference-aware relay selection schemes based on centralized or decentralized methods have been proposed for two-hop relay networks to minimize the network interference in various scenarios [52–56]. After the operation of the relay selection is carried out according to the network interference status (i.e., each of the proper communication sessions, which remains as a source-destination link or is converted to source-relay-destination link, is formed), the network interference can be further reduced by effective spectral utilization. Consequently, various dynamic SA techniques for interference coordination/avoidance have been researched [39, 40, 57–59]. If the entire spectrum is divided into a set of subchannels, e.g., as in orthogonal frequency division multiplexing (OFDM) systems, each node can autonomously select the best subchannels in terms of the interference sta-

tus.[6] Additionally, since these SA algorithms result in increased SNIR distributions, they can also be potential solutions for energy efficiency in collaboration with power allocation algorithms [60–64]. These joint optimization methods are generally based on the water-filling (WF) algorithm, which is an optimal power allocation method used to design interference-limited systems as an enabling technique based on the spectral diversity for interference and energy management [65, 66]. However, a common assumption in the above algorithmic solutions proposed in [39, 40, 52–64] is that all communication sessions carry out data streaming by using all possible subchannels simultaneously. Therefore, in a half-duplex relaying (HDR) system, there always exist source-to-relay interference links in the first time slot (i.e., the first phase of a subframe) and relay-to-destination interference links in the second time slot (i.e., the second phase of a subframe). In this study, I would like to answer the following questions: i) is this structure of symmetric data streaming by all communication sessions the best choice in the context of interference minimization? ii) What would happen if there was a temporal crack[7] in the structure of the symmetric transmission?

In this work, I propose a new concept of temporal diversity to efficiently reduce the network interference in a multiuser two-hop HDR system with a decode-and-forward (DF) protocol. It has not been reported yet to study the asymmetric transmission, which is an interference-aware backoff technique where each communication session (source-relay-destination link) adaptively chooses a certain subset of the spectrally-parallel data streaming that should be delayed by the duration of one time slot (i.e., half

[6] On the other hand, block diagonalization or interference alignment [67, 68] are also powerful techniques for interference cancellation by proper beamforming algorithms. However, these schemes are commonly used in multiple-input multiple-output (MIMO) systems, which may face challenges when applied to ad-hoc networks that only consist of devices with a small size, and generally require a significant signaling overhead for exchanging the dedicated data and the global CSI of all users in the network. Thus, they are inappropriate for use with wireless ad-hoc networks of consisting many communication sessions.

[7] This should be easily understood, in consideration of random backoff techniques that aim to avoid data collision in Wi-Fi systems [69].

of one subframe). A part of the entire interference links in the networks are changed according to the autonomous asymmetric transmission of each communication session. It should be interpreted that the degree of freedom based on temporal diversity is created for interference minimization. On the basis of this intuition, I formulate an asymmetric transmission based interference coordination problem. Depending on the generation of interference links in the network, I model 0-1 integer linear programming in the HDR system. Since this problem is known to be NP-hard [70], it requires an immense amount of calculation in order to obtain the corresponding optimal solutions. Consequently, I consider a game theoretic asymmetric transmission scheme for minimizing the total network interference in multiuser ad-hoc HDR systems. The first version of the asymmetric transmission game (ATG) is modeled in the form of the exact potential game [2], and is based on actual interference on every subchannel among the communication sessions. In ATG, a set of players is a set of communication sessions. The utility function of each player is formulated by adding the interference experienced and generated by a player. All players sequentially update their best-response strategies on the basis of a round-robin rule. According to the property of this exact potential game, the Nash equilibrium (NE) of ATG is guaranteed. Furthermore, I develop an approximated version of ATG denoted as A-ATG, which is also an exact-potential game in order to reduce signaling and computational complexity. In A-ATG, a set of communication sessions select their own transmission strategies by exchanging potential interference based on the average value of interference over the spectral domain. I summarize my main contribution as follows:

i) New concept of temporal diversity: I formulate a new interference coordination problem based on asymmetric transmission in the HDR system.

ii) General game formulation and derivation of convergence properties: I propose a game-theoretical algorithm as the suboptimal solution, and derive its convergence properties.

iii) Performance improvement in terms of network interference and energy efficiency: I

show that the proposed algorithms significantly reduce network interference compared to the SA scheme. Furthermore, in the context of power consumption while satisfying rate requirements, the corresponding performance gains are measured up to 17.4% over the joint SA [39, 40] and WF algorithm [66].

1.4 Dissertation Outline

The reminder of this dissertation is organized as follows. In Chapter 2, an application of supermodular game, which is titled *"Distributed Power Control based Connectivity Reconstruction Game in Wireless Localization"*, is introduce to effectively construct the network connectivity when operating connectivity and RSS based localization. In Chapter 3, an application of exact potential game, which is titled *"Adaptive Sector Coloring Game for Geometric Network Information based Inter-Cell Interference Coordination in Wireless Cellular Networks"*, is introduced to resolve various shortcomings of conventional static and dynamic ICIC in LTE networks. In Chapter 4, another application of exact potential game, which is titled *"Asymmetric Transmission Game for Interference Coordination in Wireless Ad-hoc Relay Networks"*, is introduced to apply new concept of temporal diversity utilization for minimizing network interference in wireless ad-hoc relay networks. Finally, conclusions were drawn in Chapter 5. The main abbreviations can be found in Table 1.1.

Table 1.1: List of main abbreviations

WSN	Wireless sensor network
RSS	Received-signal-strength
dw-MDS	Distributed weighted multidimensional scaling
NE	Nash equilibrium
CRG	Connectivity reconstruction game
LTE	Long-term evolution
OFDMA	Orthogonal frequency division multiple access
eNB	evolved Node-B
UE	User equipment
RB	Resource block
SINR	Signal-to-interference-plus-noise ratio
CSI	Channel state information
GNI	Geometric network information
ICIC	Inter-cell interference coordination
FDPS	Frequency-domain packet scheduling
ASCG	Adaptive sector coloring game
ASCG-D	ASCG with a dominant strategy space
HDR	Half-duplex relaying
DF	Decode-and-forward
SA	Subchannel allocation
WF	Water-filling
ATG	Asymmetric transmission game
A-ATG	Approximated version of ATG

Chapter 2

APPLICATION OF SUPERMODULAR GAME: Distributed Power Control based Connectivity Reconstruction Game in Wireless Localization

2.1 Brief Introduction

This study proposes a game-theoretical power control based connectivity reconstruction algorithm, called CRG, suitable for wireless localization in energy-limited wireless sensor network (WSN). The solution of CRG, which is obtained by the properties of supermodular game, results in the effective connectivity for wireless localization with energy savings. I think that my proposed algorithm can be effectively utilized in WSNs according to the system's objective, e.g., energy consumption or quality of localization. Additionally, I believe that my contribution can be more valuable in future WSNs when distribution of sensor nodes would become denser.

2.2 System Model

Assume that there is a set of anchor nodes $\mathcal{M} = \{1, ..., M\}$ and a set of sensor nodes $\mathcal{L} = \{1, ..., L\}$ in a two-dimensional WSN. The actual location of the node is denoted

by $\mathbf{x}_m$, where $m \in \mathcal{M} \cup \mathcal{L}$. Sensor nodes have unknown positions, while anchor nodes have priori known positions themselves. Sensor nodes are randomly located in the circle area with radius R. The anchor nodes are uniformly located on the edge of the same circle area. $\mathcal{P}_i$ is the set of feasible transmission power of node i in a linear scale, and $P_i \in \mathcal{P}_i$ is the transmission power at node i. In the case of node i's transmission and node j's reception, the maximum likelihood estimator of the one-sided distance can be denoted by $\bar{\delta}_{ij} = d_0\big(\gamma_0 P_i / P_{ij}\big)^{1/n_p}$, where γ_0 is the power of attenuation measured at a reference distance d_0 from transmitter i and P_{ij} is the power received by node j from transmitter i. P_{ij} follows the lognormal distribution, in which the mean value is $\bar{P}_{ij}$ and the standard deviation is σ. The standard deviation σ represents the shadowing effect, and it is constant for a sufficiently long period. n_p is the path loss exponent, and it is known to all nodes. So, for all $i, j \in \mathcal{M} \cup \mathcal{L}$, $\bar{\delta}_{ij}$ can be measured when $P_{ij} \geq P_{\text{sen}}$, where P_{sen} is the sensitivity level for correct demodulation. Considering the inaccuracy due to the relationship between σ and P_{ij}, even though the same distance is measured, more reliable values of the measured distance are obtained by a high transmission power compared to a low one. Finally, the estimated distance between node i and j, δ_{ij}, would be $\bar{\delta}_{ij}$, if $P_i > P_j$, and vice versa. δ_{ij} is valid when both $\bar{\delta}_{ij}$ and $\bar{\delta}_{ji}$ are measurable (i.e., $P_{ij}, P_{ji} \geq P_{\text{sen}}$), and it is constant during a sufficiently long period because of the temporal property of σ.

2.3 Proposed Power Control Algorithm

2.3.1 Reliability Function

To solve the network-wide localization problem by using the set of all the δ_{ij}, I have to quantify the expected accuracy of δ_{ij}. I set a reliability function denoted as w_{ij}, which reflects that less accurate measurements are down-weighted in the local optimization

function for localization in a distributed manner.[1] Although σ is concurrently influenced regardless of the received power, this influence is differentially reflected to the viewpoint of the estimated distance because the function of the estimated distance versus the received power is decreasing and convex form. As a result, the range of error would be wider, when estimating distance with low transmission power. To reflect this property, I choose a well-known form of reliability function between nodes i and j as follows [8]:

$$w_{ij}\big(=w_{ji}\big)=\begin{cases} exp\{-(\delta_{ij}/h_{ij})^2\}, & \text{if } \delta_{ij} \text{ is measured} \\ 0, & \text{otherwise.} \end{cases} \tag{2.1}$$

h_{ij} is determined by the larger value between the possible transmission coverage of nodes i and j, (i.e., $h_{ij} \triangleq \max\big[d_0(\gamma_0 P_i/P_{\text{sen}})^{1/n_p}, d_0(\gamma_0 P_j/P_{\text{sen}})^{1/n_p}\big]$); consequently, the reliability function w_{ij} is in terms of P_i or P_j. Further, by definition of δ_{ij}, w_{ij} should be zero when $P_{ij} < P_{\text{sen}}$ or $P_{ji} < P_{\text{sen}}$. These characteristics imply that I can control the reliability function along with the connectivity for network-wide localization through the adequate allocation of transmission power. Let us optimize the energy-efficient localization by means of controlling transmission power.

2.3.2 Game Formulation

My objective is the relaxation of connectivity while maintaining a similar level with localization error using full power transmission. Let us address the problem of assigning a transmission power to each node in a distributed fashion. Because of its distributed nature, game theory is a valuable tool for this problem, which I can model in a strategic form as follows:

Definition 1. Connectivity reconstruction game (CRG): $< \mathcal{L}, P_i, \{C_i\}_{i\in\mathcal{L}} >$

[1] In the SMACOF algorithm of dW-MDS [8], each sensor node solves iteratively the local optimization formulated by minimizing $S_i = \sum_{j=1,j\neq i}^{L+M} w_{ij}(\delta_{ij} - ||\tilde{\mathbf{x}}_i - \tilde{\mathbf{x}}_j||_2)^2$ for all i, where $\tilde{\mathbf{x}}_i$ is the estimated position of node i. The higher values and the lesser nonzero terms all w_{ij} are, this algorithm shows a higher performance in terms of localization error.

i) Player set: $\mathcal{L} = \{1, ..., L\}$ (a set of sensor nodes)

ii) Strategy of player i: $P_i \in \mathcal{P}_i$, where $i \in \mathcal{L}$

iii) Cost function of player i:

$C_i(\mathbf{P}) = \sum_{j \in \mathcal{L} \setminus i} C_{ij}(P_i, P_j) = \sum_{j \in \mathcal{D}_i} C_{ij}(P_i, P_j)$, where C_{ij} is the partial cost function of i related to j and $\mathcal{D}_i$ is the set of nodes connected to node i, i.e., $\mathcal{D}_i = \{j | w_{ij} \neq 0\}$.

The set of players $\mathcal{L}$ is exactly the same as the set of sensor nodes. Therefore I will use the terms "player i" and "node i" interchangeably. $\mathcal{P}_i$ is the set of feasible strategies of player i. Without loss of generality, $\mathcal{P}_i \triangleq [P_{i,\min}, P_{i,\max}]$. P_i is the strategy of player i. For each player i, I write $\mathbf{P}_{-i}$ as the joint strategy set of all players in the set excluding player i. Hence, $\mathbf{P}$ is the joint strategy of all the players. Best response of player i is defined as $P_i^* \triangleq \text{argmin}_{P_i} C_i(P_i, \mathbf{P}_{-i})$ under given $\mathbf{P}_{-i}$. CRG proceeds by each player sequentially to update the strategy of each player by round-robin rule.

Consideration for designing the cost function of CRG is twofold: C_i should contain i) provision for reducing P_i while maintaining its reliability to others (selfish philosophy); ii) information about the neighboring nodes' benefit or damage in terms of reliability according to the change of P_i (cooperative philosophy). Using these conditions, I formulate the partial cost function of player i related to j as follows:

$$C_{ij} = \begin{cases} -\frac{[w_{ij}(P_j)]^\alpha}{P_i}, & \text{if } j \in \mathcal{A}_i \\ -\frac{[w_{ij}(P_i)]^\alpha}{P_i} - (P_i - P_j)\frac{\partial([w_{ij}(P_i)]^\alpha / P_j)}{\partial P_i}, & \text{if } j \in \mathcal{B}_i \\ 0, & \text{otherwise.} \end{cases} \tag{2.2}$$

where $\mathcal{A}_i = \{j | w_{ij} \neq 0 \text{ and } P_j > P_i\}$ and $\mathcal{B}_i = \mathcal{D}_i \setminus \mathcal{A}_i$, respectively. The collection $\mathcal{A}_i$ is the subset of $\mathcal{D}_i$ and transmit a power higher than node i. Further, the collection $\mathcal{B}_i$ is the subset of $\mathcal{D}_i$ excluding $\mathcal{A}_i$. Recall from (2.1), w_{ij} is a function of P_j or P_i depending on whether player j is in $\mathcal{A}_i$ or $\mathcal{B}_i$, if the conditions $P_{ij}, P_{ji} \geq P_{\text{sen}}$ are satisfied. Based on that, C_{ij} is represented in (2.2). If $j \in \mathcal{A}_i$, w_{ij} is dependent on P_j, not P_i. On the other hand, if $j \in \mathcal{B}_i$, w_{ij} is dependent on P_i. Assuming that the value of $(P_i - P_j)\frac{\partial([w_{ij}(P_i)]^\alpha / P_j)}{\partial P_i}$ in (2.2) is approximately linear in $[P_i, P_j]$, the corresponding

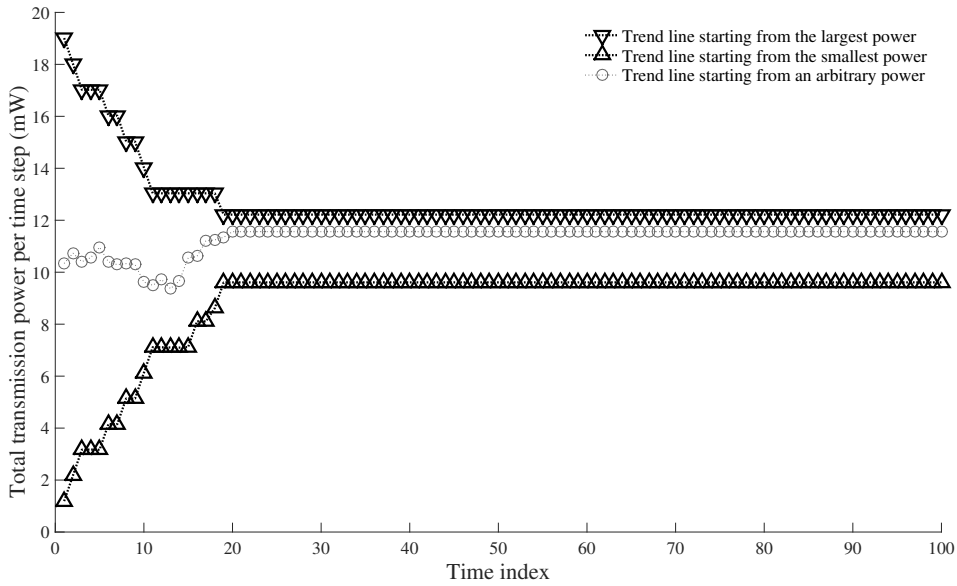

Figure 2.1: NEs of CRG ($L = 20$, $M = 4$, and $R = 20$m).

term is the value of estimated benefit of the player j according to variation of P_i. Further, system parameter α, which is given by $0 < \alpha < 1$, determines a trade-off between localization reliability and power consumption. When α goes to 0, CRG gives a higher priority to energy consumption compared to the case when α goes to 1. Therefore, I can choose the value of α according to the characteristics of the target system.

2.3.3 Convergence Properties of CRG

In this section, I discuss the existence of the NE solution. The NE of CRG is defined as a given strategy $\mathbf{P}^* \triangleq \{P_1^{\text{NE}}, ..., P_L^{\text{NE}}\}$, if I have $C_i(\mathbf{P}^*) = C_i(P_i^*; \mathbf{P}_{-i}^*) \geq C_i(P_i; \mathbf{P}_{-i}^*)$ under given $\mathbf{P}_{-i}^*$ for all $i \in \mathcal{L}$. The NE of CRG is the state in which all players are satisfied with the current transmission power and connectivity with the neighboring nodes, and there is no further update until the next localization. To show the existence of the NE of CRG, I can prove that CRG is a supermodular game, as it

satisfies the Definition 2 in [1]. In a supermodular game, there always exists the pure-strategy NE when it is played by a sequential best-response dynamic [1]. I will show that CRG is a supermodular game to prove the assured existence of the NE.

Theorem 1. CRG is supermodular and there exists an NE solution.

$Proof$: It is trivial to show that the CRG satisfies the first two conditions[2] (compactness and lower semi-continuity) in [1]. To verify the third condition of supermodularity (increasing difference) in [1], I separate all possible changes of P_i and P_j into the following two scenarios according to whether C_i is twice continuously differentiable or not.

i) *Moving in continuous region*

In this scenario, I obtain the second cross-derivative of C_i, $\partial^2 C_i(\mathbf{P})/\partial P_i \partial P_j$. If $j \in \mathcal{A}_i$, the second cross-derivative is given by $\frac{1}{(P_i)^2}\frac{\partial [w_{ij}(P_j)]^\alpha}{\partial P_j}$. Otherwise, if $j \in \mathcal{B}_i$, the second cross-derivative is given by $\frac{1}{(P_j)^2}\frac{\partial [w_{ij}(P_i)]^\alpha}{\partial P_i} + \frac{P_i}{(P_j)^2}\frac{\partial^2 [w_{ij}(P_i)]^\alpha}{\partial (P_i)^2}$. In the case of $h_{ij} = d_0(\gamma_0 P_i/P_{\text{sen}})^{1/n_p}$, the corresponding reliability function, $[w_{ij}(P_i)]^\alpha = exp(-\alpha(\delta_{ij}/h_{ij})^2)$, can be represented in the form of $exp(-(\alpha/kP_i^{2/n_p}))$, where $k = \left(d_0\gamma_0/P_{\text{sen}}^{1/n_p}\delta_{ij}\right)^2 \geq 0$. Further, $\alpha > 0$ by its definition. Thus, I can easily verify that $\frac{\partial [w_{ij}(P_i)]^\alpha}{\partial P_i} \geq 0$ and $\frac{\partial^2 [w_{ij}(P_i)]^\alpha}{\partial (P_i)^2} \geq 0$ in $\mathcal{P}_i$. Obviously, $\frac{\partial [w_{ij}(P_j)]^\alpha}{\partial P_j} \geq 0$ in $\mathcal{P}_j$. Finally, if $j \in \mathcal{L} \setminus \mathcal{D}_i$, $w_{ij} = 0$ and $C_{ij} = 0$; consequently, $\partial^2 C_i(\mathbf{P})/\partial P_i \partial P_j = 0$. Thus, $\partial^2 C_i(\mathbf{P})/\partial P_i \partial P_j \geq 0$ is satisfied for any i and j.

ii) *Passing through semicontinuous point*

Assuming that $\hat{P}_i \in \{P_i | P_{ij} < P_{\text{sen}}\}$ and $\tilde{P}_i \in \{P_i | P_{ij} \geq P_{\text{sen}}\}$, $\forall i, j \in \mathcal{L}$. Let the operator '$\rightarrow$' to the change of strategy. Simultaneous changes (e.g., $(\hat{P}_i \rightarrow \tilde{P}_i, \hat{P}_j \rightarrow \tilde{P}_j)$) are invalid because of the sequential update rule of CRG. Then, there are four following cases in this scenario of passing through a semicontinuous point: $(\hat{P}_i, \hat{P}_j \rightarrow \tilde{P}_j)$, $(\hat{P}_i \rightarrow \tilde{P}_i, \hat{P}_j)$, $(\tilde{P}_i, \hat{P}_j \rightarrow \tilde{P}_j)$, and $(\hat{P}_i \rightarrow \tilde{P}_i, \tilde{P}_j)$. By properly substituting these

[2] $\mathcal{P}_i$ is in $\mathbb{R}$ for all i; thus, $\mathcal{P}_i$ is compact. To ensure that $P_i^*\big(\triangleq \text{argmin}_{P_i} C_i\big)$ can be found in the closed region, C_i should be lower semi-continuous in $\mathbf{P}_{-\mathbf{i}}$ as well as P_i. CRG satisfies this condition according to the definition of C_{ij} in (2.2). If P_i^* is $\text{argmax}_{P_i} C_i$, the upper semi-continuity of C_i is necessary; however, it is not suitable to achieve my objective.

cases to the definition 1 of [1], the corresponding condition related to C_{ij} can be verified, which concludes the proof. ■

Figure 2.1 represents a snapshot of NE of CRG through plotting trend lines of the network energy consumption per time step, $\sum_{i=1}^{L} P_i$, starting from $P_i = P_{i,\max} = 1\text{mW}$, $P_i = P_{i,\min} = 0\text{mW}$, and an arbitrary point for all i. In this case, the values of $\sum_{i=1}^{L} P_i$ for the largest and smallest NE are 12.1mW and 9.5mW, respectively. The two important properties of CRG can be summarized as follows: i) If the users' best responses are single-valued, and each user uses the best response updates starting from the smallest (or largest) element of its strategy space, then the strategies converge to the smallest (or largest) NE. ii) If each user starts from any feasible strategy, the strategies will eventually lie in the set bounded by the smallest and largest NE of each component.

Algorithm 2.1 summarizes the steps of the algorithm for CRG, where $\mathbf{P}^{(k)}$ and $\mathcal{D}_i^{(k)}$ are the joint strategy of all players, $\mathbf{P}$, and the set of sensor nodes communicating with node i, $\mathcal{D}_i$, at the k-th time index, respectively.

Algorithm 2.1 CRG with dw-MDS

Start with arbitrary initial strategy state vector $\mathbf{P}^{(0)}$.

while $\mathbf{P}^{(k)} \neq \mathbf{P}^{(k-1)}$ **do**

Select player i according to the round-robin rule.

Collect P_j and measure δ_{ij}, $\forall j \in \mathcal{D}_i^{(k)}$

Calculate $C_i(\mathbf{P}^{(k)})$ based on (2.2) and solve new best response strategy P_i^* at time index k and update P_i to P_i^*.

Set $k \leftarrow k + 1$.

end while

Run the dw-MDS [8] with w_{ij}, $\forall i, j$, determined by $\mathbf{P}^*$.

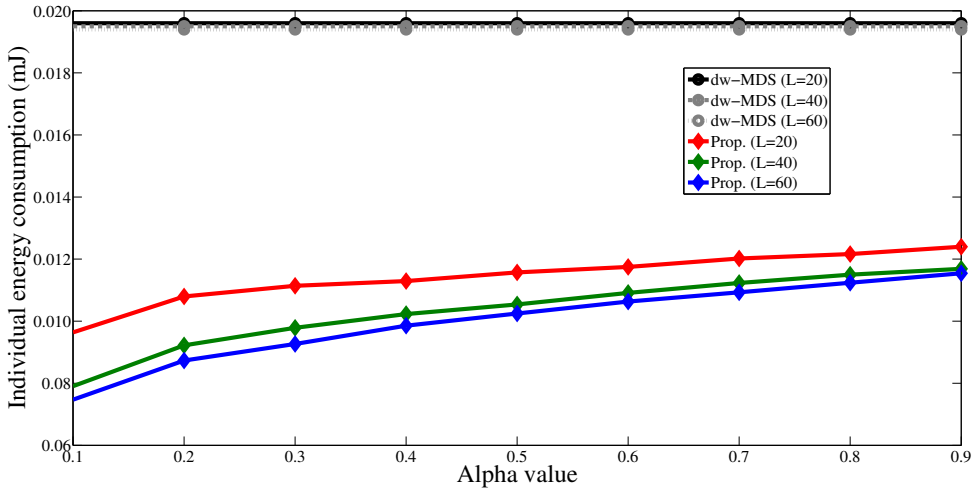

Figure 2.2: Individual energy consumption for localization versus α.

2.4 Simulation Results

I apply the proposed algorithm to the localization problem in a WSN. The dw-MDS [8] is chosen as the baseline algorithm for the analysis of the performance of dw-MDS combined with CRG. I demonstrate the performance of the proposed algorithm on the network with anchor nodes, $M = 4$, in a circle area with radius $R = 20$m. Set of sensors are randomly located in the same circle area. $P_{i,\text{min}}$ and $P_{i,\text{max}}$ are 0mW and 1mW, respectively, for all i. Thermal noise power is assumed by 1×10^{-18}mW. Further, the sensitivity level for the reception and correct demodulation P_{sen} is 1×10^{-9}mW. In addition, $n_p = 3$, $d_0 = 1$m, $\gamma_{0,\text{dB}}(\triangleq 10\log_{10}\gamma_0) = -35$dB, and $\sigma_{\text{dB}}(\triangleq 10\log_{10}\sigma) =$ 2dB. I run 200 Monte Carlo simulation trials to evaluate the proposed algorithm in terms of energy consumption and root mean square error (RMSE).

Figure 2.2 shows the trend lines of each algorithm in terms of individual energy consumption according to variation of α and L. Although CRG is an additional process in localization, it can ensure the efficiency of energy consumption. Naturally, $||\mathbf{P}^*||_1 \leq \sum_i P_{i,\text{max}}$. In addition, the number of iterations necessary for dw-MDS starting at $\mathbf{P}^*$ is almost the same as that of dw-MDS starting at full power transmis-

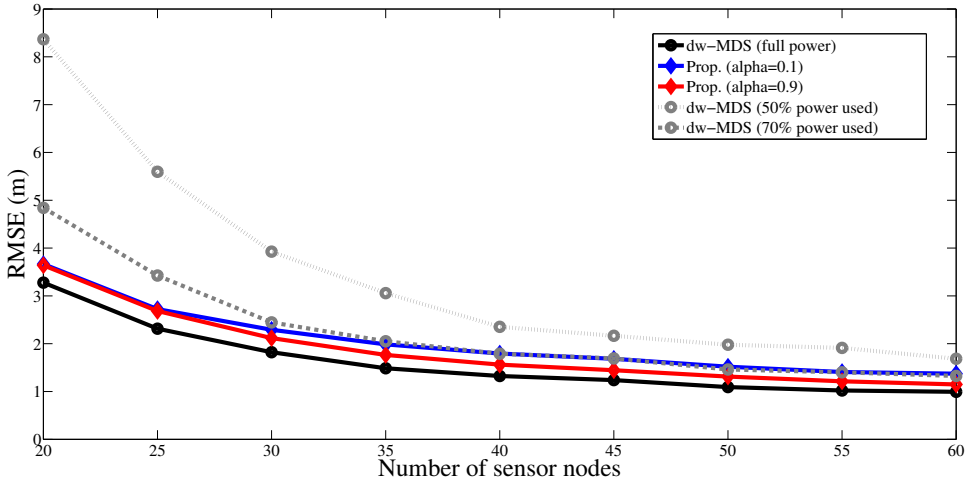

Figure 2.3: RMSE versus L.

sion. Further, energy consumption during finding NE, i.e. $||\mathbf{P}^{(0)}||_1 + \cdots + ||\mathbf{P}^*||_1$, is much smaller than the energy consumption for localization, because CRG converges to NE very fast. Iteration number of CRG converging to NE is only 1-2 on average. Assuming the transmit time interval is 1ms, each algorithm in terms of individual energy consumption is depicted in Figure 2.2. The difference in the individual energy consumption gains between baseline and proposed algorithms is around 50.8%-61.9% in the case of $\alpha = 0.1$ and 36.8%-41.1% in the case of $\alpha = 0.9$. In addition, CRG significantly changes the energy consumption according to variation of L. This is why, if density of sensor nodes is higher, each node easily gathers information about localization by virtue of a large number of neighboring nodes. Consequently, $\mathbf{P}^*$ would be smaller. It implies that CRG is suitable as a preprocess of distributed localization in highly dense and energy-limited system.

Next, I show how much damage is caused by the reduction of energy consumption through CRG to the performance of localization in Figure 2.3. RMSE is chosen as the metric of performance of localization, and it is defined as $(1/L)\sum_i \sqrt{(\mathbf{x}_i - \tilde{\mathbf{x}}_i)^{\mathrm{T}}(\mathbf{x}_i - \tilde{\mathbf{x}}_i)}$ where $\tilde{\mathbf{x}}_i$ is the estimated location of node i. The average RMSE margins between

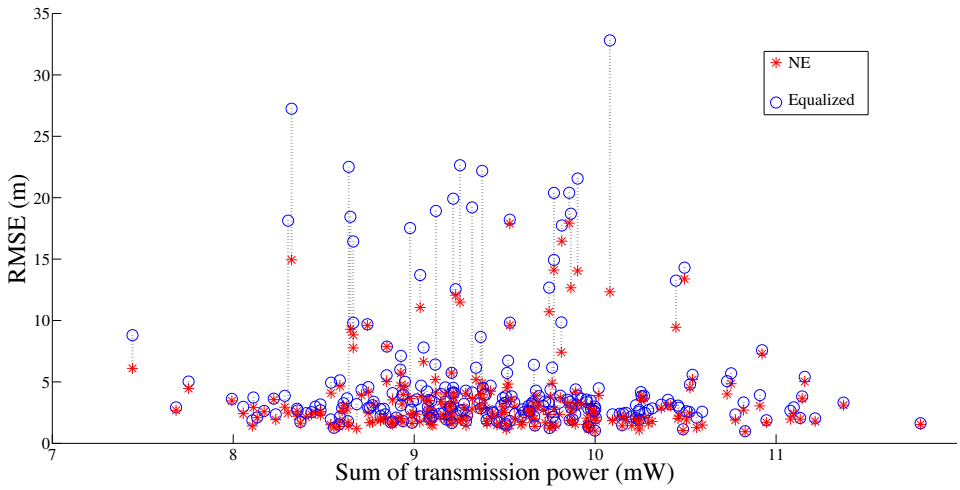

Figure 2.4: Comparison between $\mathbf{P}^*$ and $\tilde{\mathbf{P}}^*$ in terms of RMSE ($\alpha = 0.1$ and $L = 20$).

dw-MDS with full power transmission and that with CRG is only 0.43m in the case of $\alpha = 0.1$ and only 0.26m in the case of $\alpha = 0.9$. Further, I compare my algorithm to dw-MDS with each setting of $\mathbf{P}_{50\%} \triangleq \{0.5 \times P_{1,\max}, ..., 0.5 \times P_{L,\max}\}$ and $\mathbf{P}_{70\%} \triangleq \{0.7 \times P_{1,\max}, ..., 0.7 \times P_{L,\max}\}$. Although CRG allows for greater reduction of power consumption than dw-MDS with $\mathbf{P}_{70\%}$, they show similar levels of RMSE. The most interesting outcome is observed in the comparison between dw-MDS with CRG and $\mathbf{P}_{50\%}$. The average RMSE margins between dw-MDS with CRG and that with $\mathbf{P}_{50\%}$ is 1.40m if $\alpha = 0.1$ and 1.58m if $\alpha = 0.9$. It implies that CRG performs better in terms of energy consumption and localization error rather than equal power allocation by heuristic thresholds.

Figure 2.4 shows the effectiveness of CRG when the scenarios that set of sensor nodes have irregular geometric layouts, through comparison between $\mathbf{P}^*$ and $\tilde{\mathbf{P}}^*$ in terms of RMSE margin. $\tilde{\mathbf{P}}^*$ is defined as $\{\frac{\sum_i P_i^{\text{NE}}}{L}, ..., \frac{\sum_i P_i^{\text{NE}}}{L}\}$, which is an equalized form of $\mathbf{P}^*$. The RMSE margin on average in the entire simulation is 1.75m. Most significantly, the RMSE margin on average for the scenarios that have RMSE higher than 10m is 16.42m. It means that differential power allocation based on the state of sensor

node distribution is more efficient than equal power allocation while the performance in terms of reduction of power consumption is the same. Thus, my algorithm performs significantly well when sensor node distribution is irregular so that geographically isolated sensor nodes exist.

Chapter 3

APPLICATION OF EXACT POTENTIAL GAME: Adaptive Sector Coloring Game for Geometric Network Information based Inter-Cell Interference Coordination in Wireless Cellular Networks

3.1 Brief Introduction

I propose the ASCG and ASCG with a dominant strategy space (ASCG-D), which are new coordinated-distributed scheme that optimize GNI based ICIC problem. It is worth noting that ASCG-D requires smaller signaling overhead and computational load for ICIC implementation than the conventional dynamic ICIC schemes do and is robust with respect to the latency of X2 interface. Moreover, ASCG-D is an exact potential game, so it has the advantage of an NE solution always existing. Given that this study is conducted in a homogeneous cellular network, further studies are required for a heterogeneous cellular network including femtocells, relay cells, and picocells. Moreover, my study is expected to lead to interesting results when ASCG-D is combined with beamforming problems in massive multiple-input multiple-output (MIMO) cellular networks using millimeter-wave technology. The main symbols can be found in Table 3.1.

Table 3.1: List of symbols

$\mathcal{L}$	The set of eNBs (or cells)
$\mathcal{L}_{-l}$	The set of eNBs excluding the eNB l
κ^l	The sector set of the l-th cell
$\mathcal{M}^{l,k}$	The user set located in sector $\kappa_{l,k}$
$\mathcal{N}^{l,k}$	The RB set mapped into the sector $\kappa_{l,k}$
T_c	The shortest time-resolution
T_{X2}	The latency over the X2 interface
T_{su}	The strategy update period
T_{ud}	The longest time-resolution
$\mathbf{Y}^l$	The sector coloring matrix of cell l
$\mathbf{X}^{l,k}$	The user scheduling matrix of the k-th sector $\kappa_{l,k}$ of cell l
PG_l	Potential gain without considering interference
PI_l	Potential interference experienced by eNB l
$PI_{\mathcal{L}_{-l}}$	Potential interference generated by eNB l
U_l	The utility function of eNB l
$\aleph_l$	The total feasible strategy space of Y^l
$\aleph_l^D$	The dominant strategy space of Y^l

3.2 Network Model

3.2.1 System Preliminaries

I consider a downlink hexagonal cellular network with the eNB (or cell) set $\mathcal{L} \triangleq \{1, ..., L\}$ and the user set $\mathcal{M} \triangleq \{1, ..., M\}$. Each eNB is located at the center of each cell and have K sectors, where $\mathcal{K}^l \triangleq \{\mathcal{K}_{l,1}, ..., \mathcal{K}_{l,K}\}$ denotes the sector set of the l-th cell. The user subset $\mathcal{M}^{l,k} \subset \mathcal{M}$ is randomly located in the sector $\mathcal{K}_{l,k}$ by uniform distribution. To consider some load imbalance scenarios, I define the concentration factor $\lambda^l \triangleq$(number of users in the hot sector in the cell)/(number of users in the cell) where the hot sector is the most populated sector in the cell. For simplicity, the equal number of users are located in each cell and the concentration factor λ is applied to all cells such as $\sum_k |\mathcal{M}^{1,k}| = ... = \sum_k |\mathcal{M}^{L,k}| = M/L$ and $\lambda^1 = ... = \lambda^L = \lambda$, respectively. The set of eNBs $\mathcal{L}_{-l}$ is the set of eNBs excluding the eNB l from the eNB set $\mathcal{L}$.

Each eNB can communicate with other eNBs by using the X2 interface in LTE-A. The RB set is denoted as $\mathcal{N}$, and the system bandwidth is divided into N RBs as $|\mathcal{N}| = N$, where $|\cdot|$ implies the cardinality. Each RB is the smallest 2-D scheduling unit consisting of one subframe (=1 ms) and 12 subcarriers (=12×15 kHz). I assume that each eNB can utilize N RBs. P_l^n denotes the transmit power of the l-th eNB on the n-th RB. For simplification, I assume that each eNB allocate the equal power to each RBs, i.e., $P_l^n = P/N$ for all l and n, where P is the total transmit power of an eNB. At each instant, multiple RBs can be assigned to a single user; however, each RB can be assigned to at most one user. In this study, I assume an infinitely backlogged model; in other words, at each time instance, the eNB has data available for transmission to every user.

3.2.2 Determination of Time Policy

Assuming that T_c is the shortest time-resolution parameter of the entire network. It is related to the physical features changing fast, such as signal strength experiencing fast fading, SINR, and instantaneous achievable rate. On the other hands, T_{ud} is the longest time-resolution parameter of the entire network. They are related to the physical features changing slowly, such as the large-scale attenuation factors and geometric topology of the entire network. T_c and T_{ud} denote the minimum values among a set of individual channel coherence times and individual user distribution coherence times, respectively. Generally, the geometrical decorrelated distance is set to 50m in a system-level simulation [73]; hence, T_{ud} is taken as the time in which the user with the highest speed passes through the 50m distance. T_{X2} is the latency over the exchange of information among the eNBs, and I assume that $T_c \ll T_{\mathrm{X2}} \ll T_{ud}$.

3.2.3 Two-Stage Framework of RB Allocation

Let us define two RB allocation matrices. The sector coloring matrix of cell l, $\mathbf{Y}^l \in \aleph^l = \{0,1\}^{N\times K}$, represents a mapping the RB set $\mathcal{N}$ to the sector set of $\mathcal{K}^l$, where $\aleph^l$ is the set of all possible $\mathbf{Y}^l$. Further, $y^l_{n,k}$ is the n-th row and the k-th column element of $\mathbf{Y}^l$, and it is equal to 1 if RB n is assigned to sector $\mathcal{K}_{l,k}$ and 0 otherwise. These two constraints $\sum_k y^l_{n,k} \leq 1$ and $\sum_n \sum_k y^l_{n,k} \leq N$ should be satisfied. $\mathcal{N}^{l,k}$ is an RB subset that is mapped into the sector $\mathcal{K}_{l,k}$. Thus, $\sum_n y^l_{nk} = |\mathcal{N}^{l,k}|$. The set of sector coloring matrices in the entire network is $\mathbf{Y} = \mathbf{Y}^1 \times \cdots \times \mathbf{Y}^L \in \{0,1\}^{N\times K\times L}$. The set of sector coloring matrices $\mathbf{Y}$ optimize the feasible FDPS space according to every T_{ud}.

Similar to the sector coloring matrix $\mathbf{Y}^l$, the user scheduling matrix of the k-th sector $\mathcal{K}_{l,k}$ of the cell l, $\mathbf{X}^{l,k} \in \{0,1\}^{|\mathcal{N}^{l,k}|\times|\mathcal{M}^{l,k}|}$, represents a mapping $\mathcal{N}^{l,k}$ to $\mathcal{M}^{l,k}$ by the eNB l. $x^{l,k}_{nm}$ is the n-th row and the m-th column element of $\mathbf{X}^{l,k}$, and it is equal to 1 if RB n is assigned to user m and 0 otherwise. Two constraints $\sum_k x^{l,k}_{nm} \leq 1$ and $\sum_n \sum_k x^{l,k}_{nm} \leq |\mathcal{N}^{l,k}|$ should be satisfied.

3.3 PROBLEM FORMULATION: Geometric Network Information based ICIC

3.3.1 Outline

Naturally, the performance of[1] $\mathbf{X}^{l,k}$ is considerably dependent on the set of sector coloring matrices $\mathbf{Y}$. Given $\mathbf{Y}$, the user scheduling matrix $\mathbf{X}^{l,k}$ optimizes the general objective function of FDPS, such as maximizing $\sum_{m \in \mathcal{M}^{l,k}} \log(R_m)$ where R_m is the long-term service rate of user m, during the time resolution T_c. A well-formulated problem for optimizing the set of sector coloring matrices $\mathbf{Y}$ depends on which physical channel features are selected as the variables of optimization problem. Further, the time-correlation property of the variables of optimization problem determine how frequently $\mathbf{Y}$ has to be optimized. In this study, I use the GNI, which is the newly defined substitute for CSI, as the optimization variable to optimize the set of sector coloring matrices $\mathbf{Y}$. Let us establish the optimization problem through three questions. i) What is the GNI? ii) Why do I choose the GNI, and not CSI? iii) How do I formulate the utility function through the GNI?

3.3.2 What Is the GNI?

GNI is the indicator of geometric information related to the eNBs and users. I denote the absolute locations of the eNB l and user m to $G(l)$ and $G(m)$, respectively. Further, $\mathbf{G}(\mathcal{L}) = \{[G(l)]\}^{L \times 1}$ and $\mathbf{G}(\mathcal{M}) = \{[G(m)]\}^{M \times 1}$ are geometric information vectors of the eNB set $\mathcal{L}$ and the entire user set $\mathcal{L} = \bigcup_l \bigcup_k \mathcal{L}^{l,k}$, respectively. By the definition of T_{ud}, I assume that $\mathbf{G}(\cup_k \mathcal{M}^{l,k})$ is estimated by the eNB l and every eNB exchange the estimated GNI of users each other at every T_{ud}.

[1] In [16], the authors proved that the optimal solution of FDPS, $\mathbf{X}^{l,k}_{opt}$, is NP-hard. They also obtained the suboptimal solution $\mathbf{X}^{l,k}_{1/2}$, which guarantees more than a half of $\mathbf{X}^{l,k}_{opt}$ in terms of the performance of FDPS, by an approximation algorithm in polynomial time. By virtue of this contribution, I use this algorithm in the user scheduling phase and focus on the sector coloring phase for the ICIC problem.

3.3.3 Temporal Perspective: Why GNI?

The global knowledge of CSI is the best choice as the variable of optimization problem. However, in a system that has X2 interface latency, such as an LTE-A system, this choice results in some temporal disadvantages. These disadvantages are much more critical in high-mobility scenarios. Based on the time-correlation properties, the global CSI should be updated in every T_c, but GNI should be updated in every T_{ud}. I can exploit three temporal benefits by virtue of this property: i) relaxation of time restriction for optimization, ii) reduction of signaling overhead, and iii) insensitivity to the X2 interface latency T_{X2}. Then, let us consider how I achieve optimization by using only GNI instead of the global knowledge of CSI.

3.3.4 Spatial Perspective: How do I Design a Suitable Utility Function?

Despite several merits of the temporal perspective, an appropriate objective with spatial consideration is necessary. Designing the utility function by using GNI, I need new concepts of potential gain and suffered/suffering interference for optimizing the GNI based ICIC by sector coloring. Potential gain and suffered/suffering interference are determined by the function of both $\mathbf{Y}$ and $\mathbf{G}(\mathcal{L};\mathcal{M})$. The performance of sector coloring is judged by how much potential gain and interference have occurred.

If a user m is associated with the eNB l, the closer the user m comes to the boresight and the absolute location of the the eNB l, the higher desired signal power the user m receives. On the other hand, if the user m is not associated with the eNB l, the closer the user m comes to the boresight and the absolute location of eNB l, the higher interference signal power the user m receives. Thus, each eNB tries to find the optimal sector coloring matrix for not only maximizing their potential gain, but also minimizing the two types of potential interference. The potential gain and interference concepts summarized in Figure 3.1 are concretely explained as follows:

- Potential gain (PG_l): This is the concept that the eNB l considers taking advan-

tage of only the user set of the cell l, $\mathcal{M}^l\Big(= \bigcup_{k=1}^{K} \mathcal{M}^{l,k}\Big)$, while not considering the interaction between $\mathbf{Y}^l$ and $\mathbf{Y}^{\mathcal{L}_{-l}}(\triangleq \mathbf{Y} \setminus \mathbf{Y}^l)$. PG_l is the function of $\mathbf{G}(l; \mathcal{M}^l)$ and $\mathbf{Y}^l$. PG_l consists of three pieces of information. The first piece of information is the set $\{|\mathcal{M}^{l,1}|, ..., |\mathcal{M}^{l,K}|\}$. The second piece of information is the distance between the eNB l and user $m \in \mathcal{M}^{l,k}$. The third piece of information is the concentration of the user set $\mathcal{M}^{l,k}$ on the line of boresight direction to sector $\mathcal{K}_{l,k}$. The concept of potential gain is effective in maximizing the system throughput in the single cell scenario. However, there are many uncoordinated sources of interference causing degradation of the system throughput, because potential gain does not consider the interaction between $\mathbf{Y}$ and $\mathbf{Y}^{\mathcal{L}_{-l}}$.

• Suffered potential interference (PI_l): It is an estimated interference of users in the target cell l by other eNBs. To avoid interference, the eNB l is to receive the information on $\mathbf{Y}^{\mathcal{L}_{-l}}$ of other eNBs through the X2 interface. All eNBs share sector coloring information with each other. After receiving the information on $\mathbf{Y}^{\mathcal{L}_{-l}}$ of other eNBs, the eNB l determines the optimal $\mathbf{Y}^l$ for avoiding interference and maximizing the potential gain. Thus, PI_l, the potential interference experienced by the target cell l, is the function of $\mathbf{G}(\mathcal{L}_{-l}; \mathcal{M}^l)$ and $\mathbf{Y}$. Even though the throughput of user set $\mathcal{M}^l$ would increase by this interference coordination, this kind of selfish sector coloring causes the degradation of the throughput of users of adjacent cells.

• Suffering potential interference ($PI_{\mathcal{L}_{-l}}$): $PI_{\mathcal{L}_{-l}}$ is the function of $\mathbf{G}(l; \mathcal{M}^{\mathcal{L}_{-l}})$ and $\mathbf{Y}$, where $\mathcal{M}^{\mathcal{L}_{-l}} \triangleq \mathcal{M} \setminus (\mathcal{M}^l)$. From the network-level perspective, the information on the user distribution in other cells is utilized for predicting how much the current $\mathbf{Y}^l$ aggravate the performance of other cells.

Considering the above cause-and-effect relationship, let us define the formulae for the potential gain and interference as follows.

Definition 2. Potential gain, suffered potential interference, and suffering potential interference.

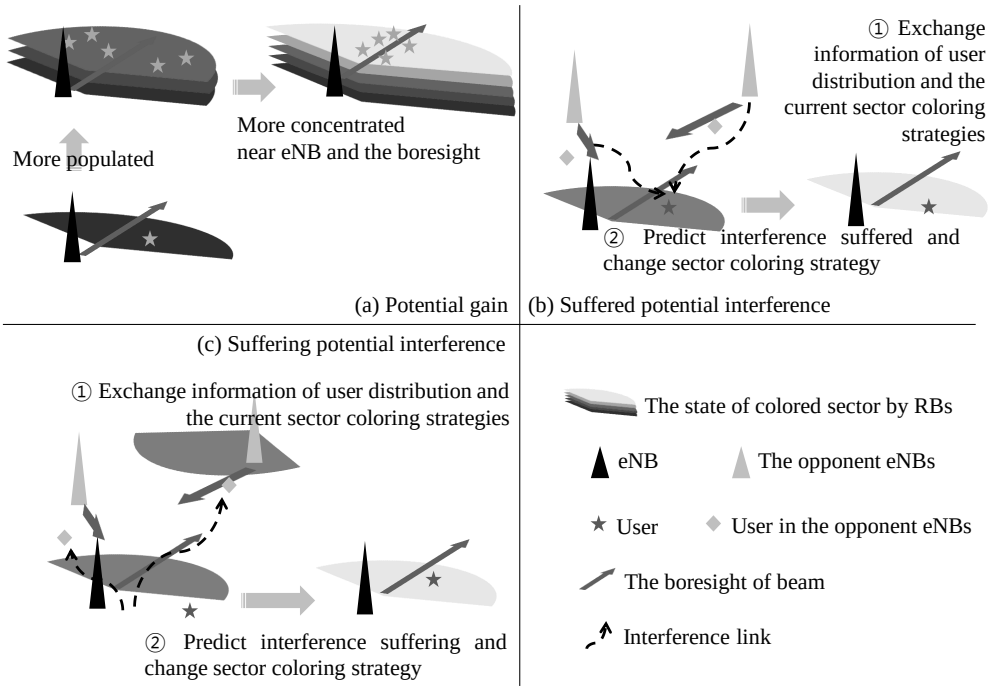

Figure 3.1: Concepts of potential gain and suffered/suffering interference.

$$
\begin{aligned}
&PG_l\big(\mathbf{G}(l;\mathcal{M}^l),\mathbf{Y}^l\big) \triangleq \sum_{n\in\mathcal{N}}\sum_{k\in\mathcal{K}^l}\Big[y^l_{nk}\cdot\sum_{m\in\mathcal{M}^{l,k}}(\gamma_l\\
&+P^n_l+\bar{h}+\phi^n_{l,m}-\mu_{l,m}-s_{l,m})\Big],\\
&PI_l\big(\mathbf{G}(\mathcal{L}_{-l};\mathcal{M}^l),\mathbf{Y}\big) \triangleq\\
&\sum_{j\in\mathcal{L}_{-l}}\sum_{n\in\mathcal{N}}\sum_{k\in\mathcal{K}^l}\Big[y^l_{nk}\cdot PG_j\big(G(j;\mathcal{M}^{l,k}),\mathbf{Y}^j\big)\Big],\\
&PI_{\mathcal{L}_{-l}}\big(\mathbf{G}(l;\mathcal{M}^{\mathcal{L}_{-l}}),\mathbf{Y}\big) \triangleq\\
&\sum_{j\in\mathcal{L}_{-l}}\sum_{n\in\mathcal{N}}\sum_{k\in\mathcal{K}^j}\Big[y^j_{nk}\cdot PG_l\big(G(l;\mathcal{M}^{j,k}),\mathbf{Y}^l\big)\Big].
\end{aligned}
\tag{3.1}
$$

Recalling that P^n_l is the transmit power of the eNB l on RB n and T_{ud} is sufficiently larger than T_c, I can approximate the useful signal power received by the user m from

the eNB l on RB n as the term $(P_l^n + \bar{h} + \phi_{l,m}^n - \mu_{l,m} - s_{l,m})$ in the above equation for the potential gain PG_l in dB scale. This approximation can be applied to the interference signal. $\bar{h}$ captures the time-averaged value of fast-fading (due to the Doppler shifts and the superposition of each multipath components) effects during the period T_{ud}. This fast-fading effect is assumed by Rayleigh distribution. The mean value of normalized Rayleigh fading is $\sqrt{\frac{\pi}{2}}$. Thus, I choose $\bar{h}$ as $10 \cdot \log_{10}\sqrt{\frac{\pi}{2}} \simeq 0.9806$ in dB scale, which is independent of RB n, because the fast-fading effects on each RB n has the same stochastic process. According to the number of sectors, the antenna gain is represented as $\phi_{l,m}^n = -\min[12\left(\frac{\theta_{l,m}}{\theta_{\text{3dB}}}\right), A_{\text{max}}]$ where $\theta_{\text{3dB}} = 70\,\text{deg}$, $A_{\text{max}} = 20$dB in the three-sector case, $\theta_{\text{3dB}} = 35\,\text{deg}$, $A_{\text{max}} = 23$dB in the six-sector case and $-180 \leq \theta < 180$ [73]. $\theta_{l,m}$ is defined as the angle between the boresight of sector antenna and the LOS direction between the eNB l and the user m. The boresight is defined to be the direction at which the beam shows the maximum antenna gain. The pathloss gain is given by $\mu_{l,m} = 128.15 + 37.6\text{log}(d_{l,m})$, where $d_{l,m}$ is the distance between the eNB l and the user m measured in km [73]. $s_{l,m}$ is the shadowing factor from the eNB l to the user m. This factor should be calculated by eNB l's geometric grid with appropriate spatial correlation [73]. Observing the statistics of the approximated signal power, I set γ_l as the threshold for regulating the proper calculations of potential gain and interference. The regulation threshold γ_l according to user m satisfies the following conditions.

$$\begin{cases} \gamma_l + P_l^n + \bar{h} + \phi_{l,m}^n - \mu_{l,m} - s_{l,m} \geq 0, & \text{if } m \in \mathcal{M}^l. \\ \gamma_l + P_l^n + \bar{h} + \phi_{l,m}^n - \mu_{l,m} - s_{l,m} < 0, & \text{otherwise.} \end{cases} \tag{3.2}$$

I choose the regulation threshold γ_l as the term $(-P_l^n - \bar{h} + A_{\text{max}} + \bar{\mu})$, where $\bar{\mu} = 128.15 + 37.6\text{log}(R)$ and R is the fixed cell-radius. This regulation threshold implies that a proper cell-breathing algorithm controlling γ_l can solve the load balancing problem. However, in this study, I assume $\gamma_l = \gamma_j$, where $\forall l, j \in \mathcal{L}$, for focusing on ICIC. For simplicity, if there are two or more eNBs satisfying the condition (4.7) on the user m, the user m is associated to an eNB which has the maximum approximated signal power.

By integration of PG_l, PI_l, and $PI_{\mathcal{L}_{-l}}$, the utility function of the eNB l, $U_l\Big(\mathbf{G}(l;\mathcal{M}),\mathbf{Y}\Big)$, is defined as

$$U_l\Big(\mathbf{G}(l;\mathcal{M}),\mathbf{Y}\Big) = PG_l\Big(\mathbf{G}(l;\mathcal{M}),\mathbf{Y}^l\Big) - PI_l\Big(\mathbf{G}(\mathcal{L}_{-l};\mathcal{M}^l),\mathbf{Y}\Big) - PI_{\mathcal{L}_{-l}}\Big(\mathbf{G}(l;\mathcal{M}^{\mathcal{L}_{-l}}),\mathbf{Y}\Big). \tag{3.3}$$

3.3.5 GNI based ICIC Problem

By virtue of the proposed temporal and spatial considerations, the proposed optimization problem is defined as follows.

P1. GNI based ICIC The final objective is to find the optimal sector coloring $\mathbf{Y}^*$ that maximize $\sum_{l=1}^{L} U_l\Big(\mathbf{G}(l;\mathcal{M}),\mathbf{Y}\Big)$ in a relaxed time restriction such as the period T_{ud}.

This is a new ICIC problem based on GNI with temporal and spatial consideration. Let us optimize this problem by game theoretic approach based the coordinated-distributed scheme in Section IV.

3.4 ADAPTIVE SECTOR COLORING GAME

3.4.1 Design of ASCG

I will examine the effectiveness of the GNI based ICIC by optimizing the set of the sector coloring matrices $\mathbf{Y}$ under given $\mathbf{G}(\mathcal{L};\mathcal{M})$ during the period T_{ud}. Although the optimization problem **P1** defined in the previous section can be solved in a centralized fashion, it is a rather complex task for all eNBs or the radio network controller (RNC) to determine the optimal sector coloring $\mathbf{Y}^*$ simultaneously. The size of total search space for optimizing $\mathbf{Y}$ is $(K^N)^L$ in the centralized scheme. Therefore, I try to design the best response game for implementing the coordinated-distributed scheme with desirable X2 interface utilization, called ASCG, which finds a suboptimal solution of **P1**.

The definition of ASCG is as follows.

Definition 3. ASCG: $< \mathcal{L}, \aleph_l, \{U_l\}_{l \in \mathcal{L}} >$

i) Player set: $\mathcal{L} = \{1, ..., l, ..., L\}$ (eNB set)

ii) Strategy of player l: $\mathbf{Y}^l \in \aleph_l$

iii) Utility of player l: $U_l(\mathbf{G}(l; \mathcal{M}), \mathbf{Y})$

Based on the temporal characteristics of GNI, **P1** is periodically updated every T_{ud}. Then, every eNB sequentially and autonomously tries to find the suboptimal solution of **P1** by implementing ASCG. Let us define the strategy update period T_{su} as the sum of the signaling latency period T_{X2} and the calculation period in which the eNB l searches for the local optimal $\mathbf{Y}^l_* \triangleq \mathrm{argmax} U_l(\mathbf{G}(l; \mathcal{M}), \mathbf{Y})$ in the current state of the fixed strategies of other eNBs $\mathbf{Y}^{\mathcal{L}_{-l}}$. Strategy $\mathbf{Y}^l$ of the player l (or the eNB l) is an element of the total feasible strategy space $\aleph_l$, where $|\aleph_l| = K^N$. I assume $T_c \ll T_{\mathrm{X2}} < T_{su} \ll T_{ud}$. Therefore, let us determine $\mathbf{Y} \triangleq \times_{l \in \mathcal{L}} \mathbf{Y}^l$ which is the suboptimal solution of **P1**, while the game proceeds by each player sequentially to update the strategy of each player by round-robin rule according to every T_{su} and autonomously to maximize its individual utility $U_l(\mathbf{Y})$ searching for the best response strategy depending on the strategy of other players.

1) Strategy update policy: The strategy update policy of ASCG is that each player updates its strategy in a predetermined order. For each iteration, players update their strategies by following the round-robin rule. The players compute their own utility in their own turn and update their strategy as follows.

$$\begin{aligned} &\mathbf{Y}^l[i_{su}] \leftarrow \mathbf{Y}^l_*[i_{su}] \triangleq \mathrm{argmax} U_l(\mathbf{Y}[i_{su} - 1]), \\ &\mathbf{Y}^{\mathcal{L}_{-l}}[i_{su}] \leftarrow \mathbf{Y}^{\mathcal{L}_{-l}}[i_{su} - 1], \\ &\text{where the time index } i_{su} = L \times q + l \text{ and } q = 0, 1, 2, \cdots . \end{aligned} \tag{3.4}$$

2) Meaning of NE of ASCG: To obtain the suboptimal solution of **P1** by ASCG, let us define the NE of ASCG as follows.

Table 3.2: Minimization of number of cases of brute force search

i) Extraction of the dominant feasible strategy space
$\aleph_l^D\Big(\Im_{PS}(\aleph_l) = \{\aleph_l^1, ..., \aleph_l^{ps}, ..., \aleph_l^{PS}\}\Big)$ satisfying (3.5).
ii) Selection of the sector coloring strategy
$\mathbf{Y}_{*,D}^l\Big(\in \aleph_l^D\Big) \triangleq \text{argmin}[PI_l + PI_{\mathcal{L}_{-l}}]$.

Definition 4. NE of ASCG A given strategy $\mathbf{Y}_*$ is an NE of ASCG, if I have $U_l(\mathbf{Y}_*) = U_l(\mathbf{Y}_*^l; \mathbf{Y}_*^{\mathcal{L}_{-l}}) \geq U_l(\mathbf{Y}^l; \mathbf{Y}_*^{\mathcal{L}_{-l}})$ for all l.

At an NE, no player is able to improve its utility with a unilateral deviation. The NE is the state that all players are satisfied, and there is no more update until next update of GNI. Convergence to NE of ASCG means determination of an ideal static ICIC state through GNI based ICIC. It also means that every eNB set $\mathcal{L}$ need not change the sector coloring strategies until next update of GNI. In the following subsection, I introduce ASCG with a dominant strategy space noted as ASCG-D. The dominant strategy space $\aleph_l^D$ result in the reduction of the solution search space of ASCG and guarantee the existence of at least one NE by demonstrating that ASCG-D is an exact potential game.

3.4.2 ASCG with a Dominant Strategy Space

Although the complexity of the original ICIC problem is reduced by virtue of ASCG, the update of the best response strategy $\mathbf{Y}_*^l$ for ASCG is also challenging because of the exponentially expanding solution space. Moreover, I need to minimize this subsidiary complexity to guarantee a complexity level similar to those of conventional static ICIC schemes, which do not have any subsidiary complexity for the ICIC process. For an eNB l, there are K^N different ASCG strategies in the total feasible strategy space $\aleph_l$. In practical systems, K is generally equal to 3 or 6. However, the number of RBs N can be quite large.

Let us minimize the number of cases of brute-force search by reducing the total

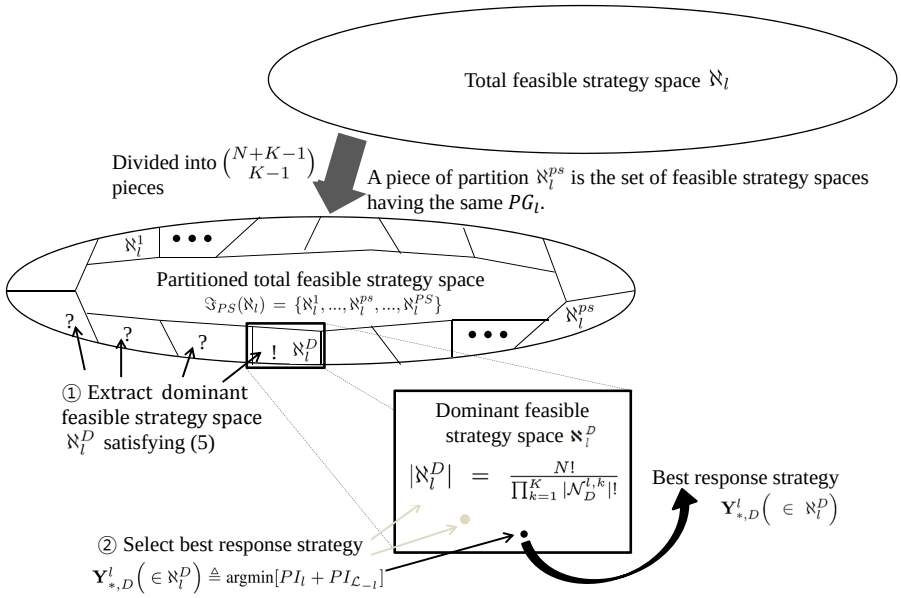

Figure 3.2: Process of minimizing number of cases of brute-force search in ASCG.

feasible strategy space $\aleph_l$ to the dominant feasible strategy space $\aleph_l^D$. My intuition is that a proper divide-and-conquer method using the property of the potential gain can drastically reduce the number of cases requiring a brute-force search for finding the best response in the total feasible strategy space. Before describing $\aleph_l^D$, let us discuss an interesting property of the potential gain.

Property 1. Homeostasis of potential gain For two different sector coloring matrices $\mathbf{Y}^l$ and $\tilde{\mathbf{Y}}^l$ with $|\mathcal{N}^{l,k}| = |\tilde{\mathcal{N}}^{l,k}|$ for $\forall k$, $PG_l(\mathbf{Y}^l) = PG_l(\tilde{\mathbf{Y}}^l)$ is always satisfied.

The potential gain PG_l of the eNB l is independent of the strategy $\mathbf{Y}^{\mathcal{L}_{-l}}$ of other players. Additionally, frequency-selective characteristic according to RBs is not reflected in the potential gain PG_l. Therefore, the potential gain PG_l is only dependent

on the cardinal number set $\{|\mathcal{N}^{l,1}|, ..., |\mathcal{N}^{l,K}|\}$. By virtue of Property 1, I add constraint (3.5) to the process to determinate the best-response strategy $\mathbf{Y}_*^l$ for reducing the total feasible strategy. [2] If $w_{l,k} = \sum_{n\in\mathcal{N}^{l,k}}(y_{nk}^l \cdot \sum_{m\in\mathcal{M}^{l,k}}(\gamma_l + (P_l^n + \bar{h} + \phi_{l,m}^n - \mu_{l,m} - s_{l,m})))$, I impose the constraint for each player l as

$$
\begin{aligned}
&|\mathcal{N}^{l,1}| = \lceil N \cdot \frac{w_{l,1}}{\sum_{k\in\mathcal{K}^l} w_{l,k}} \rceil, |\mathcal{N}^{l,2}| = \lceil N \cdot \frac{w_{l,2}}{\sum_{k\in\mathcal{K}^l} w_{l,k}} \rceil, ..., \\
&|\mathcal{N}^{l,K}| = N - \sum_{k=1}^{K-1} |\mathcal{N}^{l,k}|, \\
&\qquad \text{where } \lceil\cdot\rceil \text{ represents the ceiling operation.}
\end{aligned} \tag{3.5}
$$

Let us define $\Im_{PS}(\aleph_l) = \{\aleph_l^1, ..., \aleph_l^{ps}, ..., \aleph_l^{PS}\}$ as a partition of the feasible strategy space $\aleph_l$, where the partition number is PS and a section of partition $\aleph_l^{ps}$ is the set of possible strategies $\mathbf{Y}^l$ that have the same $PG_l = \sum_{k\in\mathcal{K}^l} w_{l,k}$. To minimize the number of cases of brute-force search, a two-step process is followed as explained in Table 3.2. Henceforth, I refer to the ASCG with the dominant feasible strategy space $\aleph_l^D$ as ASCG-D.

The solution space for extracting $\aleph_l^D$ is $|\Im_{PS}(\aleph_l)| = PS = \binom{N+K-1}{K-1}$ (Appendix A). After $\aleph_l^D$ has been determined, the best response strategy $\mathbf{Y}_{*,D}^l\Big(\in \aleph_l^D\Big)$ that minimizes $[PI_l + PI_{\mathcal{L}_{-l}}]$ is selected. Further, $|\aleph_l^D| = \frac{N!}{\prod_{k=1}^K |\mathcal{N}_D^{l,k}|!}$ (Appendix B), where $\mathcal{N}_D^{l,k}$ is the RB subset that is mapped into the sector $\mathcal{K}_{l,k}$ by a sector coloring strategy $\mathbf{Y}^l \in \aleph_l^D$. Based on the definition of dominant feasible strategy space $\aleph_l^D$, $|\mathcal{N}_D^{l,k}|$ is not changed, if $\mathbf{Y}^l$ is selected in $\aleph_l^D$. Through this two-step process, the number of cases of brute-force search K^N is drastically reduced to $\left(\binom{N+K-1}{K-1} + \frac{N!}{\prod_{k=1}^K |\mathcal{N}_D^{l,k}|!}\right)$. The process of minimizing the number of cases of brute-force search is shown in Figure 3.2.

[2] In special geometric conditions, such as the case of hot sectors in each cell geometrically concentrated, potential interference mitigation for cell-edge users by ASCG might aggravate the performances of multiuser diversity gain and user fairness. By constructing this heuristic and compulsory constraint (3.5), ASCG-D can keep the fixed and reasonable values of multiuser diversity gain and user fairness.

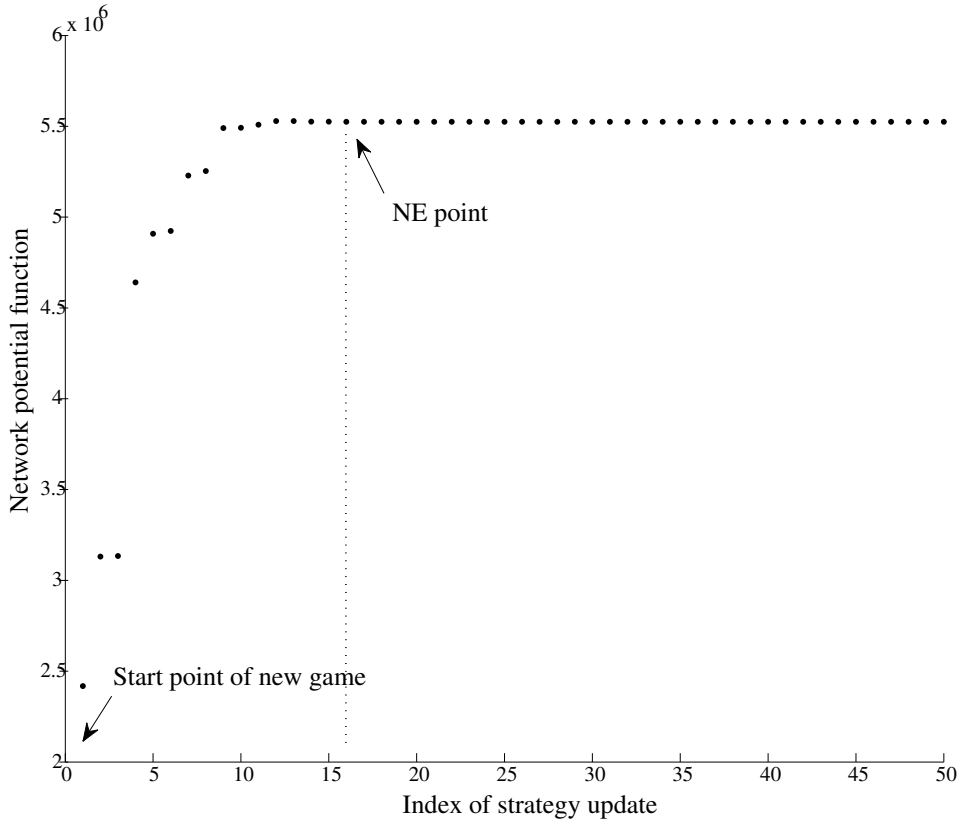

Figure 3.3: Improvement path of ASCG-D in one-drop ($L = 7, M = 140, N = 25, K = 3, P = 43\mathrm{dBm}$, and detailed parameter settings are described in section 3.5).

Moreover, I will show that ASCG-D is an exact potential game to show its guarantee of the existence of the NE. The representative characteristic of the exact potential game is that there always exists the pure-strategy NE when the corresponding players play with the sequential best-response dynamics. For any two different strategies $\mathbf{Y^1}$ and $\tilde{\mathbf{Y}}^l$, ASCG-D is an exact potential game if and only if there exists the network potential function $F(\mathbf{Y})$ satisfying the following condition.

Condition 1. Network potential function of ASCG-D If an eNB l changes its strategy from $\mathbf{Y}^l$ to $\tilde{\mathbf{Y}}^l$ while $\mathbf{Y}^{\mathcal{L}_{-l}}$ remains unchanged, then

$$U_l(\tilde{\mathbf{Y}}^l; \mathbf{Y}^{\mathcal{L}_{-l}}) - U_l(\mathbf{Y}^l; \mathbf{Y}^{\mathcal{L}_{-l}}) = F(\tilde{\mathbf{Y}}^l; \mathbf{Y}^{\mathcal{L}_{-l}}) - F(\mathbf{Y}^l; \mathbf{Y}^{\mathcal{L}_{-l}}). \tag{3.6}$$

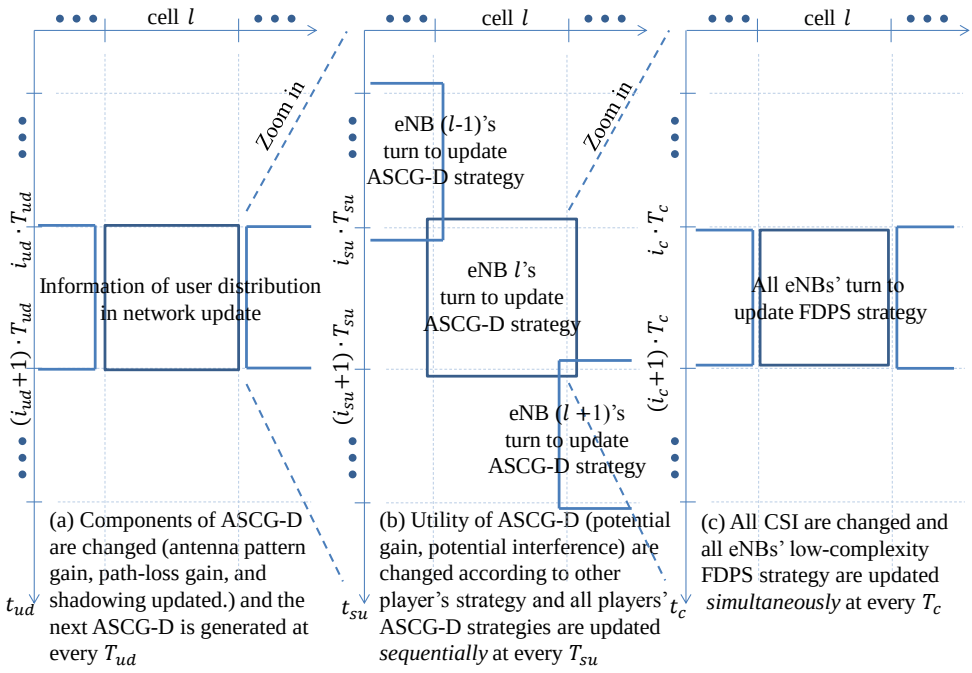

Figure 3.4: Framework of ASCG-D and FDPS.

Basically, this condition means that the change in a single player's utility due to only its own strategy deviation results in exactly the same amount of change in the exact potential function. I can verify that ASCG-D is an exact potential game if the network potential function $F(\mathbf{Y})$ is $\frac{1}{2}\sum_{l=1}^{L} U_l(\mathbf{Y})$. The corresponding proof is represented in Appendix C. The improvement path of network potential function $F(\mathbf{Y}^l; \mathbf{Y}^{\mathcal{L}-l})$ of ASCG-D according to every T_{su} of an example one-shot game is shown in Figure 3.3. I can see that as eNBs run ASCG-D, the improvement path of network potential function monotonically increases until the algorithm converges after only 16 steps, i.e., around 2 decisions of best-response strategy per player on average.

Theoretically, according to [72], the length of the improvement path converging to NE is at most L^2 using the best response dynamics in L-player game. This convergence speed implies that the computational complexity for optimizing $\mathbf{Y}$ by means

of the brute-force search, $O((K^N)^L)$, is drastically reduced to $O(L^2 \cdot \left(\binom{N+K-1}{K-1} + \frac{N!}{\prod_{k=1}^{K} |\mathcal{N}_D^{l,k}|!}\right))$. Thus, ASCG-D is a suitable suboptimal approach of **P1** by virtue of the guarantee of NE as well as the reduction of the feasible strategy space $\aleph_l$ to $\aleph_l^D$.

Algorithm 3.2 Implementation of ASCG-D and FDPS

Initialize the time index to form an expression ($i_{ud} = i_{su} = i_c = 0$, where i_{ud} and i_c is the time index related to T_{ud} and T_c, respectively).

User distribution updated and new ASCG-D generated at the time $i_{ud}T_{ud}$.

Establish the geometric loadmap $\mathbf{G}(\mathcal{L})$ and $\mathbf{G}(\mathcal{M})$ by exchanging GNI each other.

[ASCG-D part]

while $i_{ud}T_{ud} \leq i_{su}T_{su} < (i_{ud}+1)T_{ud}$ or until convergence to NE **do**

Pick player l according to the round-robin rule.

Player l extracts the dominant feasible strategy space $\aleph_l^D \in \aleph_l$ and solve the best-response strategy $\mathbf{Y}_{*,D}^l \in \aleph_l^D$.

Player l broadcasts $\mathbf{Y}_{*,D}^l$ to the other players through X2 interface during T_{X2}.

[FDPS part]

while $i_{su}T_{su} \leq i_cT_c < (i_{su}+1)T_{su}$ **do**

Given $\mathbf{Y}$, all player l solve the $\mathbf{X}_{1/2}^{l,k}$ by using the approximation algorithm [16].

Set $i_c \leftarrow i_c + 1$

end while

Set $i_{su} \leftarrow i_{su} + 1$

end while

Set $i_{ud} \leftarrow i_{ud} + 1$ and repeat steps 2-15.

3.4.3 Summary of System Operation

A summary of the overall algorithm for implementation of ASCG-D and FDPS is presented in Algorithm 3.2. Through sector coloring determined by ASCG-D, the sub-optimal FDPS space $\mathbf{Y}_*$ are achieved. During the time period T_{su}, the suboptimal

solution of $\mathbf{X}_{1/2}^{l,k}$ is solved $\lfloor \frac{T_{su}}{T_c} \rfloor$ times with fixed sector scheduling $\mathbf{Y}_*$ by ASCG-D, where $\lfloor \cdot \rfloor$ represents the flooring operation. The overall system operation over time is shown in Figure 3.4. Figure 3.4(a) shows the process of a new ASCG-D generated at every T_{ud}. Figure 3.4(b) shows the operation of an ASCG-D in which is every player sequentially updates its ASCG-D strategy to maximize its utility function at every T_{su}. Finally, Figure 3.4(c) shows the simultaneous operation of FDPS at every T_c.

3.5 PERFORMANCE EVALUATION

3.5.1 Simulation Settings and Baselines for Comparison

This section presents a system-level simulation performed for validating my proposed schemes. During the simulation, the users move by a random walk process with an arbitrary speed chosen among 3, 30, and 180 km/h. I use a simple handover method based on signal power for focusing the performance related to the ICIC problem. I set the handover margin to 8 dB. Specifically, the handover period is set to exactly the same value as T_{ud} to maintain the state of user association while operating my proposed algorithms. I run 500 Monte Carlo simulation trials and the runtime of each simulation trial is 2000 subframes. The detailed simulation assumptions are outlined in Table 3.3.

I choose the dynamic ICIC schemes (CSI based ICIC (global optimal), fractional graph coloring (FGC), and interference minimization game (IMG)) as well as the static ICIC schemes (reuse-1, reuse-3, PFR) as the baselines for the analysis of the performance of a GNI based ICIC (optimal of P1) and ASCG-D (suboptimal of P1). FGC and IMG are the conventional graph and game, respectively, theoretic approaches for the dynamic ICIC solution. To implement the FGC, I set delay time $T_{c,de}$, which contains various delays such as signaling, processing, and synchronization, to 200 ms and the update period $T_{c,period}$ to 1000 ms. Consequently, the solution of FGC continues during every 800 ms window ($T_{c,period} - T_{c,de}$). The initial state of FGC is set to reuse-

Table 3.3: System simulation parameters

Parameter	Value
Cellular layout	7 eNBs (or cells), 3 sectors per cell
Carrier frequency	2 GHz
System bandwidth/RB bandwidth	5 MHz / 180 kHz (Downlink)
Number of RBs	25
Subcarriers per RB	12
Cell-level user distribution	concentrated ($\lambda = 0.6$)
Inter-site distance (ISD)	500 m
eNB Tx power	43 dBm
Number of users per cell	20
Number of users in system	140
Scheduler	FDPS
Thermal noise	-174dBm/Hz
Channel	Rayleigh fading
Pathloss model	As in 3GPP TS 36.814 V9.0.0
Standard deviation of shadowing	8 dB
The decorrelated distance	50 m
User speed	3, 30, 180 km/h
Transmit time interval (TTI)	1 ms
T_c / T_{X2} / T_{su} / T_{ud}	1 ms / 10 ms / 20 ms / 1000 ms
Handover margin / period	8dB / 1000 ms
Traffic model	Full buffer
Observation time	2000 ms

1. The solution of FGC is obtained by means of the suboptimal heuristic Dsatur like in [30]. In addition, I have added the interference minimization game (IMG) in [39] as a conventional game theoretic approach. I set IMG's initial strategy to reuse-1. I also set RB utilization to 15 to overcome the limitation of IMG in which players select any RBs to avoid interference, which is also mentioned in [39]. In IMG, each player sequentially selects the best 15 RBs with respect to minimizing the sum of the total interference the corresponding player receives from the environment and the total interference generated by the player that is contributed to the environment. Like in ASCG-D, T_{su} and T_{ud} are adapted to IMG as the strategy update period and game generation period, respectively.

I evaluate the system performance in terms of the following parameters: the SINR distribution, system throughput, user fairness, signaling overhead, and computational load.

3.5.2 SINR Distribution and Average User Throughput

In Figure 3.5, I demonstrate an example of one-shot game to examine the average user SINR versus the subframe for each scheme. The average SINR margin between the CSI based ICIC and the GNI based ICIC is found to be 1.59 dB. Further, the average SINR margin between ASCG-D and GNI based ICIC is only 1.58 dB. I can show that ASCG-D is the well-coordinated suboptimal approach for the GNI based ICIC. In ASCG-D, a new game is generated at every T_{ud}. The average SINR margin between ASCG-D and reuse-1 is found to be 7.25 dB. An interesting point to note here is that ASCG-D shows a similar performance to (or even lower performance than) PFR in the initial point after user distribution updates. However, after every eNB proceeds with ASCG-D, ASCG-D shows a higher performance than PFR immediately. As a result, integration of results in the time grid of 0 to 2000ms reveals ASCG-D to have an average SINR gain of 4.62 dB in comparison to PFR. The average SINR margin between ASCG-D and CSI based ICIC is only 3.18 dB. ASCG-D also outperforms

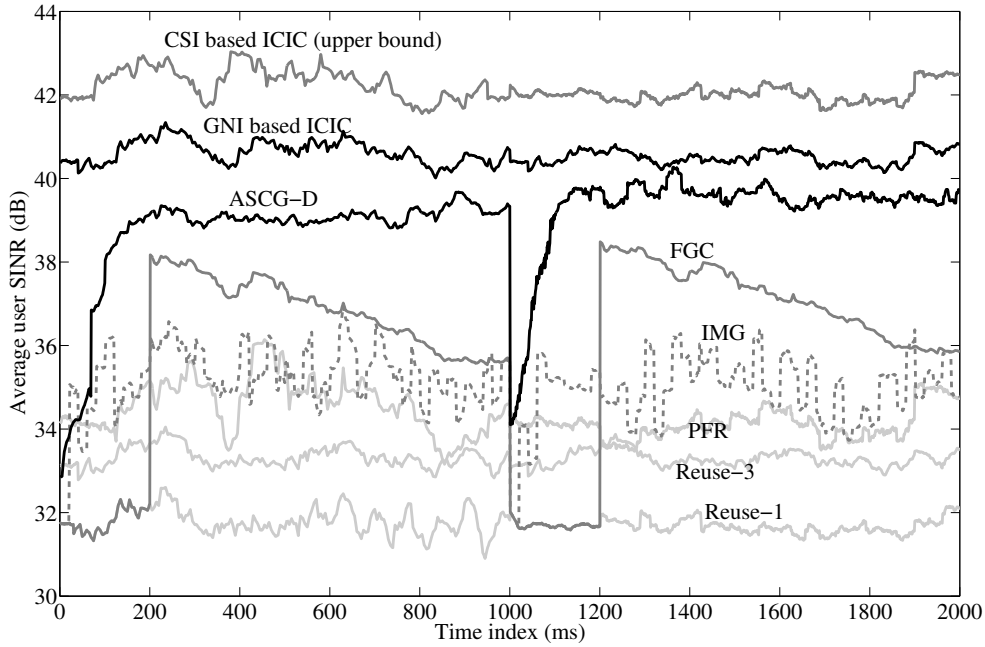

Figure 3.5: Average user SINR versus subframe for $\lambda = 0.6$.

FGC and IMG, which are conventional dynamic ICIC schemes. ASCG-D has average SINR gains of 3.05 dB and 3.81 dB in comparison with FGC and IMG, respectively. Unlike ASCG-D, FGC must need the central entity to solve ICIC optimization. To reduce the computational complexity, which explosively increases with the number of coordinated eNBs, the central entity chooses the suboptimal heuristic Dsatur method for coloring the graph. This limitation of conventional scheme causes the lower performance than ASCG-D, in spite of existence of central entity. After the delay time, which is set to 200ms, SINR distribution of FGC immediately increases by virtue of the suboptimal heuristic Dsatur method. However, this performance gain falls down due to a variation of global CSI during the rest period. Additionally, I compared ASCG-D to IMG. Since IMG operates based on CSI, this algorithm cannot find an NE in an LTE system with an X2 interface having high user mobility. If users are static, the network potential function of IMG should be monotonically increasing. However, in a realis-

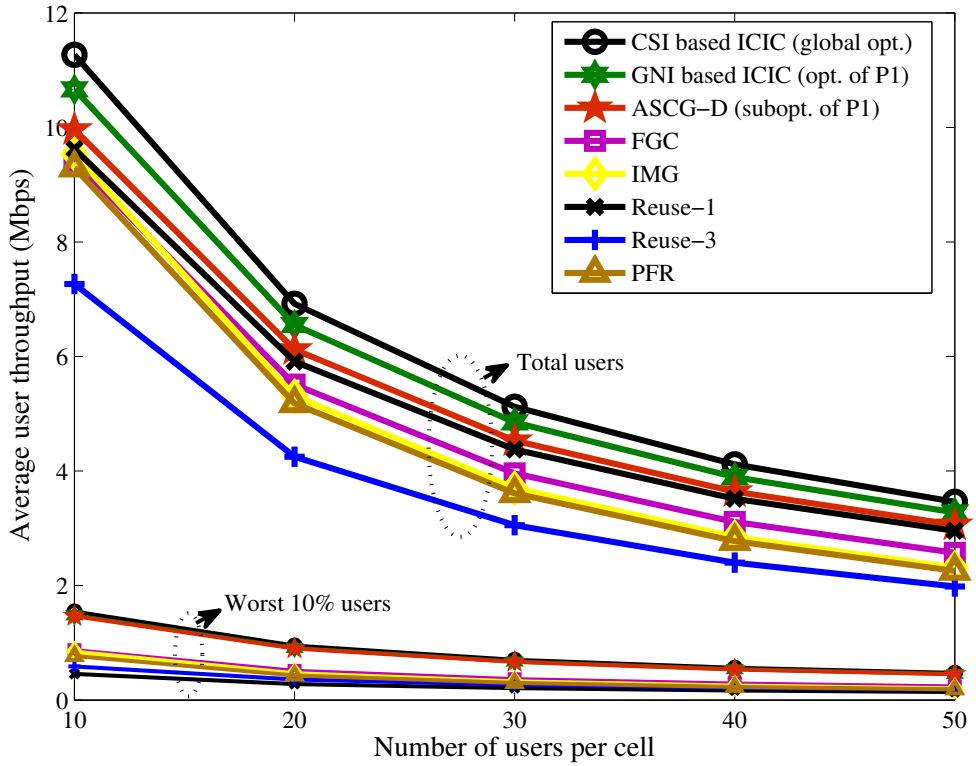

Figure 3.6: Performance of FDPS with each ICIC schemes for a varying number of users per cell ($\lambda = 0.6$).

tic system, the network potential function of IMG cannot increase steadily due to fast channel fading related to the existence of high-speed users. Moreover, SINR distribution of IMG is oscillating because each eNB calculates the best response strategy with the channel information already changed. This demonstrates that ASCG-D is a highly effective solution for maximizing the SINR distribution without the global knowledge of CSI.

Figure 3.6 shows a comparison of the average user throughput of FDPS with the various ICIC schemes for a varying number of users per cell, which is obtained by 500 Monte Carlo simulation trials. In the case of the total user throughput, ASCG-D is better than reuse-1 by only 3.5%, even though the average SINR margin between

these schemes is 7.25 dB. This result is attributed to the fact that the multiuser diversity gain of reuse-1, in which there are non-partitioning FDPS strategy spaces, is much higher than that of ASCG-D even though every strategy of the dominant strategy set guarantees good multiuser diversity gain. On the other hand, FGC and IMG show poor performance in terms of system throughput compared with ASCG-D. It is caused by both the low level of SINR distribution as shown in Figure 5 and, more crucially, an inefficient form of an FDPS strategy space. In FGC, RBs are assigned to the UEs such that no two UEs are assigned the same RB if they are connected in the graph, and the central entity performs this assignment for entire users in the network. Consequently, each user is assigned a small number of RBs. Further, in IMG, all users in a cell compete with each other to be scheduled within only 15 RBs. For these reasons, the FDPS strategy spaces made by FGC and IMG are not enough to efficiently schedule the users. As a result, ASCG-D shows better performance in terms of average user throughput than FGC and IMG, improving by 11.8% and 15.3%, respectively. However, when the number of users per cell is 10, ASCG-D shows relatively small performance gains in terms of average user throughput compared with FGC and IMG of 5.79% and 4.55%, respectively. Because the advantage of ASCG-D is highly correlated to dynamic level of environments such as the number of high-speed users, my proposed scheme shows better performance in denser and more dynamic networks. ASCG-D especially shows higher performance in the case of the worst 10% of user throughput. It comes from the proper constraint (3.5) aiming for the high performance of FDPS. The difference in the average user throughput gains between static ICIC schemes and ASCG-D is 3.5%-44.1% in the case of the total user throughput and 109.4%-221.5% in the case of the worst 10% of user throughput. The performance gains of ASCG-D compared with FGC and IMG are verified as 76.6% and 91.5%, respectively, in the case of the worst 10% of users. On the other hand, the performance of the CSI based ICIC is only 13.0% and 5.6% higher than that of ASCG-D in the cases of the total user throughput and the worst 10% of user throughput, respectively.

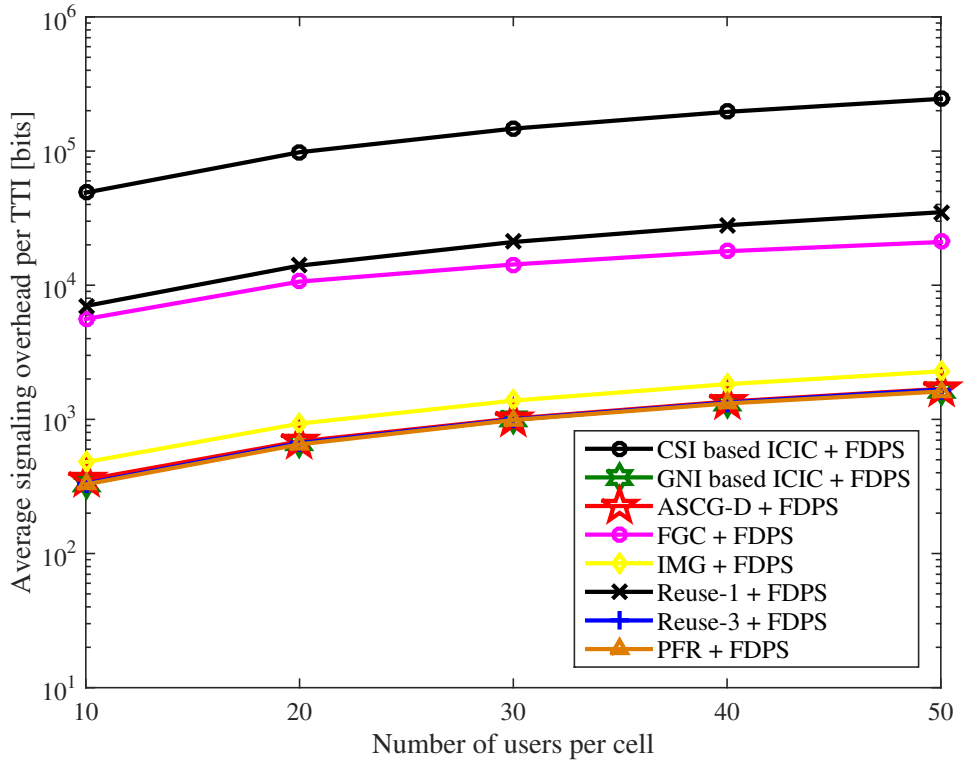

Figure 3.7: Average signaling overhead per TTI for a varying number of users per cell ($\lambda = 0.6$).

3.5.3 Signaling Overhead for ICIC and FDPS

Figure 3.7 shows the simulation results of the average signaling overhead per TTI for a varying number of users per cell. The signaling overheads of the static ICIC schemes consist of bits only for FDPS because of the absence of signaling for ICIC. The resolution for CSI B_{CSI} is 4 bits per RB in 3GPP LTE Release 8 [43]. B_{ud} is the number of bits for indicating a geometrical user distribution per T_{ud}, and is equal to $\lceil \log_2(S_{\text{network}}/S_{\text{unit}}) \rceil$, where S_{network} and S_{unit} are the area of the entire network ($\simeq 2.5 \cdot 10^6 \text{m}^2$) and the area of a de-correlated unit ($\simeq 50\text{m} \cdot 50\text{m} = 2500\text{m}^2$), respectively. Thus, the resolution for the user distribution B_{ud} is chosen to be 10 bits. B_{su} is the number of bits for representing $\mathbf{Y}^l$ per T_{su} and is equal to $N \times \lceil \log_2 K \rceil$, and

not $N \cdot K$, because one RB can be allocated to only one sector. In the simulation, $B_{su} = 25 \times 2 = 50$bits. In the case of CSI based ICIC, at every T_c, $B_{CSI} \cdot L \cdot N \cdot M$ bits are necessary for ICIC. However, additional signaling of ASCG-D results in a very relaxed time restriction on the updates, such as T_{ud} and T_{su}. ASCG-D requires $B_{ud} \cdot L \cdot M$ at every T_{ud} and $B_{su} \cdot (L-1)$ bits at every T_{su} for ICIC. The overhead of FDPS with ASCG-D is normally larger than those of FDPS with reuse-3 and FDPS with PFR by margins of 1.89% and 4.92%, respectively. The signaling overhead of FDPS with ASCG-D is 1/20th that of FDPS with reuse-1 without ICIC. This is because ASCG-D reduces the overhead of FDPS by partitioning FDPS spaces, but reuse-1 requires signaling overhead of all the CSI of all users at every TTI for the implementation of FDPS. The overhead of FDPS with FGC is 13.6 times that of FDPS with ASCG-D since FGC requires signaling overhead for all of the CSI of every user at every TTI during the delay time. Naturally, a shorter delay time ($<$ 200 ms) can reduce the overhead of FDPS with FGC; but it results in a lower performance gain in SINR distribution. Likewise, the overhead of FDPS with IMG is 1.35 times that of FDPS with ASCG-D. IMG has the benefit that each eNB can estimate the strategies of other eNBs by measuring which RBs are selected by other eNBs. Thus, IMG does not need to exchange strategy information. However, the exchange of interference information at every T_{su} is necessary to calculate the utility function, including the total interference generated by the corresponding player that is contributed to the environment and the total interference the player receives from the environment. This exchange incurs a large signaling overhead. The signaling overhead of FDPS with CSI based ICIC is up to 144 times higher than FDPS with ASCG-D. The overhead of FDPS with ASCG-D is slightly larger than that of FDPS with a GNI based ICIC by a margin of 2.01%. The overhead results from each eNB sending GNI only to the central entity in a GNI based ICIC instead of broadcasting GNI to every eNB as occurs in ASCG-D. The amount of signaling overhead is specifically explained in Appendix D.

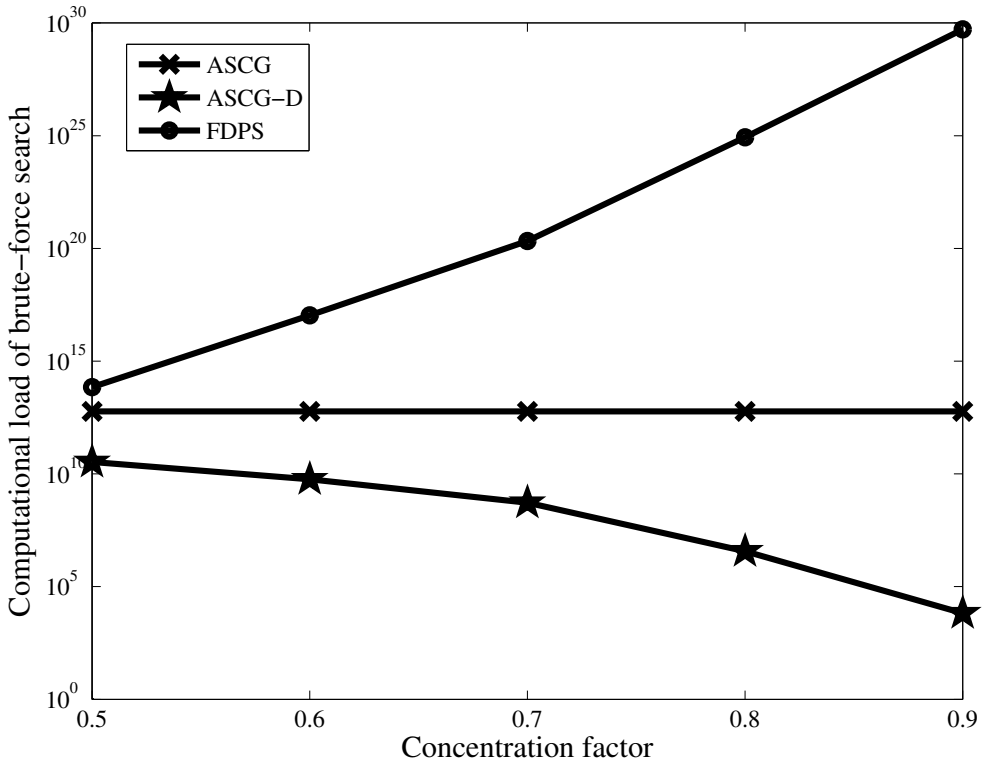

Figure 3.8: Computational load of ASCG according to irregularity of user distribution.

3.5.4 Reduction of Feasible ASCG Strategy Space

As shown in Figure 3.8, there is a considerable reduction in the computational load as compared to the time required for brute-force search on account of $\aleph_l$ being converted to $\aleph_l^D$ under variation of the concentration factor $\lambda = [0.5,\ 0.6,\ 0.7,\ 0.8,\ 0.9]$. Interestingly, when the user distribution becomes more irregular, the number of cases in the brute-force search becomes smaller by virtue of the fact that a smaller number of cases is required for searching the best response strategy $\mathbf{Y}_{*,D}^{l}$ in the dominant feasible strategy space $\aleph_l^D$ $\left(|\aleph_l^D| = \frac{N!}{\prod_{k=1}^{K} |\mathcal{N}_D^{l,k}|!}\right)$ because the term $\prod_{k=1}^{K} |\mathcal{N}_D^{l,k}|!$ is larger in the scenario of an irregular cell layout scenario. When $\lambda = 0.5$ and $\lambda = 0.9$, $\frac{|\aleph_l^D|}{|\aleph_l|}$ is 0.57% and 7.08×10^{-8}%, respectively. When the concentration factor λ is larger, the computational load of FDPS naturally converges to that of FDPS with reuse-1 (if

$\lambda = 1$ is equivalent to FDPS with reuse-1). Therefore, ASCG-D is very useful for implementing with FDPS on account of a reduction of the computational load with an increase in the concentration factor λ.

Chapter 4

APPLICATION OF EXACT POTENTIAL GAME: Asymmetric Transmission Game for Interference Coordination in Wireless Ad-hoc Relay Networks

4.1 Brief Introduction

In this work, I introduce asymmetric transmission to reduce network interference in wireless multiuser ad-hoc networks with a two-hop relaying protocol. I formulate the asymmetric transmission problems in HDR systems, and construct the game-theoretical algorithm, called ATG, for deriving suboptimal solutions. The proposed algorithm guarantees the existence of the NE. Furthermore, I developed A-ATG based on the value of spectral averaging in order to reduce signaling and computational complexity of ATG. Compared with the conventional methods, the two algorithms show a significant decrease in network interference. Ultimately, the energy consumption for satisfying the rate requirement is also reduced by 17.4%. For specific applications, I expect that the proposed algorithms can be easily applied to the autonomous outband D2D communication scenarios. With a proper change in game formulation, ATG and A-ATG can also be utilized in more various scenarios, including the underlaying inband, overlaying inband, and controlled outband D2D communication scenarios, which are

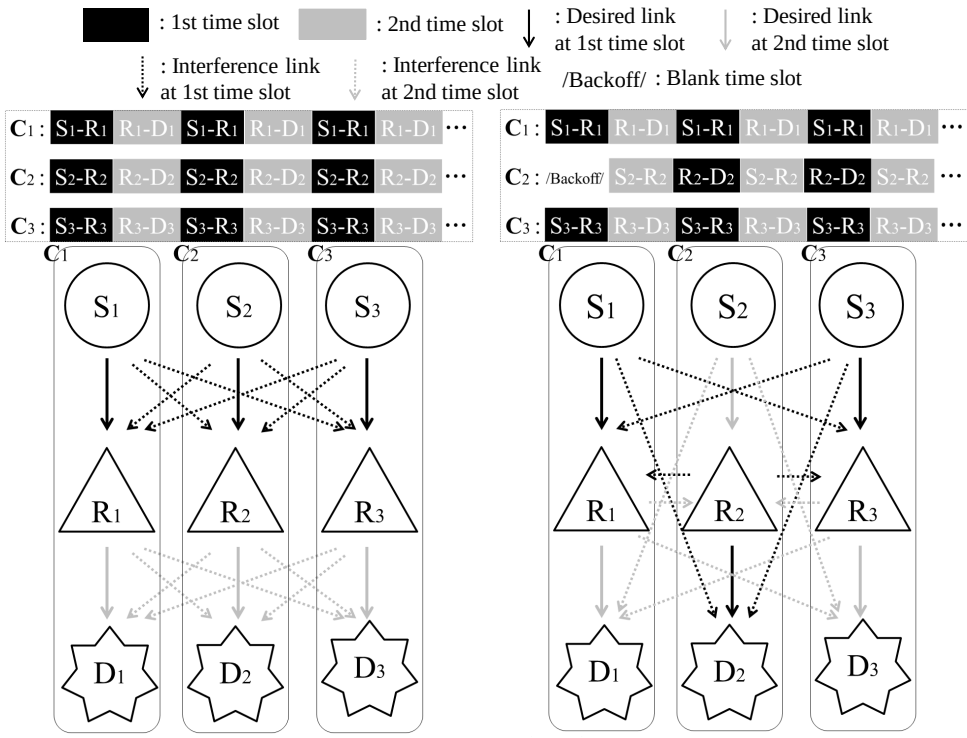

Figure 4.1: Link activation flow for data streaming and change of interference topology on a certain subchannel.

mixed with an infrastructure system consisting a central entity (e.g., evolved NodeB) and cellular users. Suggestions for further research include extending this work to multiuser ad-hoc network with MIMO systems or multi-hop relaying protocol systems.

4.2 Problem Formulation

4.2.1 System Preliminaries

I consider wireless ad-hoc networks within a multiuser SISO-OFDM framework. I assume a two-hop relaying scenario consisting of a set of communication sessions $\mathcal{C} \triangleq \{\mathbf{C}_1, ..., \mathbf{C}_M\}$ with a DF relaying protocol. The i-th communication session ($\mathbf{C}_i$) consists of three nodes: the source node (S_i), relay node (R_i), and destination node

(D_i). Every node in the network is randomly distributed over the two-dimensional region. In particular, nodes that belong to the same communication session are concentrated within their communication range. For simplicity, there is no direct link from S_i to D_i. I assume that R_i, which acts as a relay node to help the communication between S_i and D_i, is given a priori. I consider a spectrum-sharing network with a system bandwidth W divided into a set of orthogonal subchannels $\mathcal{K} = \{1, ..., K\}$. S_i and R_i each have a total transmit power P. Let H_{ab}^k denote the channel gain from a transmission node a (source or relay node) to a reception node b (relay or destination node) on subchannel k. I assume block-fading in the time-domain, which means that H_{ab}^k is stationary during a sufficiently long period. Signal power from transmission node a to reception node b on subcarrier k is defined as $P_a^k H_{ab}^k$, where P_a^k is the transmit power of node a on subchannel k. I denote $I^k(a, b)$ as interference from node a to node b on subchannel k, and it is defined in the case that if $a \in \{S_i, R_i\}$ and $b \in \{R_j, D_j\}$, where $\forall i \neq j$. Except for these cases, $P_a^k H_{ab}^k$ is a desired signal power. In this study, I assume an infinitely backlogged model, where every $\mathbf{C}_i$ has data for transmission.

4.2.2 The Concept of Asymmetric Transmission for Interference Coordination: A Simple Example

$\mathcal{C}_0^k$ and $\mathcal{C}_1^k$ are sets of communication sessions choosing symmetric and asymmetric transmission, respectively, at subchannel k. Therefore, $\mathcal{C}_0^k \cup \mathcal{C}_1^k = \mathcal{C}$ is satisfied for every subchannel k. The set of all possible K-tuple of a user set partition is defined as $\bar{\mathcal{C}} \triangleq \{\mathcal{C}_0^k, \mathcal{C}_1^k\}^{K \times 1}$. Figure 4.1 shows the link activation flow for data streaming and change of interference topology on subchannel k.

The left side of Figure 4.1 illustrates that every communication session selects symmetric transmission, i.e., $\mathcal{C}_0^k = \{\mathbf{C}_1, \mathbf{C}_2, \mathbf{C}_3\}$ and $\mathcal{C}_1^k = \emptyset$. On the other hand, the right side of Figure 4.1 represents that only the second communication session selects asymmetric transmission and the others select symmetric transmission, i.e., $\mathcal{C}_0^k = \{\mathbf{C}_1, \mathbf{C}_3\}$ and $\mathcal{C}_1^k = \{\mathbf{C}_2\}$. This means that $\mathbf{C}_2$ starts data streaming after resting

during the first time slot. By such a backoff operation, active links sharing the same time slot are altered, and consequently, network interference is changed from left to right in Figure 4.1.

In the left side of Figure 4.1 representing a HDR system, network interference would be $\sum_{i \neq j} I^k(S_i, R_j)$ at the first time slot and $\sum_{i \neq j} I^k(R_i, D_j)$ at the second time slot. However, in the right side of Figure 4.1, network interference would be $I^k(S_1, D_2)+I^k(S_1, R_3)+I^k(R_2, R_1)+I^k(R_2, R_3)+I^k(S_3, R_1)+I^k(S_3, D_2)$ at the first time slot, and $I^k(R_1, R_2)+I^k(R_1, D_3)+I^k(S_2, D_1)+I^k(S_2, D_3)+I^k(R_3, D_1)+I^k(R_3, R_2)$ at the second time slot. Such an example implies that network interference minimization could be achieved by appropriately assigning symmetric and asymmetric transmission strategies to each communication session.

4.2.3 Optimization Problem

In an HDR system, the sum of interferences for both the first and the second time slot from $\mathbf{C}_j$ to $\mathbf{C}_i$ on subchannel k, is defined as follows:

$$I_{ij}^k = \begin{cases} I^k(S_j, R_i) + I^k(R_j, D_i), & \text{if } \{\mathbf{C}_i, \mathbf{C}_j\} \in \mathcal{C}_0^k \\ I^k(S_j, R_i) + I^k(R_j, D_i), & \text{if } \{\mathbf{C}_i, \mathbf{C}_j\} \in \mathcal{C}_1^k \\ I^k(R_j, R_i) + I^k(S_j, D_i), & \text{otherwise.} \end{cases} \tag{4.1}$$

It is obvious that $I_{ij}^k = 0$ for $\forall k$, if $i = j$. Then, the optimal user set partition based on the symmetric/asymmetric transmission selection problem is formulated as the following $(K \times M)$ size of 0-1 integer programming.

P2. Asymmetric transmission in HDR system Find the optimal K-tuple of a partition of user set $\mathcal{C}^* \in \bar{\mathcal{C}}$ such that the network interference $\sum_k \sum_{i \neq j} I_{ij}^k$ is minimized.

Although the above optimization problem (termed P2) can be solved in a centralized fashion to obtain an optimal solution, it is a rather complex task because 0-1 integer programming is known to be NP-hard. Thus, I propose an game-theoretic distributed algorithm to obtain the suboptimal solution while reducing the computational complexity.

4.3 Asymmetric Transmission Game

4.3.1 Game Formulation

Definition 5. ATG: $< \mathcal{C}, \mathbb{S}, \{U_i\}_{i \in \mathcal{C}} >$

i) i) Set of players: $\mathcal{C} = \{\mathbf{C}_1, ...\mathbf{C}_M\}$

ii) Strategy of player i: $\mathbf{s}_i \in \mathbf{S}_i = \{0,1\}^{K \times 1}$

iii) Utility of player i:

$$U_i(\mathbf{s}) = \sum_{k=1}^{K} U_i^k(\mathbf{s}_i, \mathbf{s}_{-i}) = -\sum_{k=1}^{K}\sum_{j=1}^{M}(I_{ji}^k + I_{ij}^k). \tag{4.2}$$

Let the set of communication sessions $\mathcal{C} = \{\mathbf{C}_1, ..., \mathbf{C}_M\}$ denote the set of players. I will use the terms "player i" and "communication session $\mathbf{C}_i$" interchangeably. The space for the strategy profiles is defined by $\mathbb{S} = \mathbf{S}_1 \times \cdots \times \mathbf{S}_M$, where $\mathbf{S}_i \triangleq \{0,1\}^{K \times 1}$ is the set of feasible strategies of player i. A strategy of player i, $\mathbf{s}_i \in \mathbf{S}_i$, is a $(K \times 1)$-size vector. For each $\mathbf{s}_i$, I write $\mathbf{s}_{-i}$ as the joint strategy of all players except player i. Hence, $\mathbf{s} = (\mathbf{s}_i, \mathbf{s}_{-i})$ is the joint strategy of all players. Each of the elements in $\mathbf{s}_i$, $s_{i,k} \in \{0,1\}$, implies that $s_{i,k} = 0$ if $\mathbf{C}_i \in \mathcal{C}_0^k$ and 1 if $\mathbf{C}_i \in \mathcal{C}_1^k$. The utility $U_i(\mathbf{s}_i, \mathbf{s}_{-i})$ of player i means the interference generated and experienced by the player. In addition, it can be divided into K utility functions as $U_i^k(\mathbf{s}_i, \mathbf{s}_{-i}) = -\sum_{j=1}^{M}(I_{ji}^k + I_{ij}^k)$ by spectral orthogonality.

Let the strategy state $\mathbf{s}^{(n)}$ denote the joint strategy of all players at the n-th step. ATG is implemented by sequential best-response dynamics, i.e., the strategy state is updated by $\mathbf{s}^{(n)} \leftarrow \mathbf{s}^{(n-1)} \odot \mathbf{s}_{i,*}^{(n-1)}$. In other words, $\mathbf{s}^{(n)}$ is updated by substituting the i-th element of $\mathbf{s}^{(n-1)}$ to $\mathbf{s}_{i,*}^{(n-1)} = \text{argmax}_{\mathbf{s}_i}[U_i(\mathbf{s}^{(n-1)})]$.

4.3.2 Convergence and Optimality Properties of Asymmetric Transmission Game

In this section, I prove the convergence properties of ATG which is the form of the exact potential game. The exact potential games were first introduced by Monderer and

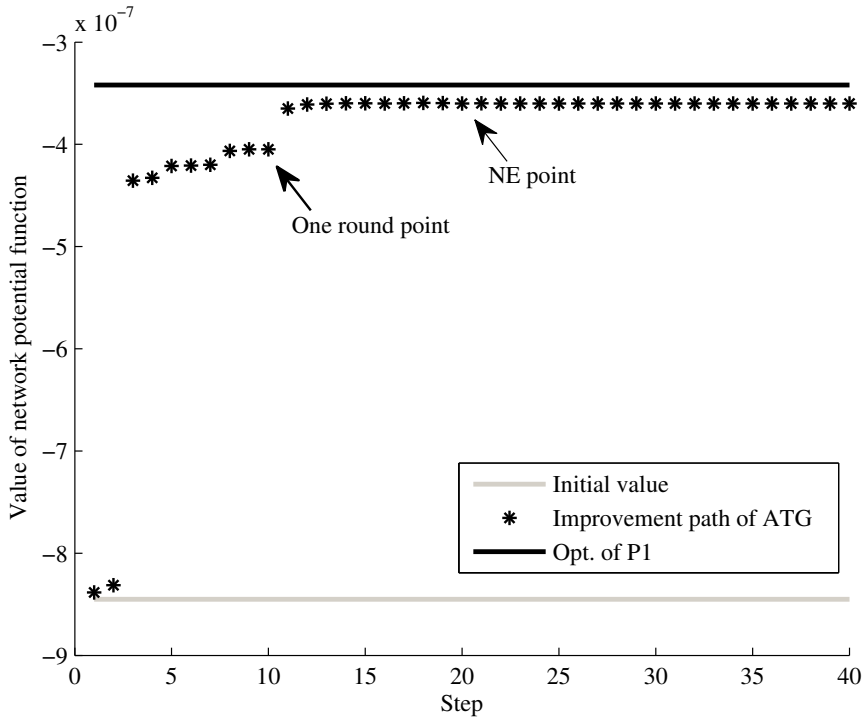

Figure 4.2: Improvement path of ATG in one drop ($M = 10$, $K = 6$, $W = 5$ MHz, $P = 23$ dBm (equal power allocation to all subchannels)); detailed parameter settings and graphical representation of the locations of the communication sessions are described in section 4.4.

Shapley. Recently, it has been widely utilized as a tool to resolve various resource allocation problems in wireless networks [38,71]. For any two different strategies $\mathbf{s}_i$ and $\tilde{\mathbf{s}}_i$, a game is an exact potential game if and only if there exists the network potential function $\Theta(\mathbf{s})$ satisfying

$$U_i(\tilde{\mathbf{s}}_i, \mathbf{s}_{-i}) - U_i(\mathbf{s}_i, \mathbf{s}_{-i}) = \Theta(\tilde{\mathbf{s}}_i, \mathbf{s}_{-i}) - \Theta(\mathbf{s}_i, \mathbf{s}_{-i}), \forall i. \tag{4.3}$$

The representative characteristic of the exact potential game is that there always exists a pure-strategy NE when it plays by sequential best-response dynamics. I will show that ATG is the exact potential game to guarantee the existence of the NE.

Theorem 2. ATG is an exact potential game, if the network potential function $\Theta(\mathbf{s}) = \frac{1}{2}\sum_{i=1}^{M} U_i(\mathbf{s})$.

$Proof$: Condition (4.3) of an exact potential game will hold if I consider the network potential function $\Theta(\mathbf{s})$ as $\frac{1}{2}\sum_{i=1}^{M} U_i$. Then,

$$\begin{aligned}\Theta(\mathbf{s}) &= \frac{1}{2}\sum_{i=1}^{M} U_i(\mathbf{s}) = -\frac{1}{2}\sum_{i=1}^{M}\Big[\sum_{k=1}^{K}\sum_{j=1}^{M} I_{ji}^{k} + I_{ij}^{k}\Big] \\ &= -\sum_{k=1}^{K}\Big[\sum_{i=1}^{M}\sum_{j=1}^{M} I_{ij}^{k}\Big] = \sum_{k=1}^{K}\Theta_k(\mathbf{s}). \end{aligned} \tag{4.4}$$

In addition, $\Theta_k(\mathbf{s}) = \Theta_k(\mathbf{s}_i, \mathbf{s}_{-i})$ is expressed as

$$\begin{aligned}\Theta_k(\mathbf{s}_i, \mathbf{s}_{-i}) &= -\sum_{l=1}^{M} I_{il}^{k} - \sum_{l=1}^{M} I_{il}^{k} - \sum_{j=1}^{M}\sum_{l=1}^{M} I_{il}^{k} I_{lj}^{k} \\ &= U_i^k(\mathbf{s}_i, \mathbf{s}_{-i}) + o(\mathbf{s}_{-i}), \end{aligned} \tag{4.5}$$

where $o(\mathbf{s}_{-i})$ takes a constant value that is independent of $\mathbf{s}_i$. It depends only on the strategies of other players with each other. Suppose that player i changes its strategy $\mathbf{s}_i$ to $\tilde{\mathbf{s}}_i$, $\Theta_k(\tilde{\mathbf{s}}_i, \mathbf{s}_{-i})$ would be changed to

$$\begin{aligned}\Theta_k(\tilde{\mathbf{s}}_i, \mathbf{s}_{-i}) &= -\sum_{l=1}^{M} \tilde{I}_{il}^{k} - \sum_{l=1}^{M} \tilde{I}_{il}^{k} - \sum_{j=1}^{M}\sum_{l=1}^{M} I_{il}^{k} I_{lj}^{k} \\ &= U_i^k(\tilde{\mathbf{s}}_i, \mathbf{s}_{-i}) + o(\mathbf{s}_{-i}). \end{aligned} \tag{4.6}$$

From the equations (4.5) and (4.6), I can conclude that $U_i^k(\tilde{\mathbf{s}}_i, \mathbf{s}_{-i}) - U_i^k(\mathbf{s}_i, \mathbf{s}_{-i}) = \Theta_k(\tilde{\mathbf{s}}_i, \mathbf{s}_{-i}) - \Theta_k(\mathbf{s}_i, \mathbf{s}_{-i})$, $\forall k \in \mathcal{K}$. Using this relationship, the condition (4.3) is satisfied.

According to Theorem 2, ATG is an exact potential game and thus guarantees a stable suboptimal solution. Let us show an example of one-drop ATG. Improvement path, $[\cdots, \Theta(\mathbf{s}^{(n-1)}), \Theta(\mathbf{s}^{(n)}), \cdots]$, is described in Figure 4.2. Each step on the horizontal axis refers to a decision made by a player. From the figure, I can observe that the network potential function increases monotonically until it achieves an NE. It is shown that the performance of ATG closely approaches to the NE even within

Algorithm 4.3 : Asymmetric transmission game

Start with arbitrary initial strategy state $\mathbf{s}^{(0)}$ (or start with $s_{i,k} = 0$ for $\forall i, k$).

while $\mathbf{s}^n \neq \mathbf{s}^{(n-1)}$ **do**

Select player i according to the round-robin rule at iteration n.

Calculate the utility of player i on basis of actual interference generated and experienced by itself.

Solve new best response strategy $\mathbf{s}_{i,*}^{(n-1)} = \text{argmax}\Big[U_i(\mathbf{s}^{(n-1)})\Big]$ and update strategy state $\mathbf{s}^{(n)} \leftarrow \mathbf{s}^{(n-1)} \odot \mathbf{s}_{i,*}^{(n-1)}$ by broadcasting $\mathbf{s}_{i,*}^{(n-1)}$.

Set $n \leftarrow n + 1$.

end while

one-round play. Furthermore, the NE point approximately achieves the optimal point ($\Theta(\mathbf{s}^{(0)}) = -0.84 \times 10^{-6}$, $\Theta(\mathbf{s}^{(M)}) = -0.40 \times 10^{-6}$, $\Theta(\mathbf{s}^{(2M)}) = -0.36 \times 10^{-6}$, $\Theta(\mathbf{s}^*) = -0.34 \times 10^{-6}$, where $\mathbf{s}^* \triangleq \text{argmax}_{\mathbf{s}}\Theta(\mathbf{s})$).

Algorithm 4.3 summarizes the steps of the algorithm for ATG. In line 1, each player starts with some random initial condition or generally starts with $s_{i,k} = 0$ for $\forall i, k$. Then, the loop from lines 2 to 6 is executed until the algorithm converges to the NE.

4.3.3 Approximated Version of Asymmetric Transmission Game

In lines 4 and 5 of Algorithm 4.3, each player individually solves the independent local optimization problems through every subchannel to resolve the best-response strategy. I introduce an approximate version of ATG (termed A-ATG) to reduce both the computational complexity and signaling overhead. Compared to ATG, which requires channel information for every subchannel, A-ATG is designed to work with the potential interference as a single representative parameter. Let us define the potential interference PI_{ij} between $\mathbf{C}_i$ and $\mathbf{C}_j$ as follows.

Table 4.1: Computational complexity and signaling overhead

	ATG	**A-ATG**
Computational complexity	$O(KMN)$	$O(MN)$
Signaling overhead	$4K(M-1)B_{\text{CSI}}$	$4(M-1)B_{\text{CSI}}$

$$PI_{ij} = \begin{cases} L(S_j, R_i) + L(R_j, D_i), & \text{if } \{\mathbf{C}_i, \mathbf{C}_j\} \in \mathcal{C}_0 \\ L(S_j, R_i) + L(R_j, D_i), & \text{if } \{\mathbf{C}_i, \mathbf{C}_j\} \in \mathcal{C}_1 \\ L(R_j, R_i) + L(S_j, D_i), & \text{otherwise.} \end{cases} \tag{4.7}$$

$\mathcal{C}_0$ and $\mathcal{C}_1$ are sets of communication sessions choosing symmetric and asymmetric transmission, respectively. $L(a, b)$ can be easily analyzed by reception node b, and it is represented by $\frac{1}{K}\sum_{k=1}^{K} I^k(a, b)$. In A-ATG, each communication session does not exchange full channel information on every subchannel, but exchange partial channel information as the spectrally averaged value of actual interference. As a result, although the efficiency degradation of a suboptimal solution would be possible, the local optimization problem of each player and the corresponding signaling overhead for exchanging information are reduced by the order of $1/K$. Let us define A-ATG as follows.

Definition 6. A-ATG: $< \mathcal{C}, \mathbb{B}, \{u_i\}_{i \in \mathcal{C}} >$

i) Set of players: $\mathcal{C} = \{\mathbf{C}_1, ...\mathbf{C}_M\}$

ii) Strategy of player i: $b_i \in \mathbf{B}_i = \{0, 1\}$

iii) Utility of player i:

$$u_i(\mathbf{b}) = u_i(b_i, \mathbf{b}_{-i}) = -\sum_{j=1, i \neq j}^{M} (PI_{ji} + PI_{ij}). \tag{4.8}$$

Let the set of communication sessions $\mathcal{C} = \{\mathbf{C}_1, ..., \mathbf{C}_M\}$ denote the set of players, same as for ATG. The space for the strategy profiles is defined by $\mathbb{B} = \mathbf{B}_1 \times \cdots \times \mathbf{B}_M$, where $\mathbf{B}_i$ is the set of feasible strategies of player i. For a specific $b_i \in B_i$, $b_i = 0$ if $\mathbf{C}_i \in \mathcal{C}_0$ and 1 otherwise. For each b_i, I write $\mathbf{b}_{-i}$ as the joint strategy set of all players

Algorithm 4.4 : Approximated asymmetric transmission game

Start with arbitrary initial strategy state $\mathbf{b}^{(0)}$ (or start with $b_i = 0$ for $\forall i$).

while $\mathbf{b}^n \neq \mathbf{b}^{(n-1)}$ **do**

Select player i according to the round-robin rule at iteration n.

Calculate the utility of player i on basis of potential interference generated and experienced by itself.

Solve new best response strategy $b_{i,*}^{(n-1)} = \text{argmax}\left[u_i(\mathbf{b}^{(n-1)})\right]$ and update strategy state $\mathbf{b}^{(n)} \leftarrow \mathbf{b}^{(n-1)} \odot b_{i,*}^{(n-1)}$ by broadcasting $b_{i,*}^{(n-1)}$.

Set $n \leftarrow n + 1$.

end while

in the set excluding player i. Hence, $\mathbf{b} = (b_i, \mathbf{b}_{-i})$ is the joint strategy of all players. $u_i(b_i, \mathbf{b}_{-i})$, the utility of player i, is defined as (4.8). $u_i(b_i, \mathbf{b}_{-i})$ is the function of potential interference generated and experienced by player i. The strategy state $\mathbf{b}^{(n)}$ is the joint strategy of all players $\mathbf{b}$ at the n-th step. A-ATG is also operated by sequential best-response dynamics. The strategy state is updated by $\mathbf{b}^{(n)} \leftarrow \mathbf{b}^{(n-1)} \odot b_{i,*}^{(n-1)}$ which means that $\mathbf{b}^{(n)}$ is updated by substituting the i-th element of $\mathbf{b}^{(n-1)}$ to $b_{i,*}^{(n-1)} = \text{argmax}_{b_i}[U_i(\mathbf{b}^{(n-1)})]$. Similar to ATG, A-ATG is also an exact potential game, and therefore guarantees the existence of the NE, which is denoted by $\mathbf{b}_*$. The following theorem is established.

Theorem 3. A-ATG is an exact potential game, if the network potential function $\theta(\mathbf{b}) = \frac{1}{2}\sum_{i=1}^{M} u_i(\mathbf{b})$.

$Proof$: The progress of proof of Theorem 2 is equivalently adopted into Theorem 3, with conversion $U_i(\mathbf{s})$ to $u_i(\mathbf{b})$.

Although A-ATG might have lower performance in terms of interference minimization and power saving than ATG, it has a significant advantage in reducing computational complexity and signaling overhead as shown in Table 4.1. The computational complexity for searching a global optimal value is $O(2^M \times K)$. However, the suboptimal solutions with ATG and A-ATG are solved in polynomial time. Compu-

tational complexity of ATG and A-ATG are $O(KMN)$ and $O(MN)$, respectively, where N is an averaged number of each player's strategy update to converge to the NE. The number of steps to converge to the NE, MN, is bounded to M^2 [72], and the computational complexities to obtain the best response strategy at each step are $O(K)$ and $O(1)$. The effect of reduction of $1/K$ is also shown in terms of signaling overhead. Term $K(M-1)$ in the ATG case and term $(M-1)$ in A-ATG case means that every opponent sends player i's suffering actual (ATG) and potential (A-ATG) interference to player i for calculating the utility function of player i. B_{CSI} is the resolution for sending CSI and is typically 4-5 bits per one subchannel. Term "4" in Table 4.1 means that information of source-to-relay, source-to-destination, relay-to-relay and relay-to-destination interference links are necessary. The steps of the algorithm for A-ATG are summarized in Algorithm 4.4.

4.4 Simulation Results

4.4.1 Parameters Settings

In this section, I evaluate the performance of my proposed algorithms. Ten communication sessions are assumed, and every node is randomly distributed within a circle of a network site, as depicted in Figure 4.3. The source, relay, and destination nodes are denoted by circles, triangles, and stars, respectively. I assume that all source and relay nodes have a 23 dBm transmit power constraint and a 5 MHz system bandwidth with six subchannels. The thermal noise power is assumed to be -174 dBm/MHz. The path loss gain is given as $128.15 + 37.6\log(d_{a,b})$ in decibels, where $d_{a,b}$ is the distance between the nodes a and b measured in kilometers. Each location's shadowing value should be calculated with a geometric grid on the basis of the standard deviation of the shadowing and the decorrelated distance with an appropriate spatial correlation [73]. The standard deviation of the shadowing is 8 dB, and the decorrelated distance is 50 m. A small-scale fading channel is generated by Jake's simulator by assuming a car-

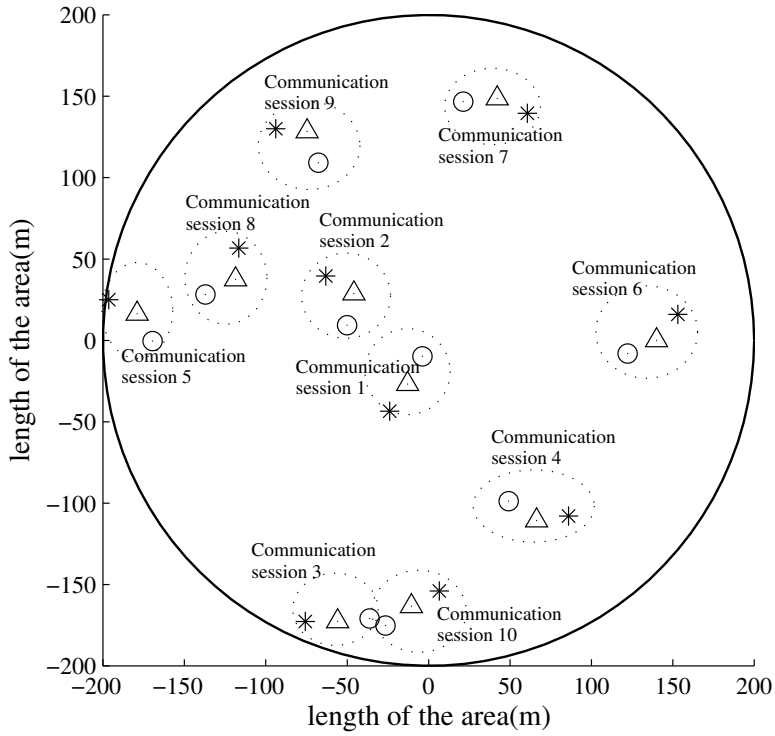

Figure 4.3: Graphical representation of the locations of the communication sessions.

rier frequency of 2 GHz, and a user's random walk velocity is 3 km/h. A transmit time interval of 1 ms is assumed.

4.4.2 Network Interference in One-shot Game

I set the SA algorithm in [39, 40] as the baseline to assess my proposed algorithms in terms of network interference.[1] The SA algorithm (also called an interference minimization game) in [39, 40] was introduced as a decentralized solution for minimizing the network interference with a low complexity in wireless ad-hoc networks with a dense geometry. In SA, each communication session is allowed to have a fixed num-

[1] Actually, SA is focused on wireless ad-hoc networks consisting of one-hop links in [39,40]. However, SA can be also directly used in wireless ad-hoc networks consisting of the two-hop links by the proper conversion of utility function of SA.

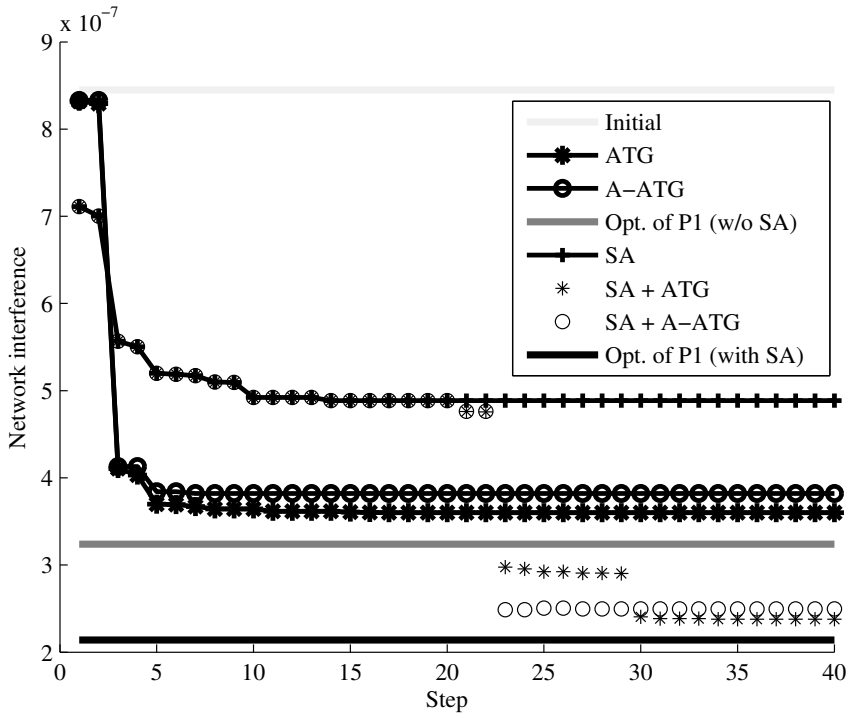

Figure 4.4: Trend of network interference with $M = 10$.

ber of subchannels K_i, where $1 < K_i \leq K$. In addition, I set $K_i = 5$ for all i. The predetermination of K_i is to resolve the limitation of SA, in which communication sessions select any subchannel to avoid interference, which is also mentioned in [39, 40]. All players belong to $\mathcal{C}_0^k$ at the initial state, i.e., the information of $I^k(R_j, R_i)$ and $I^k(S_j, D_i)$ for all i, j, k, which are related to ATG or A-ATG, is not of concern in the SA operation. In SA, for all i, each player sequentially selects the best subchannels of K_i to minimize $\sum_{k=1}^{K_i} \sum_{j=1}^{M} [I^k(S_j, R_i) + I^k(R_j, D_i) + I^k(S_i, R_j) + I^k(R_i, D_j)]$, which represents the sum of the total interference that the corresponding player receives from the environment and the total interference generated by the player that is contributed to the environment. I also set the period for operating SA to 20 steps, which is sufficient to find the solution of SA. Without SA scenarios, i.e., the case of $K_i = 6$, ATG and A-ATG start operation at the first time step. On the other hand, with

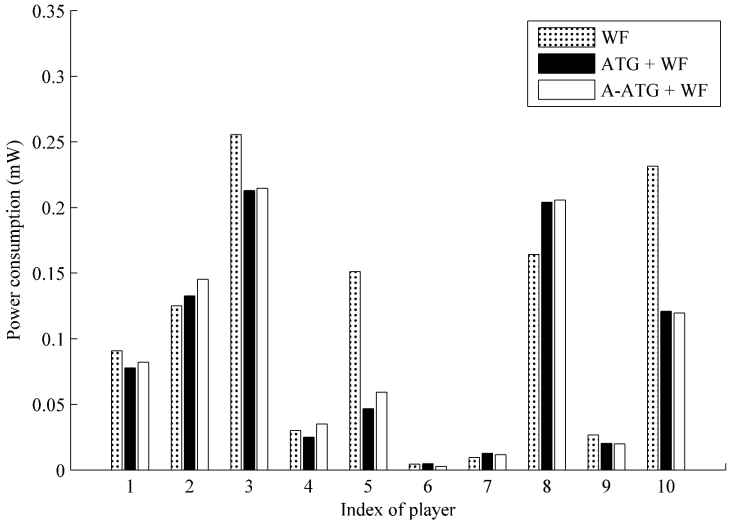

(a)

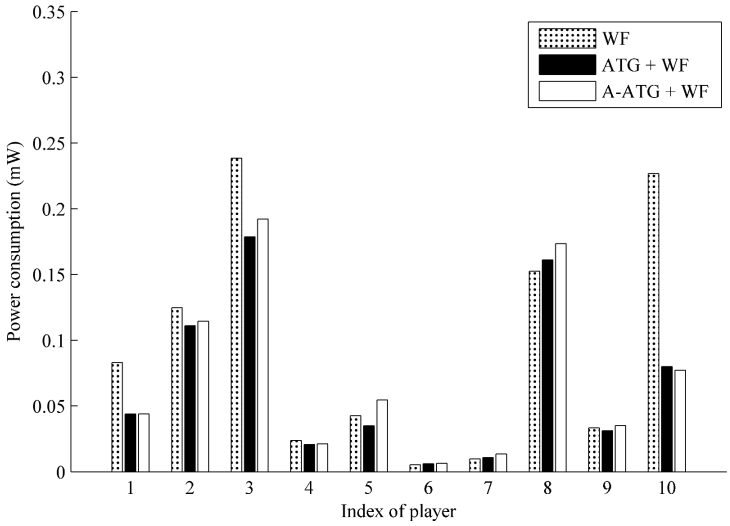

(b)

Figure 4.5: Individual power consumption for satisfying rate demand (= 6 Mbps) (a) without SA and (b) with SA.

SA scenarios, i.e., the case of $K_i = 5$, ATG and A-ATG start operation at the 21st step, which is after the period in which the SA solution is obtained. I set equal power allocation to the subchannels K_i in this subsection.

The trend of the resulting network interferences proceed along their distributed steps are shown in Figure 4.4. As the results show, cooperation between SA and my proposed schemes shows high synergistic effects by virtue of the extended degree of freedom by adding the temporal diversity of ATG or A-ATG to the spectral diversity of SA. ATG achieves 89.7% and 90.0% of the optimal values without SA (dashed line) and with SA (solid line), respectively, in terms of amount of network interference reduction, (A-ATG: 84.8% and 85.7%). In addition, the performance gain of cooperation between SA and ATG (or A-ATG) over only SA are 70.3% (67.0%). The most interesting feature of Figure 4.4 is that network interference is drastically reduced at the third step. This feature is also shown in Figure 4.2 as the increase of the network potential function at the third step. The actions of $\mathbf{C}_3$ and $\mathbf{C}_{10}$ drastically contribute to reduce the network interference (and the network potential function in Figure 4.2) as shown in Figure 4.4. This is because the geometric locations of $\mathbf{C}_3$ and $\mathbf{C}_{10}$ are very close, and this severe geometric proximity causes strong interference for each other. However, in my proposed schemes, $\mathbf{C}_3$ intelligently avoids the interference generated and experienced for $\mathbf{C}_{10}$ by virtue of the degree of freedom based on temporal diversity. While operating ATG, $\mathbf{C}_3$ selects its strategy as $\mathbf{s}_3 = [111111]$ (i.e., implement one time slot backoff in all subchannels) to minimize the interference related to $\mathbf{C}_{10}$. Although any two players are geometrically close to each other, one of these two players does not always select the perfect asymmetric transmission strategy such as $[111111]$. However, $I^k(S_3, R_{10})$ and $I^k(S_{10}, R_3)$ would be dominantly large in the situation where S_3 and S_{10} are very close and D_3 and D_{10} are relatively far. Thus, $I^k(S_3, R_{10}) + I^k(S_{10}, R_3) + I^k(R_3, D_{10}) + I^k(R_{10}, D_3)$ would be larger than $I^k(R_3, R_{10}) + I^k(R_{10}, R_3) + I^k(S_3, D_{10}) + I^k(S_{10}, D_3)$, for $\mathbf{C}_3$, which selects the best-response strategy earlier than $\mathbf{C}_{10}$ by the round-robin rule, and would select

$\mathbf{s}_3 = [111111]$. After that, $\mathbf{C}_{10}$ naturally selects $\mathbf{s}_{10} = [000000]$ at its turn of play. Likewise, the trend in the network interference is drastically reduced at the turn of $\mathbf{C}_3$ (i.e., at the 23rd step) while operating ATG and A-ATG after SA algorithm is finished. From the viewpoint of A-ATG, NE is achieved right after updating the strategy of $\mathbf{C}_3$, (i.e., every player excluding $\mathbf{C}_3$ satisfies the current state and does not update their strategies), even though network interference has more chances to be reduced. This is caused by the fact that the information of the network interference of each subchannel is blinded from the viewpoint of A-ATG. However, in ATG, the network interference is monotonically decreasing according to the updates of the strategies of the rest of the players as well as $\mathbf{C}_3$ by virtue of the specific information related to the network interference. In particular, the network interference is drastically reduced at the turn of $\mathbf{C}_{10}$ (i.e., at the 30th step), which is not observed at the corresponding turn of $\mathbf{C}_{10}$ in ATG without SA (at the 10th step). Because, in the "without SA" scenario, the entire set of subchannels is used by $\mathbf{C}_3$ and $\mathbf{C}_{10}$ naturally. Thus, $\mathbf{C}_3$ and $\mathbf{C}_{10}$ do not select the same state of transmission for all subchannels k. As a result, $\mathbf{C}_3$ and $\mathbf{C}_{10}$ select their strategies as $\mathbf{s}_3 = [111111]$ and $\mathbf{s}_{10} = [000000]$, respectively, in the "without SA" scenario. However, in the "with SA" scenario, $\mathbf{C}_3$ and $\mathbf{C}_{10}$ select different sets of subchannels to eliminate the subchannel that has the most crucial interference through the sequential updates for SA operation. As a result, the dominant influences between $\mathbf{C}_3$ and $\mathbf{C}_{10}$ should be relaxed; consequently, at the 30th step, $\mathbf{C}_{10}$ would have an additional chance to reduce the network interference related to the other players as well as $\mathbf{C}_3$ on the basis of the differently selected sets of subchannels at each communication session.

4.4.3 Individual Power Consumption in One-shot Game

Although the proposed ATG and A-ATG lead to less network interference in multiuser ad-hoc HDR systems, they are also beneficial for individual power consumption for satisfying rate demand. I compared the performance of the WF algorithm combined

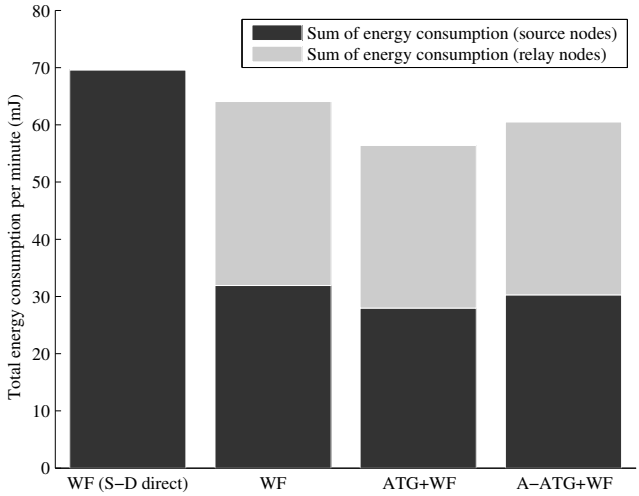

(a)

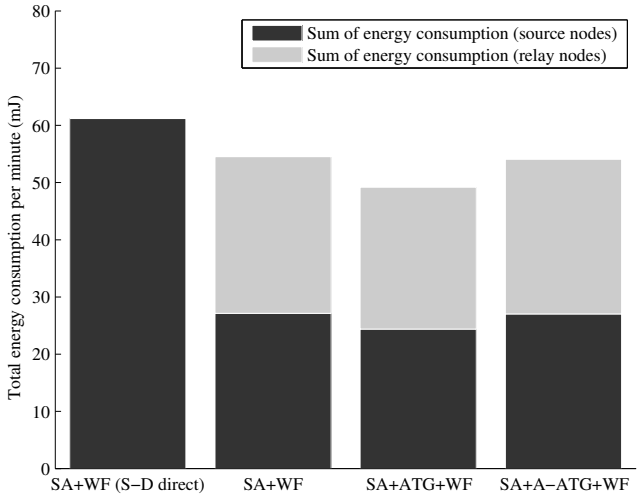

(b)

Figure 4.6: Total energy consumption per minute with $M = 10$ (a) without SA and (b) with SA.

with ATG and A-ATG (termed "ATG + WF" and "A-ATG + WF") to the WF algorithm alone and the joint SA and WF (termed "SA + WF"). Let $\bar{r}$ and r_i as the data rate requirement of all communication sessions and the achievable rate of communication session $\mathbf{C}_i$, respectively. I set that $\bar{r}$ is equal to 6 Mbps. r_i is computed according to the Shannon capacity and the basic form of rate calculation with DF protocol, i.e., $r_i = \frac{1}{2}\text{min}[r_{i,1}, r_{i,2}] = \frac{1}{2}\text{min}[\log_2(1+\gamma_{i,1}), \log_2(1+\gamma_{i,2})]$, where $\gamma_{i,1}$ and $\gamma_{i,2}$ is the SNIR at 1st time slot and 2nd time slot, respectively. WF optimizes the power allocation using the power constraint under six subchannels and five subchannels for the scenarios without and with SA, respectively. As I mentioned in Section 4.2, $\mathbf{C}_3$ and $\mathbf{C}_{10}$ are closely adjacent. In Figure 4.5, they need to consume more power to overcome the large interference using only the WF algorithm. Ironically, they are the greatest beneficiaries of my proposed schemes by virtue of the facts that they are isolated to only two of them, and the selection of the best response strategy can be observed clearly, as I mentioned in Section 4.2. As shown in the comparison of Figure 4.5(a) and Figure 4.5(b), the SA algorithm cannot lead to a reduction in the power consumption of $\mathbf{C}_3$ and $\mathbf{C}_{10}$. However, ATG and A-ATG show effective power savings for $\mathbf{C}_3$ and $\mathbf{C}_{10}$ by virtue of the degree of freedom based on the temporal diversity. Another aspect of the need for a high power consumption is shown for $\mathbf{C}_8$. It is surrounded by other players (especially $\mathbf{C}_2$, $\mathbf{C}_5$, and $\mathbf{C}_9$) at a near distance; therefore, they experience interference owing to the neighboring players. In Figure 4.5, the power consumption of $\mathbf{C}_8$ also shows that my proposed schemes do not always guarantee effective power savings for each player because ATG and A-ATG aim to optimize in terms of the global satisfaction as the exact potential game. On the other hand, $\mathbf{C}_4$, $\mathbf{C}_6$, $\mathbf{C}_7$, and $\mathbf{C}_9$ generated and experienced a small amount of network interference because they are located far from the other players. Consequently, they need a small amount of power with any scheme to achieve the rate demand in every scheme in Figure 4.5.

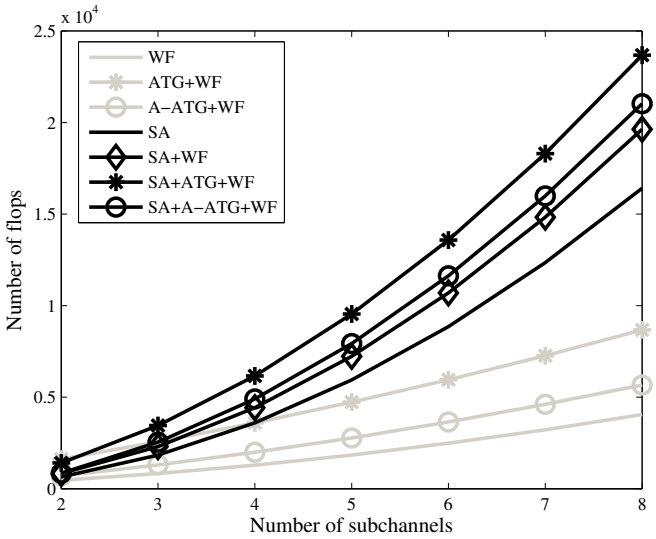

(a)

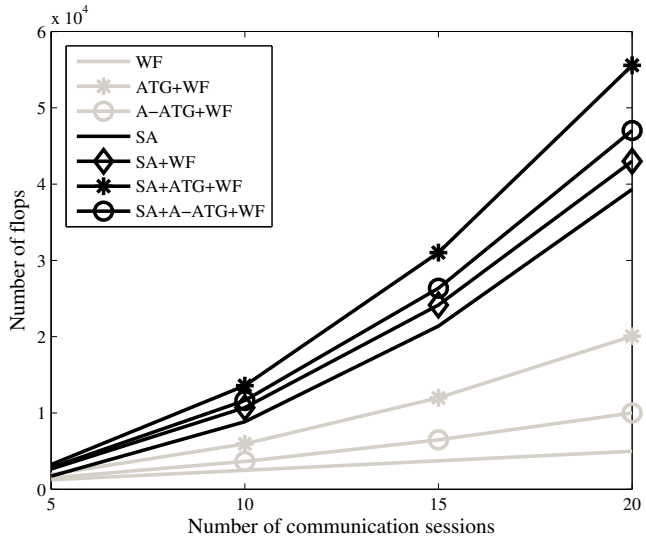

(b)

Figure 4.7: Computation load for varying (a) K (M is set to 10) and (b) M (K is set to 6).

4.4.4 Total Energy Consumption in 1000-shot Games

In addition to looking at one particular instance of ATG and A-ATG, I also analyze the energy consumption by simulating ATG and A-ATG over a long time duration. I considered 1000 replications of one-shot ATG and A-ATG, during which most of my global parameter settings were the same as before, except that the players' locations and channel conditions were randomly generated following the previously described distribution. (As Figure 4.6 shows, I additionally plotted a direct link (a source-to-destination link (termed "S-D direct") scenario to show that only changing the S-D direct link to a two-hop link with a relay node leads to significant energy savings. The performance gain of the addition of relay nodes might depend on a relay selection algorithm that is excluded in my approach. I consider it as future work to evaluate my algorithms.) In Figure 4.6, I can see that "ATG+WF" and "A-ATG+WF" show higher performance compared to the WF algorithm in terms of reducing the energy consumption in the scenarios without and with SA. Naturally, "SA+ATG+WF" in Figure 4.6(b) shows that the best performance in terms of the sum of the energy consumption of all source nodes and all relay nodes per minute is 24.4 mJ and 24.8 mJ without and with SA, respectively. More concretely, ATG attains gains of 17.4% and 9.8% over the WF algorithm in the scenarios without and with SA, respectively. A-ATG also leads to reductions in the total energy consumption per minute by 5.6% and 1.0% in the scenarios without and with SA, respectively. I can verify that my proposed schemes show a better performance gain over the WF algorithm in the scenario without SA than that with SA. This effect originates from the difference in the subchannels used K_i. ATG and A-ATG would miss opportunities to coordinate network interference because the number of co-used channels in network is naturally reduced after the SA algorithm is done. In Figure 4.6(a), six subchannels are used for every communication session; thus, my proposed schemes have many chances to demonstrate their potential ability. However, in Figure 4.6(b), each communication session utilizes five subchannels, even in different subchannel elements. The elements of the correspondingly utilized subchannels

are reduced in the scenario with SA; thus, the effectiveness of the proposed schemes would be weaker.

4.4.5 Complexity Analysis for Varying K and M

Figure 4.7(a) and Figure 4.7(b) show the complexity analysis in terms of the number of flops when varying the numbers of subchannels and communication sessions, respectively. A flop is defined as a real floating point operation. The computational complexity of an operation is counted as the total number flops required for calculating the utility function, choosing the best response, and counting the total number of iterations, and this method is applied to both the baseline algorithms and my proposed algorithms. Recall that K and M denote the numbers of subchannels and communication sessions, respectively; then, the number of flops can be calculated as follows (where $I_{(\bullet)}$ is the averaged iteration number per communication session of the corresponding algorithm, and it is commonly close to 2, which is obtained from 1000 replications of the simulation, regardless of the algorithm):

• WF: $(2K^2 + 6K)MI_{\text{WF}}$ (calculated by referring to [66, 74]).

• WF+ATG: $(2K^2 + 6K)MI_{\text{WF}} + (2(M-2)+1)(2K)MI_{\text{ATG}}$.

• WF+A-ATG:

$(2K^2 + 6K)MI_{\text{WF}} + ((2(M-2)+1)(K-1)+1)(2)MI_{\text{A-ATG}}$.

• SA: $2((K-1)(M-2)+1)\frac{K!}{K_i!(K-K_i)!}MI_{\text{SA}}$ (calculated by referring to [39]).

• SA+WF: $2((K-1)(M-2)+1)\frac{K!}{K_i!(K-K_i)!}MI_{\text{SA}} + (2K_i^2 + 6K_i)MI_{\text{WF}}$

• SA+ATG+WF:

$2((K-1)(M-2)+1)\frac{K!}{K_i!(K-K_i)!}MI_{\text{SA}} + (2(M-2)+1)(2K_i)MI_{\text{ATG}} + (2K_i^2 + 6K_i)MI_{\text{WF}}$.

• SA+A-ATG+WF:

$2((K-1)(M-2)+1)\frac{K!}{K_i!(K-K_i)!}MI_{\text{SA}} + ((2(M-2)+1)(K_i-1)+1)(2)MI_{\text{A-ATG}} + (2K_i^2 + 6K_i)MI_{\text{WF}}$.

As shown in the above equations, the increase in K greatly influences the required

numbers of flops of WF and SA compared to those of ATG and A-ATG. In Figure 4.7(a), for simplicity, I set K_i to $K-1$ for varying the number of subchannels. However, this heuristic setting is reasonable when considering the complexity of SA because of the combinatorial term $\frac{K!}{K_i!(K-K_i)!}$, which is the required number of choosing the best response in SA operation. Moreover, the lack of subchannels used may result in more power consumption in spite of the SA operation; thus, a sufficiently high value for K_i should be set to attain a synergetic effect between SA and WF. When adding ATG to "SA+WF", the required number of flops of "SA+WF" is increased by 27% on average for all of the scenarios in Figure 4.7(a). From Figure 4.7(a), it is interesting that the increase in the required number of flops owing to ATG is not very high in spite of $|\mathbf{S}_i|$ (or $|\mathbf{S}_i(K_i)|$ (or $|\mathbf{S}_i(K_i)|$), which is 2^K (or 2^{K_i}). This is the reason why finding the best response of ATG does not need a brute-force search of $|\mathbf{S}_i|$, which is also described in the above equations. The determinations of $s_{i,k}$ and $s_{i,k'}$, which are the elements of the best response, do not affect each other by virtue of the spectrum orthogonality; thus, parallel and independent operation in the frequency domain is possible to find best response of ATG, which is attractive in comparison to SA because the best response (choosing the best subchannels among K) of SA should be combinatorially determined by an exhaustive search. On the other hand, the complexity of A-ATG is $(1/K)$ of that of ATG from the viewpoint of the solution search space. However, from the viewpoint of the number of flops, the computational load of A-ATG is not $(1/K)$ of that of ATG because A-ATG needs some subsidiary flops for an average operation when calculating the utility function $u_i(\mathbf{b})$. In Figure 4.7(b), the influence of adding ATG to "WF" or "SA+WF" becomes higher than that of the scenario in Figure 4.7(a) owing to the fact that the required number of flops of ATG increases on the order of M^2, in spite of just proportionally increasing with K in Figure 4.7(a). This is the reason why both of the number of flops for calculating the utility function and counting the total number of iterations are commonly proportional to M in the ATG operation. Moreover, the number of flops for the A-ATG operation also increases in

proportion to M^2 for the same reason as ATG. However, in a WF operation, the number of flops for calculating the utility function does not depend on M; consequently, only the number of flops for counting the total number of iterations is proportional to M. In addition, "ATG+WF" results in better performance with a reduction of 49% in the required number of flops while maintaining the energy consumption performance at a level similar to that of "SA+WF". This effect on the reduction in the number of flops should be more critical when K_i approaches $K/2$ owing to the term $\frac{K!}{K_i!(K-K_i)!}$ in the equations containing the SA operation. In summary, the computational loads of ATG and A-ATG in terms of the number of flops are more sensitive to M than K, and the conversion of ATG to A-ATG in both "ATG+WF" and "SA+ATG+WF" leads an reductions of 48% and 16%, respectively, in the required number of flops for the total number of cases of the simulations.

Chapter 5

CONCLUSION

In this dissertation, by using supermodular game and exact potential game, I introduce three algorithms, which are named as CRG, ASCG, and ATG, with considerations of theoretical proof and practical issues in WSNs and wireless cellular networks.

First, I propose a game-theoretical power control based distributed algorithm, called CRG, suitable for wireless localization in energy-limited WSNs. The solution of CRG, which is obtained by the properties of supermodular game, results in the effective connectivity for wireless localization with energy savings. I think that my proposed algorithm can be effectively utilized in WSNs according to the system's objective, e.g., energy consumption or quality of localization. Additionally, I believe that my contribution can be more valuable in future WSNs when distribution of sensor nodes would become denser.

Second, I propose the ASCG and ASCG-D, which are new coordinated-distributed scheme that optimize GNI based ICIC problem. It is worth noting that ASCG-D requires smaller signaling overhead and computational load for ICIC implementation than the conventional dynamic ICIC schemes do and is robust with respect to the latency of X2 interface. Moreover, ASCG-D is an exact potential game, so it has the advantage of an NE solution always existing. Given that this study is conducted in a homogeneous cellular network, further studies are required for a heterogeneous cel-

lular network including femtocells, relay cells, and picocells. Moreover, my study is expected to lead to interesting results when ASCG-D is combined with beamforming problems in massive multiple-input multiple-output (MIMO) cellular networks using millimeter-wave technology.

Third, I introduce asymmetric transmission to reduce network interference in wireless multiuser ad-hoc networks with a two-hop relaying protocol. I formulate the asymmetric transmission problems in HDR systems, and construct the game-theoretical algorithm, called ATG, for deriving suboptimal solutions. The proposed algorithm guarantees the existence of the NE. Furthermore, I developed A-ATG based on the value of spectral averaging in order to reduce signaling and computational complexity of ATG. Compared with the conventional methods, the two algorithms show a significant decrease in network interference. For specific applications, I expect that the proposed algorithms can be easily applied to the autonomous outband D2D communication scenarios. With a proper change in game formulation, ATG and A-ATG can also be utilized in more various scenarios, including the underlaying inband, overlaying inband, and controlled outband D2D communication scenarios, which are mixed with an infrastructure system consisting a central entity (e.g., eNB) and cellular users. Suggestions for further research include extending this work to multiuser ad-hoc network with MIMO systems or multi-hop relaying protocol systems.

I deeply believe that these three algorithms can be highly potential solution for resolving the problems of limited resources in future wireless networks, such as Internet of things (IoT), vehicle-to-everything (V2X) systems, and D2D communications.

Appendix A
Derivation of number of partitions for extracting the dominant feasible strategy set

If there exists a vector $\mathbf{v} = [a_1, ..., a_K]$, where $a_k = |\mathcal{N}^{l,k}|$ for all k, how many $\mathbf{v}$ exist that satisfy $a_1 + \cdots + a_K = N$?

To solve this converted problem, integer '1' must be added to each component a_k. Consequently, the final form of problem is as follows:

$\Rightarrow$ Let a vector $\mathbf{V} = [b_1, ..., b_K] = [a_1 + 1, ..., a_K + 1]$. Then, how many $\mathbf{V}$ exist that satisfy $b_1 +, ..., + B_K = N + K$? This is equivalent to selecting $K - 1$ elements among $N + K - 1$ elements, as follows:

i) There are $N + K - 1$ holes.

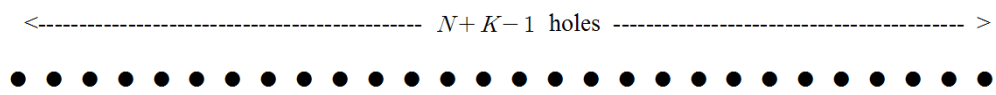

ii) Insert $K - 1$ sticks into $N + K - 1$ holes, such that they are not overlapping. In this case, two sticks are inserted into the first and second holes.

iii) In this case, the two sticks are inserted into the $(N + K - 2)$-th and the $(N +$

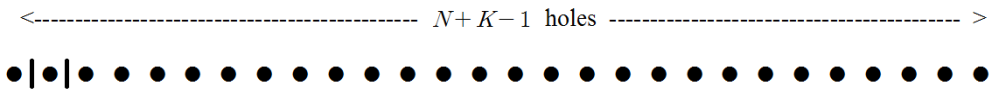

$K-1$)-th holes.

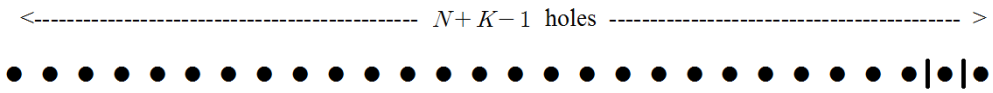

iv) In the first case, $\mathbf{V} = [1, 1, 26]$ and $\mathbf{v} = [0, 0, 25]$. In the second case, $\mathbf{V} = [26, 1, 1]$ and $\mathbf{v} = [25, 0, 0]$.

All cases of $|\aleph_l^{ps}|$ are expressed as above. Thus this is equivalent to $\binom{N+K-1}{K-1}$.

Appendix B
Derivation of the cardinal number of the dominant feasible strategy set

Let T_1 be the number of cases of possible $\mathcal{N}_D^{l,1}$ that satisfy the fixed cardinal number $|\mathcal{N}_D^{l,1}|$, and then, $T_1 = \binom{N}{|\mathcal{N}_D^{l,1}|}$. In the first iteration of choice, select arbitrary $|\mathcal{N}_D^{l,1}|$ elements among N elements. Next, in the second iteration of choice, select arbitrary $|\mathcal{N}_D^{l,2}|$ among $N - |\mathcal{N}_D^{l,1}|$, and not N. Hence, T_2 . The total number of cases T is solved as follows through iteration:

$\Rightarrow$ the total number of cases: $|\aleph_l^D| = \prod_{k=1}^{K} T_k = \binom{N}{|\mathcal{N}_D^{l,1}|} \times \binom{N-|\mathcal{N}_D^{l,1}|}{|\mathcal{N}_D^{l,2}|} \times \cdots \times \binom{|\mathcal{N}_D^{l,K}|}{|\mathcal{N}_D^{l,K}|} = \frac{N!}{\prod_{k=1}^{K} |\mathcal{N}_D^{l,k}|!}$.

Appendix C
Existence of NE in ASCG-D

For simplification, I omit the time index $i_{su}T_{su}$. Let us separate the utility functions of player l into the components of potential gain and potential interference ($PG_l(\mathbf{Y}^l) = U_l^{PG}(\mathbf{Y}^l)$ and $PI_l(\mathbf{Y}) + PI_{\mathcal{L}_{-l}(\mathbf{Y})} = U_l^{PI}$).

$$
\begin{aligned}
&U_l(\mathbf{Y}) = PG_l(\mathbf{Y}^l) + \Big(PI_l(\mathbf{Y}) + PI_{\mathcal{L}_{-l}(\mathbf{Y})}\Big) \\
&= U_l^{PG}(\mathbf{Y}^l) + U_l^{PI}(\mathbf{Y}) = U_l^{PG}(\mathbf{Y}^l) + \sum_{n=1}^{N} U_{l,n}^{PI}(\mathbf{Y}) \\
&\text{where } U_{l,n}^{PI}(\mathbf{Y}) = -\sum_{j\in\mathcal{L}_{-l}}\sum_{k\in\mathcal{K}^l}\Bigg[y_{nk}^l \cdot \sum_{k'\in\mathcal{K}^j}\Big[y_{nk'}^j \cdot \\
&\Big(\sum_{m\in\mathcal{M}^{l,k}}(\gamma_j + P_j^n + \phi_{j,m}^n - \mu_{j,m}) \\
&\quad - \sum_{m'\in\mathcal{M}^{j,k'}}(\gamma_l + P_l^n + \phi_{l,m'}^n - \mu_{l,m'})\Big)\Big]\Bigg]. \qquad (1)
\end{aligned}
$$

Necessary condition (3.6) of an exact potential game is rewritten as

$$
\begin{aligned}
&U_l^{PG}(\tilde{\mathbf{Y}}^l) - U_l^{PG}(\mathbf{Y}^l) + \sum_{n=1}^{N}[U_{l,n}^{PI}(\tilde{\mathbf{Y}}^l;\mathbf{Y}^{\mathcal{L}_{-l}}) - U_{l,n}^{PI}(\mathbf{Y}^l;\mathbf{Y}^{\mathcal{L}_{-l}})] \\
&= F^{PG}(\tilde{\mathbf{Y}}^l;\mathbf{Y}^{\mathcal{L}_{-l}}) - F^{PG}(\mathbf{Y}^l;\mathbf{Y}^{\mathcal{L}_{-l}}) \\
&\qquad + F^{PI}(\tilde{\mathbf{Y}}^l;\mathbf{Y}^{\mathcal{L}_{-l}}) - F^{PI}(\mathbf{Y}^l;\mathbf{Y}^{\mathcal{L}_{-l}}). \qquad (2)
\end{aligned}
$$

Using (2), let us find $F^{PG}(\mathbf{Y}^l;\mathbf{Y}^{\mathcal{L}_{-l}})$ and $F^{PI}(\mathbf{Y}^l;\mathbf{Y}^{\mathcal{L}_{-l}})$ according to the components $U_l^{PG}(\mathbf{Y}_l)$ and $U_l^{PI}(\mathbf{Y}^l;\mathbf{Y}^{\mathcal{L}_{-l}})$.

i) Component $U_l^{PG}(\mathbf{Y}_l)$

$U_l^{PG}(\mathbf{Y}^l)$ in ASCG-D has the following two properties:

. $U_l^{PG}(\mathbf{Y}^l)$ is independent of $\mathbf{Y}^{\mathcal{L}_{-l}}$.

. $U_l^{PG}(\tilde{\mathbf{Y}}_l) = U_l^{PG}(\mathbf{Y}^l)\,(\because \forall\tilde{\mathbf{Y}}^l, \mathbf{Y}^l \in \aleph_D^l)$.

Thus,

$$U_l^{PG}(\mathbf{Y}^l) = F^{PG}(\mathbf{Y}^l;\mathbf{Y}^{\mathcal{L}_{-l}}) \text{ is constant.} \tag{3}$$

ii) Component $U_l^{PI}(\mathbf{Y}^l;\mathbf{Y}^{\mathcal{L}_{-l}})$

To simplify, I define $w_n^{jl} = \sum_{k'\in\mathcal{K}^j}\Big(y_{nk'}^j \cdot \sum_{k\in\mathcal{K}^l}\Big(y_{nk}^l \cdot \sum_{m\in\mathcal{M}^{l,k}}(\gamma_j + P_j^n + \phi_{j,m}^n - \mu_{j,m})$ and $w_n^{lj} = \sum_{k'\in\mathcal{K}^j}\Big(y_{nk'}^j \cdot \sum_{k\in\mathcal{K}^l}\Big(y_{nk}^l \cdot \sum_{m'\in\mathcal{M}^{j,k'}}(\gamma_l + P_l^n + \phi_{l,m}^n - \mu_{l,m})$. The utility function of player l according to potential interference is reconstructed as follows:

$$U_l^{PI}(\mathbf{Y}^l;\mathbf{Y}^{\mathcal{L}_{-l}}) = \sum_{n=1}^{N}[-\sum_{j\in\mathcal{L}_{-l}} w_n^{lj} - \sum_{j\in\mathcal{L}_{-l}} w_n^{jl}]$$

$$= \sum_{n=1}^{N} U_{l,n}^{PI}(\mathbf{Y}^l;\mathbf{Y}^{\mathcal{L}_{-l}}). \tag{4}$$

Modified necessary condition (2) of an exact potential game will hold if I consider a part of network potential function $F^{PI}(\mathbf{Y}^l;\mathbf{Y}_{-l}^{\mathcal{L}})$ is $\frac{1}{2}\sum_{l=1}^{L} U_l^{PI}(\mathbf{Y})$. And then,

$$F^{PI}(\mathbf{Y}^l;\mathbf{Y}^{\mathcal{L}_{-l}}) = \frac{1}{2}\sum_{l=1}^{L} U^{PI}(\mathbf{Y}) = \frac{1}{2}\sum_{l=1}^{L}\sum_{n=1}^{N} U_{l,n}^{PI}(\mathbf{Y})$$

$$= \sum_{n=1}^{N}\Big(\sum_{l=1}^{L-1}\sum_{j\in\mathcal{L}_{-l}} w_n^{lj}\Big) = \sum_{n=1}^{N} F_n^{PI}(Y). \tag{5}$$

$F_n^{PI}(\mathbf{Y})$ is expressed as

$$F_n^{PI}(\mathbf{Y}) = -\sum_{i\in\mathcal{L}_{-l}} w_n^{li} - \sum_{i\in\mathcal{L}_{-l}} w_n^{jl} - \sum_{i\in\mathcal{L}_{-l}}\sum_{j\in\mathcal{L}_{-l}} w_n^{ij}$$

$$= U_{l,n}^{PI}(\mathbf{Y}) + o(\mathbf{Y}^{\mathcal{L}_{-l}}). \tag{6}$$

, where $o(\mathbf{Y}^{\mathcal{L}_{-l}}) = -\sum_{i\in\mathcal{L}_{-l}}\sum_{j\in\mathcal{L}_{-l}} w_n^{ij}$ takes a constant value is independent of $\mathbf{Y}^l$. It is dependent only on the strategies of other players with each other.

Suppose that player l change its strategy $\mathbf{Y}^l$ to $\tilde{Y}^l$, w_n^{li} and w_n^{jl} would be changed to $\tilde{w}_n^{jl} = \sum_{k'\in\mathcal{K}^j}\left(y_{nk'}^j \cdot \sum_{k\in\mathcal{K}^l}\left(\tilde{y}_{nk}^l \cdot \sum_{m\in\mathcal{M}^{l,k}}(\gamma_j + P_j^n + \phi_{j,m}^n - \mu_{j,m})\right.\right.$ and $\tilde{w}_n^{lj} = \sum_{k'\in\mathcal{K}^j}\left(y_{nk'}^j \cdot \sum_{k\in\mathcal{K}^l}\left(\tilde{y}_{nk}^l \cdot \sum_{m'\in\mathcal{M}^{j,k'}}(\gamma_l + P_l^n + \phi_{l,m}^n - \mu_{l,m})\right.\right.$, where $\tilde{y}_{nk}^l$ is an element of $\tilde{\mathbf{Y}}^l$. And, F_n^{PI} is changed to

$$
\begin{aligned}
F_n^{PI}(\tilde{\mathbf{Y}}^l;\mathbf{Y}^{\mathcal{L}_{-l}}) &= -\sum_{i\in\mathcal{L}_{-l}}\tilde{w}_n^{li} - \sum_{i\in\mathcal{L}_{-l}}\tilde{w}_n^{jl} \\
&- \sum_{i\in\mathcal{L}_{-l}}\sum_{j\in\mathcal{L}_{-l}} w_n^{ij} = U_{l,n}^{PI}(Y) + o(\mathbf{Y}^{\mathcal{L}_{-l}}). \qquad (7)
\end{aligned}
$$

By (6) and (7), $U_{l,n}^{PI}(\tilde{\mathbf{Y}}^l;\mathbf{Y}^{\mathcal{L}_{-l}}) - U_{l,n}^{PI}(\mathbf{Y}^l;\mathbf{Y}^{\mathcal{L}_{-l}}) = F_n^{PI}(\tilde{\mathbf{Y}}^l;\mathbf{Y}^{\mathcal{L}_{-l}}) - F_n^{PI}(\mathbf{Y}^l;\mathbf{Y}^{\mathcal{L}_{-l}})$. By integration of all $n \in \mathcal{N}$,

$$
\begin{aligned}
&U_{l,n}^{PI}(\tilde{\mathbf{Y}}^l;\mathbf{Y}^{\mathcal{L}_{-l}}) - U_{l,n}^{PI}(\mathbf{Y}^l;\mathbf{Y}^{\mathcal{L}_{-l}}) \\
&\qquad = F_n^{PI}(\tilde{\mathbf{Y}}^l;\mathbf{Y}^{\mathcal{L}_{-l}}) - F_n^{PI}(\mathbf{Y}^l;\mathbf{Y}^{\mathcal{L}_{-l}}). \qquad (8)
\end{aligned}
$$

From (3) and (8), then (2) will hold.

Appendix D
The Required Signaling overhead of ASCG-D

The signaling overhead per T_c is explained as follows (where B_{CSI}, B_{su}, and B_{ud} are defined in Section V., and N_m^c is the cardinal number of the candidate coloring RB set of user m, whose value depends on the ICIC scheme):

- CSI based ICIC + FDPS :

  $B_{CSI} \cdot L \cdot N \cdot M + B_{CSI} \cdot \sum_{m=1}^{M} N_m^c \, [bits/T_c]$.

- GNI based ICIC + FDPS :

  $\frac{B_{ud} \cdot M}{\lfloor T_{ud}/T_c \rfloor} + B_{CSI} \cdot \sum_{m=1}^{M} N_m^c \, [bits/T_c]$.

- ASCG-D + FDPS :

  $\frac{B_{ud} \cdot M \cdot L}{\lfloor T_{ud}/T_c \rfloor} + \frac{B_{su} \cdot (L-1)}{\lfloor T_{su}/T_c \rfloor} + B_{CSI} \cdot \sum_{m=1}^{M} N_m^c \, [bits/T_c]$.

- FGC + FDPS :

  $\frac{T_{c,de}}{T_{c,de}+T_{c,period}} \cdot B_{CSI} \cdot N \cdot M + B_{CSI} \cdot \sum_{m=1}^{M} N_m^c \, [bits/T_c]$.

- IMG + FDPS :

  $\frac{B_{CSI} \cdot N \cdot ((L-1) \cdot (1+\frac{M}{L}))}{\lfloor T_{su}/T_c \rfloor} + B_{CSI} \cdot \sum_{m=1}^{M} N_m^c \, [bits/T_c]$.

- Reuse-1 + FDPS : $B_{CSI} \cdot N \cdot M \, [bits/T_c]$.

- Reuse-3 + FDPS : $B_{CSI} \cdot \sum_{m=1}^{M} N_m^c \, [bits/T_c]$.

- PFR + FDPS : $B_{CSI} \cdot \sum_{m=1}^{M} N_m^c \, [bits/T_c]$.

Bibliography

[1] J. Levin, Supermodular games, Lecture Notes on Game Theory and Economic Applications, Department of Economics, Stanford University, 2006.

[2] D. Monderer and L.S. Shapley, "Potential games," Games and economic behavior, vol.14, no.1, pp.124-143, 1996.

[3] N. Patwari and A. O. Hero, III, "Using proximity and quantized rss for sensor localization in wireless networks," in *Proc. 2nd ACM Int. Conf. Wireless Sensor Netw. Appl.*, pp. 20–29, 2003.

[4] L. Lin, H.-C. So, and Y. T. Chan, "Accurate and simple source localization using differential received signal strength," *Digit. Signal Process.*, vol. 23, no. 3, pp. 736–743, May 2013.

[5] S. Lederer, Y. Wang, and J. Gao, "Connectivity-based localization of large-scale sensor networks with complex shape," *ACM Trans. Sensor Netw.*, vol. 5, no. 4, Nov. 2009.

[6] T. Van Nguyen, Y. Jeong, H. Shin, and M. Z. Win, "Machine learning for wideband localization," *IEEE J. Sel. Areas Commun.*, vol. 33, no. 7, pp. 1357–1380, Jul. 2015.

[7] Y. Shang, W. Ruml, Y. Zhang, and M. P. Fromherz, "Localization from mere connectivity," *in Proc. 4th ACM Int. Symp. Mobile Ad Hoc Netw. Comput.*, pp. 201–212, 2003.

[8] J. A. Costa, N. Patwari, and A. O. Hero, III, "Distributed weighted multidimensional scaling for node localization in sensor networks," *ACM Trans. Sensor Netw.*, vol. 2, no. 1, pp. 39–64, 2006.

[9] F. Doremani, H. Javadi, and A. Farahi, "A new distributed weighted multidimensional scaling algorithm for localization in wireless sensor networks," *Int. J. Comput. Sci. Eng. Sur.*, vol. 20, no. 1, pp. 65–76, 332 Feb. 2011.

[10] F. K. W. Chan and H. C. So, "Efficient weighted multidimensional scaling for wireless sensor network localization," *IEEE Trans. Signal Process.*, vol. 57, no. 11, pp. 4548–4553, Nov. 2009.

[11] Bejar, B., P. Belanovic, and S. Zazo. "Cooperative localisation in wireless sensor networks using coalitional game theory." *Signal Processing Conference, 2010 18th European. IEEE*, 2010.

[12] A. Moragrega, P. Closas, and C. Ibars, "Energy-efficient positioning in sensor networks by a game theoretic approach," *in Proc. 19th Eur. Signal Process. Conf.*, pp. 2014–2018, 2011.

[13] S. Sesia, I. Toufik, and M. Baker, *LTE, The UMTS Long Term Evolution: From Theory to Practice*. Wiley Publishing, 2009.

[14] K. I. Pedersen, T. E. Kolding, F. Frederiksen, I. Z. Kovacs, D. Laselva, and P. E. Mogensen, "An overview of downlink radio resource management for utran long-term evolution," *IEEE Communications Magazine*, vol. 47, no. 7, pp. 86–93, 2009.

[15] S. N. K. Marwat, "LTE channel modelling for system level simulations," Ph.D. dissertation, MS thesis, Dept. Comm. Netwo., Bremen. Univ., Bremen, Germany, 2011.

[16] S.-B. Lee, S. Choudhury, A. Khoshnevis, S. Xu, and S. Lu, "Downlink MIMO with frequency-domain packet scheduling for 3GPP LTE," in *IEEE INFOCOM*, pp. 1269–1277, 2009.

[17] A. Pokhariyal, G. Monghal, K. I. Pedersen, P. E. Mogensen, I. Z. Kovacs, C. Rosa, and T. E. Kolding, "Frequency domain packet scheduling under fractional load for the utran LTE downlink," in *IEEE Vehicular Technology Conference (VTC-Spring)*, pp. 699–703, 2007.

[18] S.-B. Lee, I. Pefkianakis, S. Choudhury, S. Xu, and S. Lu, "Exploiting spatial, frequency, and multiuser diversity in 3GPP LTE cellular networks," *IEEE Transactions on Mobile Computing*, vol. 11, no. 11, pp. 1652–1665, 2012.

[19] Y. Xu, H. Yang, F. Ren, C. Lin, and X. Shen, "Frequency domain packet scheduling with MIMO for 3GPP LTE downlink," *IEEE Transactions on Wireless Communications*, vol. 12, no. 4, pp. 1752–1761, 2013.

[20] A. S. Hamza, S. S. Khalifa, H. S. Hamza, and K. Elsayed, "A survey on inter-cell interference coordination techniques in OFDMA-based cellular networks," *Communications Surveys & Tutorials, IEEE*, vol. 15, no. 4, pp. 1642–1670, 2013.

[21] N. U. Hassan and M. Assaad, "Optimal fractional frequency reuse (FFR) and resource allocation in multiuser OFDMA system," in *International Conference on Information and Communication Technologies (ICICT)*, pp. 88–92, 2009.

[22] F. Khan, *LTE for 4G mobile broadband: air interface technologies and performance*. Cambridge University Press, 2009.

[23] M. Rahman and H. Yanikomeroglu, "Enhancing cell-edge performance: a downlink dynamic interference avoidance scheme with inter-cell coordination," *IEEE Transactions on Wireless Communications*, vol. 9, no. 4, pp. 1414–1425, 2010.

[24] M. Porjazoski and B. Popovski, “Analysis of intercell interference coordination by fractional frequency reuse in LTE,” in *Software, Telecommunications and Computer Networks (SoftCOM), 2010 International Conference on*, pp. 160–164, 2010.

[25] M. Porjazoski and B. Popovski, “Contribution to analysis of intercell interference coordination in LTE: A fractional frequency reuse case,” in *Mobile Congress (GMC), 2010 Global*, pp. 1–4, 2010.

[26] G. Li and H. Liu, “Downlink radio resource allocation for multi-cell OFDMA system,” *IEEE Transactions on Wireless Communications*, vol. 5, no. 12, pp. 3451–3459, 2006.

[27] G. Fodor, C. Koutsimanis, A. Rácz, N. Reider, A. Simonsson, and W. Müller, “Intercell interference coordination in OFDMA networks and in the 3GPP long term evolution system,” *Journal of Communications*, vol. 4, no. 7, pp. 445–453, 2009.

[28] S. H. Ali and V. Leung, “Dynamic frequency allocation in fractional frequency reused OFDMA networks,” *IEEE Transactions on Wireless Communications*, vol. 8, no. 8, pp. 4286–4295, 2009.

[29] M. Boujelben, S. Ben Rejeb, and S. Tabbane, “A comparative study of interference coordination schemes for wireless mobile advanced systems,” in *The 2014 International Symposium on Networks, Computers and Communications*, pp. 1–5, 2014.

[30] M. C. Necker, “A novel algorithm for distributed dynamic interference coordination in cellular networks,” *PIK-Praxis der Informationsverarbeitung und Kommunikation*, vol. 34, no. 2, pp. 97–101, 2011.

[31] D. Kimura, Y. Harada, and H. Seki, "De-centralized dynamic ICIC using X2 interfaces for downlink LTE systems," in *2011 IEEE 73rd Vehicular Technology Conference (VTC Spring)*, pp. 1–5, 2011.

[32] Z. Xie and B. Walke, "Resource allocation and reuse for inter-cell interference mitigation in OFDMA based communication networks," in *The 5th Annual ICST Wireless Internet Conference (WICON)*, pp. 1–6, 2010.

[33] M. Rahman, H. Yanikomeroglu, and W. Wong, "Interference avoidance with dynamic inter-cell coordination for downlink LTE system," in *IEEE Wireless Communications and Networking Conference (WCNC)*, pp. 1–6, 2009.

[34] M. Rahman and H. Yanikomeroglu, "Interference avoidance through dynamic downlink OFDMA subchannel allocation using intercell coordination," in *IEEE Vehicular Technology Conference (VTC Spring)*, pp. 1630–1635, 2008.

[35] Z. Lu, Y. Yang, X. Wen, Y. Ju, and W. Zheng, "A cross-layer resource allocation scheme for ICIC in LTE-Advanced," *Journal of Network and Computer Applications*, vol. 34, no. 6, pp. 1861–1868, 2011.

[36] D. Ling, Z. Lu, Y. Ju, X. Wen, and W. Zheng, "A multi-cell adaptive resource allocation scheme based on potential game for ICIC in LTE-A," *International Journal of Communication Systems*, vol. 27, no. 11, pp. 2744–2761, 2014.

[37] X. Wang, W. Zheng, Z. Lu, X. Wen, and W. Li, "Dense femtocell networks power self-optimization: an exact potential game approach," *International Journal of Communication Systems*, 2014.

[38] L. Liang and G. Feng, "A game-theoretic framework for interference coordination in OFDMA relay networks," *IEEE Transactions on Vehicular Technology*, vol. 61, no. 1, pp. 321–332, 2012.

[39] Q. D. La, Y. H. Chew, and B.-H. Soong, "An interference minimization game theoretic subcarrier allocation algorithm for OFDMA-based distributed systems," in *IEEE Global Telecommunications Conference (GLOBECOM)*, pp. 1–6, 2009.

[40] Q. D. La, Y. H. Chew, and B.-H. Soong, "An interference-minimization potential game for OFDMA-based distributed spectrum sharing systems," *IEEE Trans. Veh. Technol*., vol.60, no.7, pp.3374-3385, 2011.

[41] S. Sesia, I. Toufik, and M. Baker, *LTE: the UMTS long term evolution*. Wiley Online Library, 2009.

[42] L. Lindbom, R. Love, S. Krishnamurthy, C. Yao, N. Miki, and V. Chandrasekhar, "Enhanced inter-cell interference coordination for heterogeneous networks in LTE-Advanced: A survey," *arXiv preprint arXiv:1112.1344*, 2011.

[43] B. T. Scheme, "LTE: the evolution of mobile broadband," *IEEE Communications magazine*, vol. 45, 2009.

[44] P. Brucker, J. Hurink, and F. Werner, "Improving local search heuristics for some scheduling problems. Part II," *Discrete Applied Mathematics*, vol. 72, no. 1, pp. 47–69, 1997.

[45] A. Asadi, Q. Wang, and V. Mancuso, "A survey on device-to-device communication in cellular networks," *IEEE Commun. Surveys & Tutorials*, vol.16, no.4, pp.1801-1819, 2014.

[46] J. Pekka, Y. Chia-Hao, R. Cassio, W. Carl, H. Klaus, T. Olav, and K. Visa, "Device-to-device communication underlaying cellular communications systems," *Int. J. Commun, Netw., Syst. Sci*., vol. 2, no. 3, pp.169-178, 2009.

[47] T. Rault, A. Bouabdallah, and Y. Challal, "Energy efficiency in wireless sensor networks: A top-down survey," *Comput. Netw*., vol. 67, pp. 104-122, 2014.

[48] G. Anastasi, M. Conti, M. Francesco, A. Passarella, "Energy Conservation in Wireless Sensor Networks: A survey," *Ad Hoc Networks*, Vol. 7, Issue 3, pp. 537-568, 2009.

[49] A. Abrardo, G. Fodor, and B. Tola, "Network coding schemes for device-to-device communications based relaying for cellular coverage extension", *Proc. IEEE SPAWC*, pp.670-674, 2015.

[50] B. Rankov and A. Wittneben, "Spectral efficient protocols for half-duplex fading relay channels," *IEEE J. Sel. Areas Commun*., vol.25, no.2, pp.379-389, 2007.

[51] J.N. Laneman, D.N. Tse, and G.W. Wornell, "Cooperative diversity in wireless networks: Efficient protocols and outage behavior," *IEEE Trans. Inf. Theory*, vol.50, no.12, pp.3062-3080, 2004.

[52] S. Zhou, J. Xu and Z. Niu, "Interference-aware relay selection scheme for two-hop relay networks with multiple source-destination pairs," *IEEE Trans. Veh. Technol*., vol.PP, no.99, 2013.

[53] Jin, A-Long, et al. "An energy-efficient uncoordinated cooperative scheme with uncertain relay distribution intensity," *IEEE Trans. Veh. Technol*., vol.64, no.2, pp.677-688, 2015.

[54] N. Suraweera and N. C. Beaulieu, "Performance analysis of DF relaying with optimum combining in a Poisson field of interferers," *Proc. IEEE ICC*, pp. 3915-3920, 2015.

[55] A. Zanella, A. Bazzi , et al. "Performance analysis of multiuser 2-hop systems with random placement of relay nodes," *Proc. IEEE Global Communications Conference (GLOBECOM)*, 2014.

[56] T. Jing, S. Zhu, H. Li, X. Cheng, and Y. Huo, "Cooperative relay selection in cognitive radio networks," *Proc. IEEE INFOCOM*, pp.175-179, 2013.

[57] Hoang, T. Duc, L. Bao Le, and T. Le-Ngoc, "Radio resource management for optimizing energy efficiency of D2D communications in cellular networks," *Proc. IEEE Personal, Indoor, and Mobile Radio Communications (PIMRC)*, 2015.

[58] Hoang, T. Duc, L. Bao Le, and T. Le-Ngoc, "Joint subchannel and power allocation for D2D communications in cellular networks," *Proc. IEEE Wireless Communications and Networking Conference (WCNC)*, 2014.

[59] Z. Guan, T. Melodia, D. Yuan, and D.A. Pados, "Distributed spectrum management and relay selection in interference-limited cooperative wireless networks," *Proc. ACM MobiCom*, pp.229-240, 2011.

[60] W. Zhao and S. Wang, "Joint subchannel and power allocation in multiuser OFDM systems with minimal rate constraints," *Int. J. Commun. Syst.*, vol.27, no.1, pp.1-12, 2014.

[61] Chang, Zheng, "Spectrum and energy efficient solutions for OFDMA collaborative wireless networks," University of Jyväskylä, 2013.

[62] S. Gao, L. Qian, and Dhadesugoor R. Vaman. "Distributed energy efficient spectrum access in wireless cognitive radio sensor networks," *Proc. IEEE Wireless Communications and Networking Conference (WCNC)*, 2008.

[63] R. Wang, H. Ji, and X. Li, "A distributed power allocation scheme in green cognitive radio ad hoc networks," *Journal of Shanghai Jiaotong University (Science)*, pp. 195-201, 2015.

[64] Chen, Xiaomao, and S. Ouyang, "Energy-and spectral-efficiency trade-off in OFDMA-based cooperative cognitive radio networks," *International Journal of Distributed Sensor Networks*, 2014.

[65] G. Scutari, D.P. Palomar, and S. Barbarossa, "Simultaneous iterative water-filling for gaussian frequency-selective interference channels," *Proc. IEEE ISIT*, pp.600-604, 2006.

[66] G. Scutari, D.P. Palomar, and S. Barbarossa, "Asynchronous iterative water-filling for Gaussian frequency-selective interference channels," *IEEE Trans. Inf. Theory*, vol.54, no.7, pp.2868-2878, 2008.

[67] X. Wang, X. Wang, W. Gong, and Z. Huang, "Generalized block-diagonalization schemes for MIMO relay broadcasting systems," *Int. J. Digital Multimedia Broadcasting*, 2014.

[68] X. Chen, S. Song, and K. Ben Letaief, "Interference alignment in mimo interference relay channels," *Proc. IEEE Wireless Communications and Networking Conference (WCNC)*, pp.630-634, 2012.

[69] P. Brenner, "A technical tutorial on the IEEE 802.11 Protocol," *BreezeCom Wireless Communications*, 1997.

[70] R. Impagliazzo, S. Lovett, R. Paturi, and S. Schneider, "0-1 integer linear programming with a linear number of constraints," *arXiv preprint arXiv:1401.5512*, 2014.

[71] B. Ellingsæter, M. Skjegstad, and T. Maseng, "A potential game for power and frequency allocation in large-scale wireless networks," *arXiv preprint arXiv:1212.0724*, 2012.

[72] P. Brucker, J. Hurink, and F. Werner, "Improving local search heuristics for some scheduling problems. Part II," *Discrete Applied Mathematics*, vol.72, no.1, pp.47-69, 1997.

[73] D. Kim, B. Shin, D. Hong and J. Lim, “Self-configuration of neighbor cell list utilizing E-UTRAN NodeB scanning in LTE systems”, *Proc. IEEE Consumer Communications and Networking Conf (CCNC)*, pp. 1-5, 2010

[74] Z. Shen, R. Chen, J. G. Andrews, R. W. Heath and B. L. Evans, ”Low complexity user selection algorithms for multiuser MIMO systems with block diagonalization,” *IEEE Trans. Signal Process.*, vol. 54, pp. 3658-3663, 2006.

초 록

본 박사 논문집에서는, 무선 센서 네트워크와 셀룰러 네트워크에서의 다양한 목표들을 해결하기 위해, 슈퍼모듈라 게임과 이그잭트 포텔셜 게임을 이용하여 세 가지 알고리즘들 (네트워크 연결 재정립 게임, 적응적 섹터 색칠 게임, 그리고 비대칭적 신호 전송 게임) 을 개발하였다. 각 게임의 주 공헌은 다음 세 가지이다: 1) 무선 위치 측위에서의 네트워크 연결성 밀도 완화 (에너지 절약); 2) 셀룰러 네트워크에서의 셀간 간섭 조정; 3) 애드혹 릴레이 네트워크에서의 간섭 최소화. 해당 내용 설명들은 아래와 같다.

1) 지리적으로 밀집하고 에너지 소모에 민감한 무선 센서 네트워크에서는, 최대 전력 전송을 통한 네트워크 연결성 기반 위치 측위는 에너지 소모 측면에서 비효율적이라 할 수 있다. 본 연구에서는, 에너지 소모 효율과 측위 품질을 동시에 고려하는 분산적 전력 조절 기반 네트워크 연결 재정립 게임을 소개한다. 제안된 기법은 최대 전력 전송을 했을 때와 비슷한 측위 품질을 보임과 동시에 61.9% 에너지 소모 이득을 보인다.

2) 셀간 간섭 조정은 다운링크 LTE/LTE-A 네트워크에서의 사용자 스케쥴링 성능 향상에 유망한 기술이다. 하지만, 신호 대 간섭과 잡음비와 사용자 공평성에 관한 부족한 고려 탓에 정적 셀간 간섭 조정 기법들은 사용자 스케쥴링 성능 향상에 크게 기여 할 수 없다. 반면, 엄청난 양의 시그날링 오버헤드와 X2 인터페이스 지연 시간을 고려했을 때 채널 정보 기반 동적 셀간 간섭 조정 기법들 또한 효율적이라 보기 어렵다. 이러한 단점들을 극복하기위해, 지리 정보 기반의 새로운 셀간 간섭 조정 문제를 소개하며, 해당 문제의 해결책으로 적응적 섹터 색칠 게임을 제안한다. 나아

가, 내쉬 이퀼리브리엄의 존재를 제공하는 우세 전략 공간에서의 적응적 섹터 색칠 게임을 개발한다. 제시된 기법은 정적 셀간 간섭 조정 알고리즘들과 비교하였을 때, 시스템 쓰루풋 측면에서 44.1%의 성능 향상을 보이며, 특히 하위 10% 사용자들의 경우 221%의 성능 향상을 보인다. 또한, 전체 그리고 하위 10% 사용자 쓰루풋 성능에서의, 우세 전략 공간에서의 적응적 섹터 색칠 게임 대비 채널 정보 기반 동적 셀간 간섭 조정 기법의 이득은 각각 13.0% 와 5.6% 로써, 큰 차이를 보이지 않는다. 가장 흥미로운 결과는 우세 전략 공간에서의 적응적 섹터 색칠 게임은 채널 정보 기반 동적 셀간 간섭 조정 기법 대비 1/144의 시그날링 오버헤드를 필요로 한다는 점이다.

3) 투홉 반이중 릴레잉 프로토콜을 동반한 무선 애드혹 네트워크에서의 네트워크 간섭량 최소화를 위한 새로운 컨셉의 시간 다이버시티 사용 기반 비대칭적 신호 전송 기법을 제시한다. 비대칭적 신호 전송 기법은, 각 통신 세션 (소스-릴레이-데스티네이션 링크) 이 주파수 축에서 서로 직교한 여러 데이타 스트리밍 중 일부를 적응적으로 선택하는 간섭 기반 백오프 기술이다. 이러한 비대칭적 신호 전송 기법에 관한 문제를 새롭게 정의하고, 이 문제를 해결하기 위한 서브옵티말 해법으로써 비대칭적 신호 전송 게임을 개발한다. 비대칭적 신호 전송 게임이 이그잭트 포텐셜 게임임을 보임으로써 본 게임의 수렴성을 증명한다. 나아가, 시그날링 오버헤드와 계산 복잡도 감소를 위해 함축적 비대칭적 신호 전송 게임을 개발한다. 제안된 두가지 기법들은 기존 알고리즘들과 네트워크 간섭 최소화 측면에서 높은 시너지 효과를 보인다. 요구 데이타 전송량을 만족시키기 위해 필요한 에너지 소모량는 기존 알고리즘 대비 17.4%의 이득을 보인다.

주요어: 슈퍼모듈러 게임, 무선 위치 측위, 네트워크 연결성 밀도 완화, 에너지 소모, 이그잭트 포텔셜 게임, LTE 네트워크, 셀간 간섭 조정, 네트워크 지리 정보, 투홉 릴레잉 프로토콜, 간섭 조정

학번: 2009-23136